

**CHARACTERIZATION OF THREE CYSTEINE-RICH PROTEINS AND
AN ELONGATION FACTOR FROM THE SECRETOME OF *FUSARIUM*
*GRAMINEARUM***

ANAS ERANTHODI

Master of Science, University of Illinois at Urbana-Champaign, 2008

A thesis submitted
in partial fulfilment of the requirements for the degree of

DOCTOR OF PHILOSOPHY

in

BIOMOLECULAR SCIENCE

Department of Biological Sciences
University of Lethbridge
LETHBRIDGE, ALBERTA, CANADA

© Anas Eranthodi, 2020

CHARACTERIZATION OF THREE CYSTEINE-RICH PROTEINS AND AN
ELONGATION FACTOR FROM THE SECRETOME OF *FUSARIUM*
GRAMINEARUM

ANAS ERANTHODI

Date of Defence: June 23, 2020

Dr. Nora A. Foroud Dr. Elizabeth Schultz Thesis Co-Supervisors	Research Scientist Associate Professor	Ph.D. Ph.D.
Dr. Denis Gaudet Thesis Examination Committee member	Emeritus Scientist	Ph.D.
Dr. Stewart Rood Thesis Examination Committee member	Emeritus Professor	Ph.D.
Dr. James E. Thomas Thesis Examination Committee member	Emeritus Professor	Ph.D.
Dr. Nehal Thakor Internal External Examiner Department of Chemistry and Biochemistry Faculty of Arts and Science	Associate Professor	Ph.D.
Dr. Neil Brown External Examiner University of Bath	Assistant Professor	Ph.D.
Dr. Cameron Goater Chair, Thesis Examination Committee	Professor	Ph.D.

Abstract

Fusarium graminearum is one of the primary causal agents of Fusarium head blight (FHB) in cereals. Most proteins in the secretome of this pathogen are uncharacterized and their role in FHB is undefined. This study was aimed at elucidating the roles of four secreted proteins in *F. graminearum* growth and aggressiveness; a cerato-platanin, FgCPP1, two CFEM-containing proteins, FgCFEM1 and FgCFEM2 and the elongation factor 1A (FgEF1A). Characterization of gene disruption and *in locus* overexpression (OX) transformants for these proteins showed that *CPP1-OX* produced more DON in culture and also caused higher initial infection in different wheat cultivars. *CFEM1-OX* accumulated less DON in culture but showed increased disease spread in a moderately susceptible wheat cultivar. *FgEF1A* overexpression did not lead to substantially higher *FgEF1A* expression; nevertheless, a reduction in fitness and aggressiveness was observed. This study provides some basic insights into the roles of these secreted proteins in *F. graminearum* aggressiveness.

Acknowledgements

I express my deep sense of gratitude to Dr. Nora Foroud for the opportunity to work under her guidance and for the constant encouragement and concrete suggestions throughout the course of my program. I am grateful to her for helping me develop my writing skills. I owe a special debt of gratitude to Dr. Elizabeth Schultz for the all possible help for my Ph.D. program and valuable comments for my thesis.

I am grateful to Dr. Denis Gaudet, Dr. James Thomas and Dr. Stewart Rood for serving in my committee and providing encouragement and valuable suggestions for my doctoral program.

This project was funded through a Genomics Research and Development Initiative grant and I am grateful to Alberta Innovates Graduate Student Scholarship. I also acknowledge the SGS Dean's Scholarship and the International Tuition Award I received.

Candid thanks to all my lab mates: Dr. Ravinder Goyal, Dr. Daria Ryabova, Dianeveys González-Peña Fundora, Reyhaneh Pordel, Daniel Gaudet, Connor West and Marshall Smith for their help and support in the lab. Thank you Dianeveys for your emotional support.

A special thanks to Dr. Gopal Subramaniam and his lab (AAFC-Ottawa) for the *in vitro* and *in planta* DON analyses, Dr. Harpinder Randhawa (AAFC-Lethbridge) for providing Tenacious, Awesome and Penhold wheat cultivars, Dianeveys for the pictures of *Fusarium graminearum* spores and Michelle Frick, Michelle Cradduck, Dr. Sankar Pahari, Dr. Gaganpreet Dhariwal, Dr. Raman Dhariwal, Kimberly Burton-Hughes, Dr.

Fengying Jiang and Dr. Mohamed Hafez for their technical advice. My sincere thanks to the greenhouse staff at AAFC-Lethbridge for their assistance.

Thank you to Dr. Abdul Shukkoor, Dr. Aneesa and Irfan for helping me during my initial days in Canada.

My sincere gratitude to my family: my mother Fathema, father Ummer and my uncle Abdulla for their tireless efforts to educate me, and my father-in-law Omar and mother-in-law Zahra for motivating me. No words of mine would be adequate to express my indebtedness to my beloved wife Noor, and my children Mishael and Omar for standing with me with patience while passing this long journey.

Table of Contents

Abstract	iii
Acknowledgements	iv
List of Tables	xi
List of Figures	xii
List of Abbreviations	xviii
Chapter 1: Literature review	1
1.1 Introduction	1
1.2 <i>Fusarium graminearum</i>	2
1.2.1 <i>F. graminearum</i> life cycle	3
1.3 FHB symptoms and signs.....	4
1.4 A brief history of FHB in North America with emphasis on Western Canada.....	6
1.5 Trichothecenes	7
1.6 Impact of trichothecenes and FHB.....	9
1.7 FHB resistance mechanisms	11
1.8 Aggressiveness factors in <i>F. graminearum</i>	12
1.9 Potential aggressiveness factors from the <i>F. graminearum</i> secretome.....	15
1.10 Cerato-platanin proteins	16
1.11 CFEM domain-containing proteins.....	22
1.12 An elongation factor protein from the <i>F. graminearum</i> secretome	25
1.13 Conclusion and thesis objectives	26

Chapter 2: Overexpression of a cerato-platanin-encoding gene leads to a small increase in <i>Fusarium graminearum</i> aggressiveness	28
2.1 Introduction	28
2.2 Materials and Methods	31
2.2.1 <i>F. graminearum</i> strain and growth parameters	31
2.2.2 Bioinformatic analyses of FgCPP1	32
2.2.3 Generation of <i>FgCPPI</i> disruption and overexpression transformants.....	32
2.2.3.1 Generation of <i>FgCPPI</i> disruption and overexpression constructs	32
2.2.3.2 Electroporation of pRF-HU2:: <i>Δcpp1</i> and pRF-HU2E:: <i>CPPI-OX</i> constructs into <i>Agrobacterium tumefaciens</i>	37
2.2.3.3 <i>A. tumefaciens</i> -mediated transformation of <i>F. graminearum</i>	37
2.2.3.4 Verification of <i>Δcpp1</i> and <i>CPPI-OX</i> transformants	38
2.2.4 Mycelial growth and macroconidia germination assays	40
2.2.5 Sensitivity to cell wall stress agents and cell wall degrading enzymes.....	41
2.2.6 Plant infection assays on wheat spikes by spray and point inoculations	42
2.2.7 Fungal biomass estimation in wheat spikes	43
2.2.8 Cellophane penetration experiment.....	44
2.2.9 DON production in axenic culture	44
2.2.10 DON production <i>in planta</i>	46
2.2.11 <i>TRI</i> gene expression <i>in planta</i>	46
2.2.12 Statistical analyses.....	47

2.3 Results	47
2.3.1 Bioinformatic analyses of FgCPP1	47
2.3.2 Targeted deletion and <i>in locus</i> overexpression of <i>FgCPP1</i> in <i>F. graminearum</i>	48
2.3.3 <i>FgCPP1</i> disruption or overexpression has no effect on general fitness of <i>F.</i> <i>graminearum</i>	51
2.3.4 <i>FgCPP1</i> is not likely involved in <i>F. graminearum</i> cell wall protection.....	52
2.3.5 <i>FgCPP1</i> overexpression leads to increase in initial infection, but no effect on disease spread.....	53
2.3.6 <i>FgCPP1</i> seems to have no role in cell wall penetration	56
2.3.7 <i>FgCPP1</i> overexpression increases DON production in axenic culture	57
2.3.8 <i>FgCPP1</i> disruption or overexpression likely affects DON production during interaction with host.....	58
2.4 Discussion	60
Chapter 3: Roles of two secreted CFEM domain-containing proteins in growth and aggressiveness of <i>Fusarium graminearum</i>	67
3.1 Introduction.....	67
3.2 Materials and Methods.....	69
3.2.1 Bioinformatic analyses of FgCFEM1 and FgCFEM2.....	69
3.2.2 Generation of disruption and overexpression transformants of <i>FgCFEM1</i> and <i>FgCFEM2</i>	70
3.2.3 Verification of <i>FgCFEM1</i> and <i>FgCFEM2</i> transformants.....	70

3.2.4 <i>In vitro</i> characterization and plant infection assays	72
3.2.5 Statistical analyses.....	73
3.3 Results	73
3.3.1 Bioinformatic analyses of FgCFEM1 and FgCFEM2.....	73
3.3.2 Targeted disruption and <i>in locus</i> overexpression of <i>FgCFEM1</i> or <i>FgCFEM2</i> in <i>F. graminearum</i>	75
3.3.3 Neither <i>FgCFEM1</i> nor <i>FgCFEM2</i> seems to have a major influence on fungal fitness	77
3.3.4 Disruption or overexpression of <i>FgCFEM1</i> or <i>FgCFEM2</i> does not affect stress tolerance in <i>F. graminearum</i>	78
3.3.5 <i>FgCFEM1</i> or <i>FgCFEM2</i> overexpression affects DON production by <i>F.</i> <i>graminearum</i> in axenic cultures	80
3.3.6 Neither <i>FgCFEM1</i> nor <i>FgCFEM2</i> is involved in cell wall penetration.....	80
3.3.7 <i>FgCFEM1</i> overexpression leads to increased disease spread	81
3.4 Discussion	83
Chapter 4: Expression of the elongation factor 1A gene under the strong constitutive <i>GPDA</i> promoter affects fungal fitness, DON production and aggressiveness in <i>Fusarium graminearum</i>	
4.1 Introduction	89
4.2 Materials and Methods.....	93
4.2.1 Generation of <i>FgEF1A</i> overexpression transformants.....	93

4.2.2 Verification of <i>FgEF1A</i> overexpression transformants	94
4.2.3 <i>In vitro</i> characterization of <i>GPDA:EF1A</i> transformants	96
4.2.4 Infection assays on wheat spikes by spray and point inoculations	96
4.2.5 Identification of FgEF1A amino acid sequences for peptide synthesis	96
4.2.6 Eliciting activities of FgEF1A peptides	97
4.2.6.1 Callose induction in Arabidopsis	97
4.2.6.2 β -1,3-glucanase assay in wheat seedlings	98
4.2.7 Statistical analyses.....	99
4.3 Results	100
4.3.1 <i>FgEF1A in locus</i> expression from a <i>glyceraldehyde-3-phosphate</i> <i>dehydrogenase</i> overexpression promoter resulted in a limited increase in transcript levels	100
4.3.2 <i>GPDA:EF1A</i> transformants exhibit reduced fitness.....	102
4.3.3 DON production is greatly affected in <i>GPDA:EF1A-C1</i> transformant.....	103
4.3.4 <i>GPDA:EF1A</i> transformants are compromised in their ability to cause disease in wheat spikes	104
4.3.5 FgEF1A peptides do not elicit plant immune responses	107
4.4 Discussion	109
Chapter 5: Summary of findings and future directions.....	116
Bibliography	122

List of Tables

Table 1.1: Variation in functional groups of major Type A and Type B trichothecenes in <i>Fusarium</i> species. OAc = <i>O</i> -acetyl, OIsoval = <i>O</i> -isovalerate. The table was modified from Foroud et al. (2019).	9
Table 1.2: <i>Fusarium graminearum</i> disruption mutants with reduced aggressiveness.....	14
Table 2.1: Primers used for various experiments in this chapter	65
Table 2.2: Major resistance mechanisms of wheat cultivars used in this study.....	66
Table 3.1: Primers used for various experiments in this chapter	87
Table 4.1: Primers used for various experiments in this chapter	115

List of Figures

Figure 1.1: The life cycle of <i>F. graminearum</i> . Images are not drawn to scale.	3
Figure 1.2: (a) Perithecia on carrot agar medium; (b) Perithecia releasing ascospores; (c) Enlarged ascospores; (d) <i>F. graminearum</i> on potato dextrose agar (PDA) medium; (e) Macroconidia; (f) A single enlarged macroconidium; (g) A healthy wheat spike; (h) An FHB-infected spike; (i) Spikelets and rachis of a spike.	5
Figure 1.3: Trichothecene backbone structure. The drawing was prepared in ChemDraw 19.0 and adapted from Foroud et al. (2019).	9
Figure 1.4: Alignment of amino acid sequences of fungal CPPs (without signal peptide) known to elicit immune response in plants. The alignment includes CPPs from <i>C. platani</i> , <i>B. cinerea</i> , <i>S. sclerotiorum</i> , <i>F. graminearum</i> , <i>Magnaporthe grisea</i> , <i>V. dahliae</i> , <i>F. graminearum</i> , <i>Trichoderma virens</i> and <i>T. atroviride</i> in the order shown in the alignment. The conserved regions corresponding to two peptide motifs, PepA and PepB proved to be essential for the eliciting activity of BcSpl1 are highlighted in yellow. Four conserved cysteine residues are highlighted in cyan. The cysteine residues on two peptide motives form a disulfide bond connecting the two motives. CPPs contain conserved aspartate residue (highlighted in grey), which might be essential for the expansin-like activity of fungal CPPs, when they occur alone or in combination with other residues. The alignment was created using the Clustal Omega Multiple Sequence Alignment software from EMBL-EBL.	21
Figure 2.1: Preparation of (a) <i>FgCPPI</i> disruption (pRF-HU2:: <i>Δcppl</i>) and (b) overexpression (pRF-HU2E:: <i>CPPI-OX</i>) constructs. Part I. pRF-HU2 and pRF-HU2E were both digested with PacI and NtBbvCI to generate two fragments with sticky ends from each vector. Part II. Inserts were prepared by two rounds of PCRs; <i>FgCPPI</i> gene, its upstream and downstream regions were amplified by first round of PCR, and adaptors containing deoxy-uridine base at both ends of the amplicons were attached by a second round of PCR. Part III. USER cloning of upstream and downstream amplicons into digested pRF-HU2 or upstream and gene into digested pRF-HU2E. GoI stands for gene of interest. Drawings were adapted from Frandsen et al. 2008.	36
Figure 2.2: Strategy used for disruption (left) and overexpression (right) of <i>FgCPPI</i> in <i>F. graminearum</i> (Frandsen et al., 2008). Transformants were developed by a double crossover event between the construct and WT.	38
Figure 2.3: Schematic representation of (a) annealing sites of the primers used for verification of successful cross over in <i>Δcppl</i> and <i>CPPI-OX</i> , and (b) restriction sites and probe binding positions in WT, <i>Δcppl</i> and <i>CPPI-OX</i> transformants for Southern blotting.	40
Figure 2.4: Phylogenetic analysis of CPPs from a group of ascomycete fungi. The Neighbor-Joining phylogenetic tree was constructed with the bootstrap method (500 replicates) using MEGA-X software.	48

Figure 2.5: Verification of *Δcppi1* and *CPPI-OX* transformants. (a) Amplification using primers that bind outside the homologous recombination sites were used for verification of crossover at desired sites in the genome of the transformants. (b) Southern blot showing a single band of 2479 bp for WT and 1582 bp for *Δcppi1* and *CPPI-OX* transformants indicating single copy integration of *FgCPPI* disruption and overexpression construct in *Δcppi1* and *CPPI-OX*, respectively. (c) *FgCPPI* expression in *Δcppi1* and *CPPI-OX* compared to WT as determined by RT-qPCR. *F. graminearum* β -*TUBULIN* gene was used for normalization. Bars represent standard error from three replicates, each performed in triplicate. Asterisk indicates statistically significant difference compared with the WT ($p < 0.05$). (d) *FgCPP2* expression in *Δcppi1* and *CPPI-OX* compared to WT as determined by RT-qPCR. *F. graminearum* β -*TUBULIN* gene was used for normalization. Bars represent standard error from three replicates, each performed in triplicate.50

Figure 2.6: (a) Percentage germination of macroconidia of *FgCPPI* transformants and WT on water agar after 6 and 9 h incubation at 27°C. Bars represent standard error from two independent experiments, each with five replicates. (b) Radial mycelial growth of *FgCPPI* transformants and WT over 4 days of growth on PDA at 27°C. Bars represent standard error from five replicates.51

Figure 2.7: Sensitivity of *FgCPPI* transformants to chemicals targeting fungal cell wall/membranes. (a) Mycelial growth from different macroconidia dilutions of *FgCPPI* transformants and WT on PDA containing cell wall/membrane stress agents. SDS= sodium dodecyl sulfate, CFW= calcofluor white and CR= congo red. Images were taken after 40 h of growth at 25°C. Images are representative of two independent experiments, each with three replicates. (b) Macroconidia of *FgCPPI* transformants and WT germinating in YMA containing cell wall degrading enzyme, Glucanex. Images were taken after 14 h of incubation at 28°C. Scale bar = 200 μ m. Images are representative of two independent experiments, each with three replicates.53

Figure 2.8: Disease severity of *FgCPPI* transformants on wheat. (a) Percentage of diseased spikelets of susceptible wheat cultivar Roblin, moderately susceptible Penhold and moderately resistant Awesome 3, 6, 9 and 18 days after spray inoculation with *Δcppi1*, *CPPI-OX* or WT. Bars represent standard error from three independent experiments, each with five replicates (b) Number of diseased spikelets of Roblin, Penhold and resistant wheat cultivar Tenacious 7, 12 and 18 days after point inoculation with *Δcppi1*, *CPPI-OX* or WT. Bars represent standard error from three independent experiments, each with five replicates (c) Quantity of *Δcppi1*, *CPPI-OX* or WT in spikes of Penhold 3 days after spray inoculation as determined by qPCR. Bars represent standard error from three replicates, each performed in triplicate. Asterisks indicate statistically significant difference compared with the WT ($p < 0.05$).56

Figure 2.9: Cellophane penetration experiment. Before: *FgCPPI* transformants and WT grown on cellophane sheet placed over minimal medium for 4 days at 28°C in dark. After: The cellophane sheets were removed and the plates were incubated

- at 28°C for 2 days allowing penetrated hyphae to grow from the medium. Images are representative of two independent experiments, each with five replicates.....57
- Figure 2.10: DON production by *FgCPP1* transformants or WT in axenic cultures under DON-inducing conditions. Bars represent standard error from six replicates. Asterisk indicates statistically significant difference compared with the WT ($p < 0.05$).58
- Figure 2.11: DON production by *FgCPP1* transformants or WT during interaction with wheat spikes. (a) DON production in spray inoculated Penhold spikes at 1, 2 and 3 dpi with *FgCPP1* transformants or WT. Bars represent standard error from three replicates. (b) DON production in point inoculated Penhold spikelets at 1, 2 and 3 dpi with *FgCPP1* transformants or WT. Bars represent standard error from three replicates. (c) Expression of *TRI5* and *TRI6* by *FgCPP1* transformants compared to WT 3 days after spray inoculation of Penhold spikes. *F. graminearum* β -*TUBULIN* and *EF1A* genes were used for normalization. Bars represent standard error from three replicates, each performed in triplicate. Asterisks indicate statistically significant difference compared with the WT ($p < 0.05$).59
- Figure 3.1: Schematics showing annealing position of primer pairs used for the verification of crossover in (a) *FgCFEM1* and (b) *FgCFEM2* transformants, and restriction enzyme cutting sites and probe binding positions in (c) WT, $\Delta cfem1$ and *CFEM1-OX* and (d) WT, $\Delta cfem2$ and *CFEM2-OX* for Southern blotting.....72
- Figure 3.2: **(a)** Phylogenetic analysis of CFEM proteins from ascomycetes and saccharomycetes. The Neighbor-Joining phylogenetic tree was constructed with the bootstrap method (500 replicates) using MEGA-X software. **(b)** Multiple sequence alignment of CFEM domains of FGSG_02077 and FGSG_08554 along with four other putatively secreted *F. graminearum* CFEM proteins. The alignment was created using the Clustal Omega Multiple Sequence Alignment software from EMBL-EBI. Eight highly conserved cysteine residues of CFEM domains are highlighted in cyan.75
- Figure 3.3: Verification of *FgCFEM1* and *FgCFEM2* disruption and overexpression transformants. (a) Amplification using primers that bind outside the homologous recombination sites was performed for verification of cross over at desired sites in the genome of the transformants. (b) Southern blot showing a single band of 4201 bp for WT and 5021 bp for $\Delta cfem1$ and *CFEM1-OX* indicating single copy integration of *FgCFEM1* disruption and overexpression construct in $\Delta cfem1$ and *CFEM1-OX*, respectively. A single band of 4546 bp for WT and 3516 bp for $\Delta cfem2$ and *CFEM2-OX* transformants indicates single copy integration of *FgCFEM2* disruption and overexpression construct in $\Delta cfem2$ and *CFEM2-OX*, respectively. (c) Transcript levels of *FgCFEM1* and *FgCFEM2* in the transformants compared to the WT estimated by RT-qPCR. *F. graminearum* β -*TUBULIN* was used for normalization. Bars represent standard error from three replicates, each performed in triplicate. Asterisks indicate statistically significant difference compared with the WT ($p < 0.05$).76

- Figure 3.4: (a) Percentage of macroconidia germination in *FgCFEM1* and *FgCFEM2* transformants and the WT after 6 and 9 h of incubation on water agar at 27°C. Bars represent standard error from two independent experiments, each with five replicates. Asterisk indicates statistically significant difference compared with the WT at $p < 0.05$. (b) Radial mycelial growth of *FgCFEM1* and *FgCFEM2* transformants as well as the WT over 4 days of growth on PDA at 27°C. Bars represent standard error from five replicates.77
- Figure 3.5: Stress tolerance of *FgCFEM1* and *FgCFEM2* transformants. (a) Mycelial growth following inoculation with different macroconidia dilutions of *FgCFEM1* and *FgCFEM2* transformants and the WT on PDA containing various stress agents. Images were taken after 40 h of growth at 25°C. Images are representative of two independent experiments, each with three replicates. (b) Germination of macroconidia of *FgCFEM1* and *FgCFEM2* transformants and the WT in YMA containing the cell wall degrading enzyme, Glucanex. Images were taken after 14 h of incubation at 28°C. Scale bar = 200 μ m. Images are representative of two independent experiments, each with three replicates.....79
- Figure 3.6: Amount of DON produced by *FgCFEM1* and *FgCFEM2* transformants as well as the WT in axenic culture. Bars represent standard error from six replicates. Asterisks indicate statistically significant difference compared with the WT at $p < 0.05$80
- Figure 3.7: Cellophane penetration experiment. Before: *FgCFEM1* and *FgCFEM2* transformants and WT grown on cellophane sheet placed over minimal medium for 4 days at 28°C in dark. After: The cellophane sheets were removed, and the plates were returned to the incubator for 2 more days allowing penetrated hyphae to grow through the medium. Images are representative of two independent experiments, each with five replicates.81
- Figure 3.8: Disease severity of *FgCFEM1* and *FgCFEM2* transformants following point or spray inoculation on susceptible (Roblin), moderately susceptible (Penhold), moderately resistant (Awesome) and resistant (Tenacious) wheat cultivars. (a) Number of diseased spikelets of Roblin, Penhold and Tenacious at 7, 12 and 18 days after point inoculation with the transformants or WT. Bars represent standard error from three independent experiments, each with five replicates. Asterisks indicate statistically significant difference compared with the WT ($p < 0.05$). (b) Percentage of diseased spikelets of Roblin, Penhold and Awesome at 3, 6, 9 and 18 days after spray inoculation with the transformants or WT. Bars represent standard error from three independent experiments, each with five replicates. Asterisks indicate statistically significant difference compared with the WT ($p < 0.05$).82
- Figure 4.1: Role of EF1A in eukaryotic translation elongation. EF1A when bound to GTP transports aminoacyl-tRNA (aa-tRNA) to the A-site of ribosome. Codon-anticodon pairing stimulates the GTPase activity of EF1A leading to the hydrolysis of GTP and the release of aa-tRNA to the A-site of ribosome. The GDP bound to EF1A is exchanged for GTP by a guanidine nucleotide exchange factor (GEF), which in higher eukaryotes consists of three subunits, EF1B, EF1D

- and EF1G. The EF1A-GTP is now ready to participate in another round of elongation. The drawing was adapted from Li et al., 2013.....93
- Figure 4.2: Schematics showing (a) annealing sites of the primers used for verification of successful crossover during the integration of the expression cassette for *GPDA:EF1A* transformants, and (b) restriction enzyme cutting sites and probe binding sites in WT and *GPDA:EF1A* transformants for Southern blotting.95
- Figure 4.3: Alignment of FgEF1A sequence with elf18 (a), EFa50 (b & c) or Arabidopsis EF1A (d). The amino acid sequence used for peptide synthesis are indicated as P1 (a), P2 (b), P3 (c) and P4 (d).....97
- Figure 4.4: Verification of *GPDA:EF1A* transformants. (a) Amplification using primers that bind outside the homologous recombination sites was performed for verification of cross over at desired sites in the genome of the transformants. (b) Amplification of *hph* from *GPDA:EF1A* transformants. (c) Southern blot showing a single band of 2492 bp for WT and 1215 bp for *GPDA:EF1A* transformants indicating single copy integration of *FgEF1A* overexpression construct in *GPDA:EF1A* transformants. (d) Transcript levels of *FgEF1A* in *GPDA:EF1A* transformants compared to the WT estimated by RT-qPCR. *F. graminearum* β -*TUBULIN* was used for normalization. Bars represent standard error from three replicates, each performed in triplicate. Asterisks indicate statistically significant difference compared with the WT ($p < 0.05$).101
- Figure 4.5: (a) Percentage macroconidia germination of WT and *GPDA:EF1A* transformants after 6 and 9 h of incubation on water agar at 27°C. Bars represent standard error from two independent experiments, each with five replicates. Asterisks indicate statistically significant difference compared with the WT ($p < 0.05$). (b) Radial mycelial growth of WT and *GPDA:EF1A* transformants over 5 days of growth on PDA at 27°C. Bars represent standard error from five replicates. Asterisks indicate statistically significant difference compared with the WT ($p < 0.05$).103
- Figure 4.6: Amount of DON produced by *GPDA:EF1A-C1* transformant and the WT in axenic culture. Bars represent standard error from six replicates. Asterisks indicate statistically significant difference compared with the WT ($p < 0.05$).....104
- Figure 4.7: Disease severity of *GPDA:EF1A* transformants following spray or point inoculation on susceptible (Roblin), moderately susceptible (Penhold), moderately resistant (Awesome) and resistant (Tenacious) wheat cultivars. (a) Percentage of diseased spikelets of Roblin, Penhold, Awesome and Tenacious at 7, 12, and 18 days after spray inoculation with *GPDA:EF1A-C1* or WT. Bars represent standard error from three independent experiments, each with five replicates. Asterisks indicate statistically significant difference compared with the WT ($p < 0.05$). (b) Number of diseased spikelets of Roblin, Penhold, Awesome and Tenacious at 7, 12 and 18 days after point inoculation with *GPDA:EF1A-C1* or WT. Bars represent standard error from three independent experiments, each with five replicates. Asterisks indicate statistically significant difference compared with the WT ($p < 0.05$). (c) Number of diseased spikelets of Roblin at 7, 12 and 18 days after point inoculation with *GPDA:EF1A-C1*, *GPDA:EF1A-C2*,

GPDA:EF1A-C3, *GPDA:EF1A-C4* or WT. Bars represent standard error from three independent experiments, each with five replicates. Asterisks indicate statistically significant difference compared with the WT ($p < 0.05$). (d) FHB disease symptoms in Roblin, Penhold, Awesome and Tenacious at 18 days after spray inoculation with WT or *GPDA:EF1A-C1* and (e) in Roblin, Penhold, Awesome and Tenacious at 18 days after point inoculation with WT or *GPDA:EF1A-C1*. 107

Figure 4.8: Eliciting activities of FgEF1A peptides. (a) Arabidopsis seedlings were treated with 1 μ M each of P1, P2, P3 and P4 for 24 h, stained with 0.01% aniline blue in 150 mM K_2HPO_4 for 2 h and observed for callose under a microscope using DAPI filter. Treatments with 1 μ M flg22 and water served as positive and negative controls, respectively. Images are representative of two independent experiments. (b) β -1,3-glucanase activity in 10-day-old Roblin seedlings at 12, 24 and 48 h after spraying with 1 μ M each of P1, P2, P3, P4, flg22 or water. Bars represent standard error from two independent experiments, each with three replicates per treatment per time point. Asterisk indicates statistically significant difference compared with the WT ($p < 0.05$). 108

List of Abbreviations

aa-tRNA	aminoacyl-tRNA
ANOVA	Analysis of variance
ATA	Alimentary toxic aleukia
Cas9	CRISPR-associated protein 9
CDK	cyclin-dependent kinase
CFEM	Common in fungal extracellular membrane
CFW	Calcofluor white
CMC	Carboxymethylcellulose
CPPs	Cerato-platanin proteins
CR	Congo red
CRISPR	Clustered regularly interspaced short palindromic repeats
DNS	3,5-dinitrosalicylic acid
DON	Deoxynivalenol
EF1A	Elongation factor 1A
EFR	Elongation factor receptor
EF-Tu	Elongation factor-thermo unstable
ETI	Effector-triggered immunity
FDK	Fusarium damaged kernels
FHB	Fusarium head blight
GDP	Guanosine diphosphate
GEF	Guanidine nucleotide exchange factor
GFP	Green fluorescent protein
GPCR	G-protein-coupled receptor
GPDA	Glyceraldehyde-3-phosphate dehydrogenase
GPI	Glycosylphosphatidylinositol
GTP	Guanosine triphosphate
GUS	β glucuronidase
HAT	histone acetyltransferase
HDAC	histone deacetylase
hph	Hygromycin phosphotransferase
LB	Luria-Bertani

LSD	Least significant difference
miRNAs	miRNA-like RNAs
miRNAs	microRNAs
mRNA	messenger RNA
MS	Murashige and Skoog
NIV	Nivalenol
PAMPs	Pathogen-associated molecular patterns
PDA	Potato dextrose agar
PRRs	Pattern recognition receptors
PTI	PAMP-triggered immunity
qPCR	quantitative PCR
ROS	Reactive oxygen species
RT-qPCR	Reverse transcription-quantitative PCR
SDS	Sodium dodecyl sulfate
SNAREs	Soluble N-ethylmaleimide-sensitive factor attachment protein receptors
tRNA	transfer RNA
USER	Uracil-specific excision reagent
WT	Wild-type
YMA	Yeast mannitol agar

Chapter 1: Literature review

1.1 Introduction

Canada is a leading producer of premium quality wheat (*Triticum aestivum*). In 2019, Canada produced 32.3 million tonnes of wheat, of which 10.3 million tonnes came from Alberta (<https://www150.statcan.gc.ca/n1/daily-quotidien/191206/dq191206b-eng.htm>). Canada is one of the world's leading wheat exporters; in 2018, Canada exported \$ 5.4 billion (USD) worth of wheat amounting to 14.1% of total international wheat exports worldwide (<http://www.worldstopexports.com/wheat-exports-country/>). One of the major threats to maintain/improve this production level and grain quality is the fungal disease Fusarium head blight (FHB). FHB is a problem, not only in wheat, but also in other cereals including barley (*Hordeum vulgare*), oats (*Avena sativa*) and corn (*Zea mays*) (Goswami and Kistler, 2004). While multiple *Fusarium* species can be associated with FHB, *Fusarium graminearum* is the primary causal agent in North America (Goswami and Kistler, 2004). The pathogen not only causes yield losses, but also contaminates grains with trichothecene mycotoxins produced by the fungus. Deoxynivalenol (DON) is the major trichothecene produced by *F. graminearum* in North America (Goswami and Kistler, 2004; Trail, 2009). In this chapter, I will review biology and genetics of *F. graminearum*, economic losses due to FHB and DON, and impact of DON on human and animal health. This chapter will also describe several aggressiveness factors identified in *F. graminearum*. Finally, the role of cysteine-rich proteins in plant-fungal interactions and the importance of studying cysteine-rich proteins from *F. graminearum* secretome will also be discussed.

1.2 *Fusarium graminearum*

The *Fusarium* genera belongs to Kingdom Fungi, Phylum Ascomycota, Subphylum Pezizomycotina, Class Sordariomycetes, Order Hypocreales, Family Nectriaceae (Goswami and Kistler, 2004). As an ascomycete, *F. graminearum* has both sexual and asexual stages, referred to as the teleomorph and anamorph, respectively. Its teleomorphic name is *Gibberella zeae*, whereas *F. graminearum* is the anamorphic name.

The genome of *F. graminearum* PH-1 strain has been completely sequenced. It contains 36.6 Mb, assembled into four chromosomes (King et al., 2015). The fungus is haploid for most of its life cycle. Formation of hyphae containing binucleate cells (dikaryotic phase) is the initial step in sexual development. The binucleate cells develop into fruiting body initials which further develop into flask-shaped perithecia containing asci. Asci are tubular sacs containing ascospores (sexual spores) that are formed as a result of meiosis (Trail and Common, 2000). *F. graminearum* does not require a sexually distinct partner to produce ascospores. This is known as homothallism and is due to the presence of both mating types (MAT1-1 and MAT1-2) in the haploid genome (Yun et al., 2000).

F. graminearum is the primary *Fusarium* species in North America which causes FHB in cereals (Goswami and Kistler, 2004). Other *Fusarium* species such as *F. culmorum*, *F. avenaceum*, *F. pseudograminearum* and *F. poae* are also associated with FHB. Variations in the prevalence of species have been observed depending on the temperature of the cultivating regions. For instance, *F. graminearum* is mainly associated with wheat grown in warmer areas such as North America and China, whereas *F.*

culmorum prefers cooler regions such as Northern Europe (Desjardins, 2006). For the purpose of this review, I will focus my discussion on *F. graminearum*.

1.2.1 *F. graminearum* life cycle

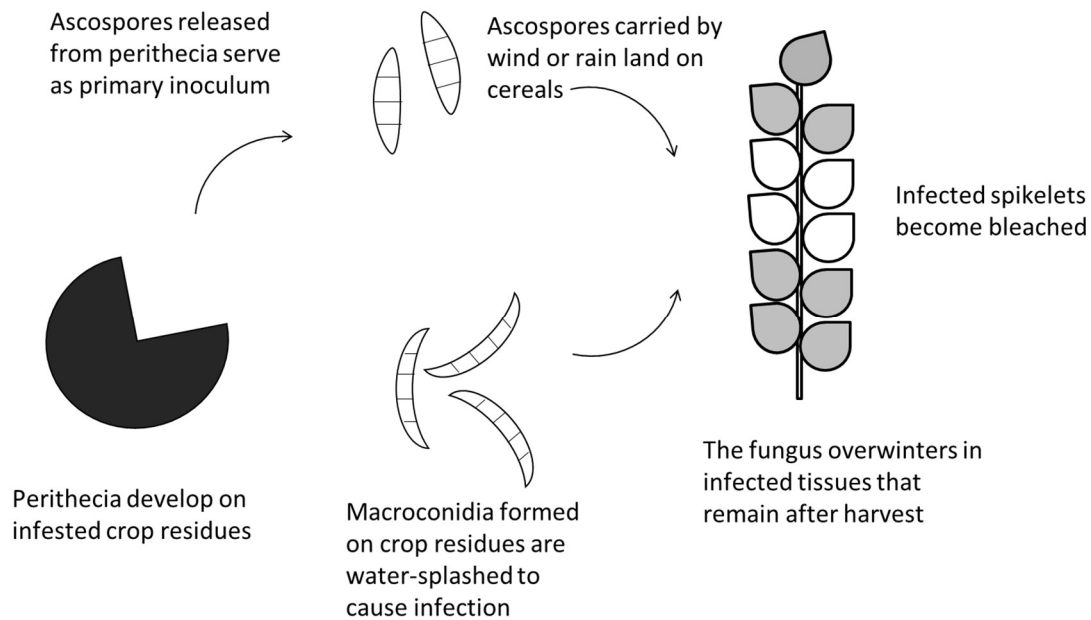


Figure 1.1: The life cycle of *F. graminearum*. Images are not drawn to scale.

F. graminearum can overwinter saprophytically in crop residues, grasses and in the soil. The fungus produces perithecia (Figure 1.2 a) on the infested crop residues. Ascospores (Figure 1.2 b & c) released from perithecia act as primary inoculum for the disease (Trail et al., 2002). The ascospores are carried by the wind and when they land on susceptible cereals, they can start new infections. The infection can also be caused by asexual spores, called macroconidia, formed on crop residues (Figure 1.2 e & f). When the host plant dies or is removed by harvest, the fungus produces survival structures, such as perithecia, on the infested crop residues (Trail, 2009) (Figure 1.1).

1.3 FHB symptoms and signs

In wheat, each spike (also called head) is composed of many spikelets located on alternate sides of the spike's stem, which is called a rachis (Figure 1.2 i). *F. graminearum* gains access to host plants through natural openings such as stomata (Bushnell et al., 2003) or by penetrating host epidermal cell walls using DON producing short infection hyphae, lobate appressorium and infection cushions (Boenisch and Schäfer, 2011). FHB causes premature bleaching of infected spikelets (Figure 1.2 h). The fungus spreads from diseased spikelets to the rachis resulting in dark brown discoloration of the rachis. Over time, the remaining spikelets also become infected leading to premature bleaching of the whole spike. Under moist conditions, the fungus produces light pink or salmon-coloured sporodochia on the infected rachis and/or the spikelets. Sporodochia are a compact mass of hyphae that bear conidiophores on which macroconidia are produced. As disease progresses, the fungus colonizes the developing grain leading to shrivelled and wrinkled kernels (Schmale III and Bergstrom, 2003); these are called Fusarium damaged kernels (FDK). Even though FHB is favoured by wet and warm weather at anthesis, infection can occur at any stage from anthesis to kernel filling if the favourable conditions persist. Infection during anthesis can either completely affect kernel development or result in FDK (Schaafsma et al., 2001). FDK are lighter compared to healthy grains and are largely responsible for the yield losses associated with FHB.

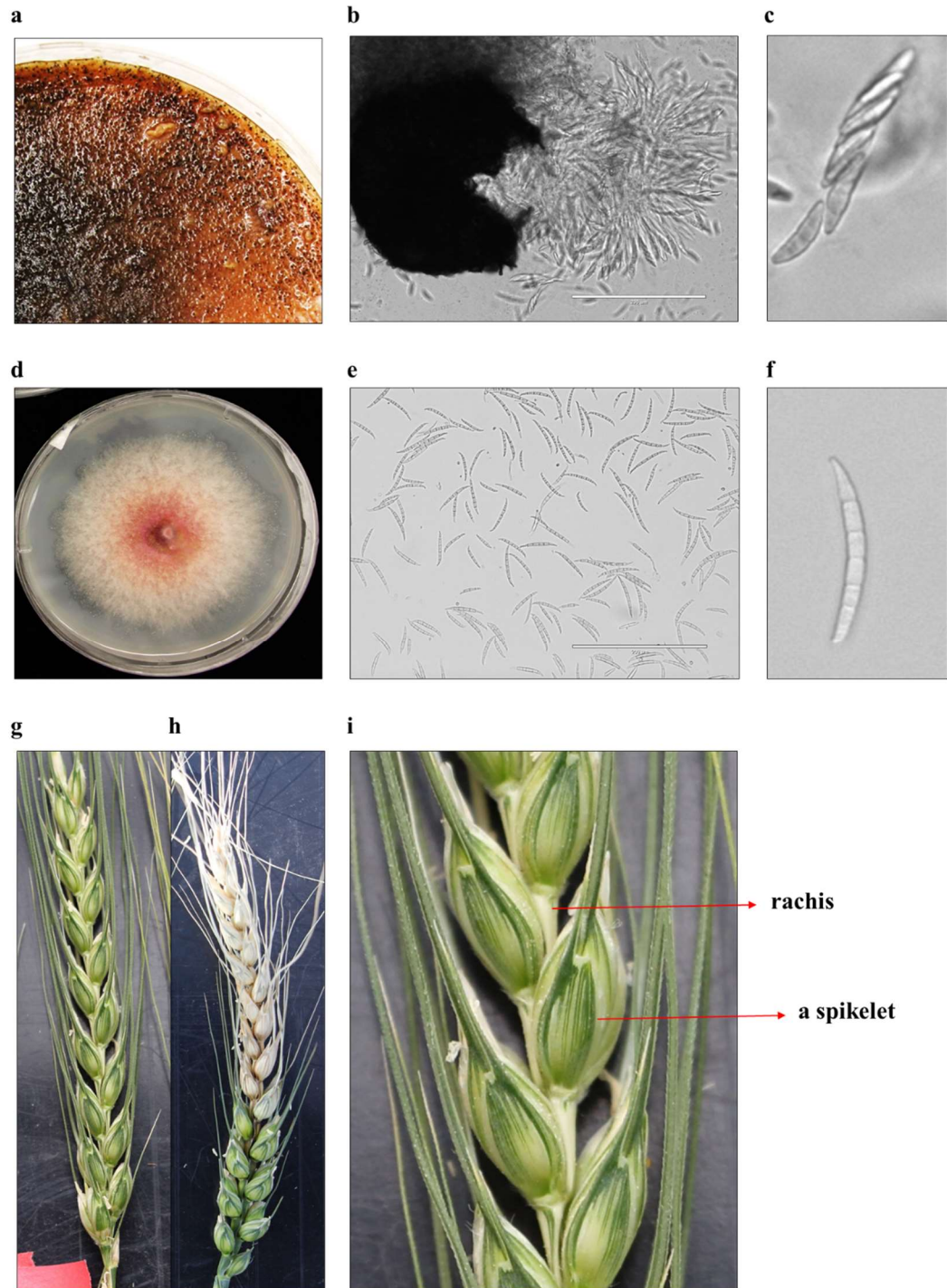


Figure 1.2: (a) Perithecia on carrot agar medium; (b) Perithecia releasing ascospores; (c) Enlarged ascospores; (d) *F. graminearum* on potato dextrose agar (PDA) medium; (e) Macroconidia; (f) A single enlarged macroconidium; (g) A healthy wheat spike; (h) An FHB-infected spike; (i) Spikelets and rachis of a spike.

1.4 A brief history of FHB in North America with emphasis on Western Canada

FHB was first described in 1884 in England, where it was called wheat scab (Stack, 2003). While the disease occurred in Eastern Canada and United States for many years, no major outbreaks were reported until 1984 (<https://www.grainscanada.gc.ca/en/grain-research/scientific-reports/fhb-western/fhb-1.html>), when wheat samples from a field in the Southern Manitoba were reported to contain FDK and considerable levels of DON (Clear and Abramson, 1986). One year later, more FHB-affected wheat samples were identified from the same field, as well as in nearby fields (Abramson et al., 1987).

From 1991-1996, damaging levels of FHB were reported across the US, especially in the Midwest and Manitoba (reviewed in McMullen et al., 1997). The year 1993 witnessed the most severe FHB outbreak in North America, which resulted in an estimated \$ 1 billion (USD) loss (Busch, 1994). This epidemic hit Minnesota, South Dakota, North Dakota and Manitoba which produce hard red spring wheat, durum wheat and spring barley (McMullen et al., 1997). The 1993 outbreak was mainly attributed to wet weather due to unusually heavy rainfall since precipitation during flowering to grain development are conducive to infection (McMullen et al., 1997). In 1993, Minnesota, South Dakota and North Dakota received some of the highest rainfalls in the month of July, when spring-planted cereals in these regions reach anthesis and kernel development stages (Enz, 1995). The same year, Manitoba also received above normal levels of rainfall throughout the growing season (Gilbert et al., 1994). The coincidence of long moist weather with anthesis and grain filling stages of wheat and barley favoured disease outbreak in these areas in 1993 (McMullen et al., 1997).

FHB continued to be a problem in western Canada. During 1998, 75% of cereals in Manitoba were planted 2-3 weeks earlier than usual leading to early crop heading in mid-June to early July, at which time, the eastern and central regions of Manitoba received heavy rainfall, resulting in increased FHB levels. In the same year, regions of Western Manitoba and Eastern Saskatchewan also experienced frequent and heavy precipitation during June, July, and August leading to higher FHB levels (Tekauz et al., 2000).

There has been a change in the distribution of *F. graminearum* over the prairies. In 1994, the pathogen was mainly restricted to Manitoba and Eastern Saskatchewan; however, by 2002, it reached Alberta. Since then, *F. graminearum* has been isolated from infected crops in Southern Alberta. Since 2013, it has also been isolated from areas of Alberta outside of southern Alberta, showing that *F. graminearum* is now distributed all over the province. While only nine counties in Alberta reported *F. graminearum* in 2001, 26 counties reported the presence of this pathogen in 2016 (<https://www.alberta.ca/fusarium-head-blight-overview.aspx>).

1.5 Trichothecenes

Trichothecenes are sesquiterpenoid secondary metabolites produced by fungi from different genera including *Fusarium* (Grove, 2007). Trichothecenes are composed of three fused rings consisting of a cyclohexene ring fused to a tetrahydropyran ring and a cyclopentyl moiety attached to the tetrahydropyran ring through C₂ and C₅. The structure also contains an epoxide functionality at C₁₂, which is known to be essential for its toxicity (reviewed in: Desjardins et al., 1993; Foroud et al., 2019) (Figure 1.3). Four types of trichothecenes have been reported from different trichothecene-producing fungi. Type

A and B vary in their functional groups at positions C₃, C₄, C₇, C₈ and C₁₅ (Table 1.1). Type C trichothecenes possess an additional epoxide at C_{7,8}, whereas type D contains a macrocyclic ring between C₄ and C₁₅. Type C and D are non-*Fusarium* trichothecenes that are not associated with FHB (Bata et al., 1985; Ueno, 1985) and will not be further discussed here. Among Type A trichothecenes produced by *Fusarium* sp., those with highest economic importance includes T-2 toxin and HT-2 toxin and are mainly produced by *F. langsethiae* and *F. sporotrichioides* (reviewed in Foroud et al., 2019). Type B trichothecenes are generally more prevalent in FHB infected heads, and these include nivalenol (NIV), 4-deoxynivalenol (DON) and their derivatives (4-*O*-acetyl-NIV, 3-*O*-acetyl-DON and 15-*O*-acetyl-DON). Of the FHB causing species, *F. graminearum* and *F. culmorum* are the main producers of Type B trichothecenes (reviewed in Foroud and Eudes, 2009), and DON is the most widespread mycotoxin identified in cereal grains.

Historically, 15-ADON producing strains of *F. graminearum* were more abundant in North America (Mirocha et al., 1989; Miller et al., 1991). Since its introduction during 1990s, the 3-ADON strains has been increasing in Canada and the United states (Ward et al., 2008). Emergent 15-ADON producing strains with genetic similarities to 3-ADON chemotypes have also been identified in North America (Ward et al., 2008). Both 3-ADON and emergent 15-ADON strains were reported to accumulate higher levels of DON and to be more aggressive in wheat than the traditional 15-ADON strains (Ward et al., 2008; Puri and Zhong, 2010; Foroud et al., 2012). It is not known whether the increased aggressiveness is due to their ability to accumulate more DON. However, comparison of genomes of 15-ADON and 3-ADON strains revealed some genetic

variation which is believed to contribute to their differences in aggressiveness (Walkowiak et al., 2015; Walkowiak et al., 2016).

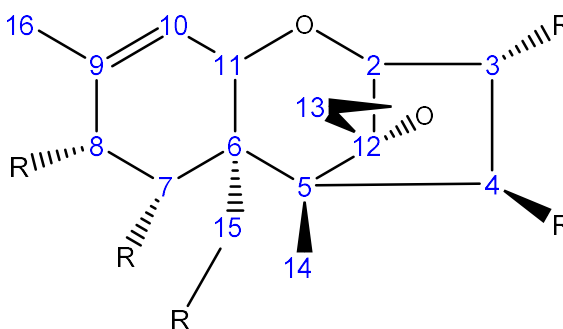


Figure 1.3: Trichothecene backbone structure. The drawing was prepared in ChemDraw 19.0 and adapted from Foroud et al. (2019).

Table 1.1: Variation in functional groups of major Type A and Type B trichothecenes in *Fusarium* species. OAc = *O*-acetyl, OIsoval = *O*-isovalerate. The table was modified from Foroud et al. (2019).

Trichothecenes	C ₃	C ₄	C ₇	C ₈	C ₁₅
T-2 toxin	-OH	-OAc	-H	-OIsoval	-OAc
HT-2 toxin	-OH	-OH	-H	-OIsoval	-OAc
Nivalenol (NIV)	-OH	-OH	-OH	=O	-OH
4- <i>O</i> -acetyl-NIV (4ANIV)	-OH	-OAc	-OH	=O	-OH
4-deoxynivalenol (DON)	-OH	-H	-OH	=O	-OH
3- <i>O</i> -acetyl-DON (3-ADON)	-OAc	-H	-OH	=O	-OH
15- <i>O</i> -acetyl-DON (15-ADON)	-OH	-H	-OH	=O	-OAc

1.6 Impact of trichothecenes and FHB

FHB is a devastating cereal disease which causes huge economic losses. The combined activity of fungal proliferation and trichothecene mycotoxin production in infected grains results in shrivelled and lightweight kernels (FDK) leading to yield and quality losses. Contamination of grains with toxic levels of trichothecenes causes further downgrading of grains which negatively impacts grain exporting and processing

(McMullen et al., 1997). Economic losses due to FHB outbreaks during 1990s were estimated at around \$ 520 million and 2.5 billion (USD) for Canadian and American wheat growers, respectively (Windels, 2000).

In addition to economic losses, trichothecenes also pose serious health risks. Trichothecenes can bind to 60S ribosomes where it inhibits protein synthesis in eukaryotes (Ueno, 1977; Garreau de Loubresse et al., 2014). In addition to the protein synthesis inhibitory action, other trichothecenes-induced cellular toxicities such as oxidative stress-mediated DNA damage, cell cycle arrest and membrane structure alteration have also been reported (reviewed in Arunachalam and Doohan, 2013). Consumption of Type A trichothecene-contaminated grains can cause a condition in humans called alimentary toxic aleukia (ATA) which is initially manifested by intestinal irritation, vomiting and diarrhoea, followed by aleukia and anemia. ATA was reported to have killed at least 100,000 people in Russia in 1940s due to accidental consumption of T2-toxin contaminated grains (Mayer, 1953; Yagen and Joffe, 1976). DON, probably the most common contaminant of grains and grain products (Sobrova et al., 2010) is less toxic to mammals compared to T-2 toxin. However, DON is a potent inducer of vomiting and is also referred to as ‘vomitoxin’ (Rotter et al., 1996) and DON poisoning can lead to emesis, anorexia, reduced feed intake and weight loss in animals, growth retardation, gastroenteritis and adverse effects on immune function and reproduction (Pinton et al., 2008; Pestka, 2010; Pinton et al., 2010). Since DON is stable at high temperatures, standard cooking processes cannot degrade this mycotoxin (Scott, 1984).

Regulations are in place to ensure that DON levels in food stuffs do not exceed the maximum allowable quantities. In Canada, maximum tolerable levels for DON in

food products are established by Health Canada and are enforced by the Canadian Food Inspection Agency. As of January 2018, maximum allowable DON level in uncleaned soft wheat for use in staple foods is 2 ppm and that in soft wheat for use in baby foods is 1 ppm; however, these limits are under review (<https://www.canada.ca/en/health-canada/services/food-nutrition/food-safety/chemical-contaminants/maximum-levels-chemical-contaminants-foods.html>).

1.7 FHB resistance mechanisms

Two types of immunity have been identified in plants against pathogens; pathogen-associated molecular pattern-triggered immunity (PTI) and effector-triggered immunity (ETI). The former is activated when plasma membrane-localized pattern recognition receptors (PRRs) of plants recognize conserved molecular signatures of pathogens called pathogen-associated molecular patterns (PAMPs). Some well-studied PAMPs include bacterial flagellin, elongation factor-thermo unstable (EF-Tu) and fungal chitin (Boller and Felix, 2009). The PRR for flagellin in *Arabidopsis thaliana* (common name, Arabidopsis) is the flagellin sensing 2 (FLS2) receptor which perceives a 22-amino acid flagellin epitope, flg22 (Chinchilla et al., 2006). The EF-Tu receptor EFR in *Arabidopsis* recognizes an N-acetylated elf18 epitope (Zipfel et al., 2006). A chitin elicitor receptor kinase 1 (AtCERK1) serves as the PRR in *Arabidopsis* for chitin oligomers (Miya et al., 2007; Wan et al., 2008), whereas chitin elicitor binding protein (CEBiP) functions in coordination with OsCERK1 to activate PTI in *Oryza sativa* (common name, rice) (Kaku et al., 2006; Shimizu et al., 2010). PTI is a race-nonspecific resistance and is active against all kinds of pathogens (Jones and Dangl, 2006; Boller and Felix, 2009). ETI is a race-specific immunity which is elicited when a specific pathogen

effector is recognized directly or indirectly by a cognate host receptor (Jones and Dangl, 2006). Resistance due to ETI is qualitative and involves gene-for gene interaction leading to discrete phenotypes—either resistant or susceptible (Flor, 1971). In contrast, a quantitative plant-pathogen interaction gives rise to a continuous distribution of disease phenotypes from resistant to susceptible (Poland et al., 2009; St.Clair, 2010).

FHB resistance is quantitative in nature and is due to the additive effect of several genes (Poland et al., 2009; St.Clair, 2010). Of the various types of resistance reported in cereals, resistance to initial infection (Type I) and resistance to fungal spread from an infected spikelet (Type II) are the best documented (Schroeder and Christensen, 1963). Other forms of resistance such as low rate of kernel infection (Type III) (Mesterházy, 2003), tolerance to FHB and trichothecenes (Type IV) (Wang and Miller, 1988), and resistance to trichothecene accumulation (Type V) (Miller et al., 1985) have also been described.

1.8 Aggressiveness factors in *F. graminearum*

The terms pathogenicity, aggressiveness and virulence are sometimes used interchangeably, but they have specific meanings with respect to pathogen-host interactions. I will be using these terminologies according to Vanderplank (1968) and D'Arcy et al. (2001). Pathogenicity indicates the ability of a pathogen to infect a host, whereas aggressiveness is a quantitative measure of pathogenicity. Virulence refers to the ability of a pathogen to cause disease in a specific host genotype and relates to gene-for-gene interactions.

Over the last two decades, a series of aggressiveness factors have been identified in *F. graminearum*. DON, a trichothecene mycotoxin produced by *F. graminearum*, is an

important and well-characterized aggressiveness factor in this pathogen. The importance of DON in FHB disease was first shown by Proctor et al. (1995) who demonstrated that a trichodiene synthase (*TRI5*) disruption mutant was less aggressive in wheat. *TRI5* catalyzes the first committed step in the trichothecene biosynthesis pathway (Hohn and Beremand, 1989). Several studies using DON non-synthesising strains showed that in the absence of DON, the pathogen is unable to move from the inoculated spikelet(s) into the wheat rachis to cause disease spread (Bai et al., 2002; Langevin et al., 2004; Jansen et al., 2005; Maier et al., 2006; Cuzick et al., 2008). It was shown that this restriction in movement is a result of cell wall thickenings in the wheat rachis node, a defense response which is inhibited by trichothecenes (Jansen et al., 2005). However, the absence of DON did not influence disease spread in barley due to its inherent resistance to disease spread (Jansen et al., 2005; Maier et al., 2006). Thus, trichothecenes are not necessary for initial infection in wheat, but are required for the spread of the fungus in the rachis.

Apart from DON, numerous other aggressiveness factors have also been identified in *F. graminearum* (Table 1.2). They include, but are not limited to, genes related to G-protein signaling, metabolism, cell wall synthesis, cell membrane formation, vesicle trafficking and membrane fusion. Several protein kinases and phosphatases, transcription factors, GTPases, phospholipases, NADPH oxidases and a secreted lipase are also important for *F. graminearum* aggressiveness.

Table 1.2: *Fusarium graminearum* disruption mutants with reduced aggressiveness

Category	Gene (s) disrupted	Reference
GPCR	<i>GIV1</i> to <i>GIV5</i>	(Jiang et al., 2019)
	<i>FGRRES_07792</i> , <i>16536</i> , <i>16221</i> , <i>02155</i> , <i>07839</i>	(Dilks et al., 2019)
	<i>STE2</i>	(Sridhar et al., 2020)
G protein	G α subunit (<i>GzGPA2</i>) ^c , G β subunit (<i>GzGPB1</i>) ^{b c}	(Yu et al., 2008)
cAMP-dependent signaling	Adenylate cyclase (<i>FAC1</i>) ^{a c} , cAMP-dependent protein kinase A (<i>CPK1</i>) ^{a c}	(Hu et al., 2014)
Phospholipases	Phospholipase C (<i>FgPLC1</i>) ^{a c}	(Zhu et al., 2016)
	Phospholipase D (<i>FgPLD1</i>) ^{a c}	(Ding et al., 2017)
Protein kinases	<i>MGV1</i> ^{a c}	(Hou et al., 2002)
	<i>GPMK1</i> ^c	(Jenczmionka et al., 2003)
	Hog1 pathway genes (<i>SSK2-PBS2-HOG1</i>) ^{a c}	(Zheng et al., 2012)
	<i>FgSCH9</i> ^{a c}	(Chen et al., 2014)
	<i>GIL1</i> ^c	(Yu et al., 2017)
Protein phosphatases	<i>FgPTC1</i>	(Jiang et al., 2010)
	<i>FgPTC3</i> ^{a c}	(Jiang et al., 2011)
	<i>FgTEP1</i>	(Zhang et al., 2010)
Transcription factors	<i>FgTFM1</i> ^{a c}	(Liu et al., 2019a)
	<i>ZIF1</i> ^a	(Wang et al., 2011)
	<i>FgCRZ1A</i> ^{a c}	(Chen et al., 2019a)
	<i>FgMCM1</i> ^{a c}	(Yang et al., 2015)
	<i>FgSTE12</i>	(Gu et al., 2015)
	<i>MYT3</i> ^{a c}	(Kim et al., 2014)
	<i>TRI6</i> ^{a d} , <i>TRI10</i> ^{a d}	(Seong et al., 2009)
Regulators of gene expression	HATs (<i>FgSAS3</i>) ^{a c} , (<i>FgGCN5</i>) ^{a c}	(Kong et al., 2018)
	HAT (<i>FgEAF6</i>) ^c	(Qin et al., 2019)
	HDAC (<i>FTL1</i>) ^c	(Ding et al., 2009)
	HDAC (<i>HDF1</i>) ^{a c}	(Li et al., 2011)
	CDK (<i>FgSSN3</i>) ^{a c}	(Cao et al., 2016)
	Topoisomerase (<i>FgTOP1</i>) ^c	(Baldwin et al., 2010)
GTPases	<i>RAS2</i> ^c	(Bluhm et al., 2007)
	<i>FgRAB51</i> ^{a c} , <i>FgRAB52</i> ^{a c} , <i>FgRAB6</i> ^c , <i>FgRAB7</i> ^{a c} , <i>FgRAB8</i> ^{a c} , <i>FgRAB11DN</i> ^c , <i>FgRAB2</i> ^{b c} , <i>FgRAB4</i> ^{b c} , <i>FgYPTA</i> ^b , <i>FgRABX</i> ^{b c} , <i>FgRAB11CA</i> ^c	(Zheng et al., 2015)
GEF	<i>FgMON1</i> ^{a c}	(Li et al., 2015)
SNAREs	<i>FgVAM7</i> ^{a c}	(Zhang et al., 2016b)
	<i>FgPEP12</i> ^{a c}	(Li et al., 2019a)
	<i>FgSYN8</i> ^{a c}	(Adnan et al., 2019a)
	<i>FgSEC22</i> ^{a c}	(Adnan et al., 2019b)
Trichothecene biosynthesis	<i>GzSYN1</i> ^c , <i>GzSYN2</i>	(Hong et al., 2010)
	<i>TRI5</i> ^a	(Proctor et al., 1995) (Bai et al., 2002)
Catalase	<i>KatG2</i>	(Guo et al., 2019)
NADPH oxidases	<i>NoxA</i>	(Wang et al., 2014)
	Regulatory subunit of <i>NoxA</i> and <i>NoxB</i> (<i>FgNoxR</i>) ^c	(Zhang et al., 2016a)
ABC transporter	<i>FgABCC9</i> ^{a c}	(Qi et al., 2018)
Related to cell wall synthesis	Chitin synthase (<i>FgCHS8</i>) ^{a c}	(Zhang et al., 2016d)
	Chitin synthase (<i>GzCHS5</i> & <i>GzCHS7</i>) ^c	(Kim et al., 2009)
	Cell wall mannoprotein (<i>FgCWM1</i>) ^c	(Zhang et al., 2019)
Cell membrane components	<i>MES1</i> ^c	(Rittenour and Harris, 2008)
	Sphingolipid C-9 methyltransferase (<i>FgMT2</i>) ^c	(Ramamoorthy et al., 2009)

Category	Gene (s) disrupted	Reference
Plant Cell wall degrading enzyme	Xylanase (<i>XylA</i>)	(Tini et al., 2019)
Plant defence compound degrading enzyme	Tomatinase-like enzyme (<i>FgTOM1</i>)	(Carere et al., 2017)
Related to metabolism	Lactate dehydrogenases <i>FgLDHL1</i> ^c & <i>FgLDHL2</i> ^c	(Chen et al., 2019b)
	Threonine deaminase (<i>FgILV1</i>) ^{a c}	(Liu et al., 2015)
	Dihydroxyacid dehydratase (<i>FgILV3A</i>) ^{a c}	(Liu et al., 2019c)
	Hexokinase (<i>FgHXK1</i>) ^{a c}	(Zhang et al., 2016c)
	Linoleic acid isomerase (<i>FgLA12</i>) ^{a c}	(Zhang et al., 2017a)
	Thioredoxin reductase <i>FgTRR</i> ^{a c}	(Fan et al., 2019)
	Acetylglutamate synthase (<i>ARG2</i>) ^c	(Kim et al., 2007)
	Phosphoribosylamine-glycine ligase (<i>ADE5</i>) ^c	
	Cystathionine beta-lyase (<i>CBL1</i>) ^c	(Seong et al., 2005)
	Methionine synthase (<i>MSY1</i>) ^c	
	Glutamine amidotransferase (<i>GzHIS7</i>) ^c	(Seo et al., 2007)
	Ornithine N5-oxygenase (<i>SID1</i>) ^c	(Greenshields et al., 2007)
Secreted lipase	<i>FGL1</i>	(Voigt et al., 2005)

HAT (histone acetyltransferase). HDAC (histone deacetylase). CDK (cyclin-dependent kinase). SNAREs (Soluble N-ethylmaleimide-sensitive factor attachment protein receptors). ^aGene disruption affected DON production. ^bGene disruption led to increased DON accumulation. ^cGene disruption affected fungal fitness. ^d*TRI6* and *TRI10* regulate expression of *TRI* genes involved in trichothecene biosynthesis.

1.9 Potential aggressiveness factors from the *F. graminearum* secretome

F. graminearum secretome consists of proteins and secondary metabolites. DON is an example of a secreted secondary metabolite whose role in *F. graminearum* aggressiveness has been well-documented. Another secondary metabolite important for aggressiveness is an extracellular siderophore triacetyl fusarinine C (TFC). Deletion of an *NPS6* gene required for the biosynthesis of TFC led to hypersensitivity to iron starvation and oxidative stress. Malonichrome is also an extracellular siderophore, but its absence alone does not affect aggressiveness (Oide et al., 2014). Paper et al. (2007) identified 289 proteins from the *F. graminearum* secretome. Of the secreted proteins, a lipase encoded by *FGL1* inhibits vascular callose depositions and facilitates colonization of wheat rachis (Blümke et al., 2014). Infection by *FGL1* disruption mutant was found to be restricted to the inoculated and adjacent spikelets (Voigt et al., 2005). While a multitude of aggressiveness factors have been studied in *F. graminearum*, most of the proteins in the secretome remain uncharacterized. A common characteristic of secreted proteins with

known roles in plant-fungal interaction is the presence of multiple cysteine residues (Van den Ackerveken et al., 1993; Luderer et al., 2002; Fudal et al., 2007; Bolton et al., 2008). These cysteine residues might form intramolecular disulfide bonds which is believed to be a mechanism to provide stability for these secreted proteins in the protease-rich environment of the host plant apoplast (Stergiopoulos and de Wit, 2009). The *F. graminearum* secretome is enriched with cysteine-rich proteins (Brown et al., 2012; Sperschneider et al., 2015); however, very little is known about the role of these proteins in aggressiveness. Among the secreted cysteine-rich proteins are cerato-platanins and common in fungal extracellular membrane (CFEM) domain-containing proteins. The orthologues of these cysteine-rich proteins are associated with aggressiveness in other fungal species, and in the following sections, I will review their role in fungal growth and plant infection. Literature reviews for cerato-platanins and CFEM proteins specific to *F. graminearum* are provided in the introduction section of chapter 2 and chapter 3, respectively. In addition to cysteine rich proteins, *F. graminearum* secretes other proteins that may or may not be involved in host plant infection, including the housekeeping gene elongation factor 1A (Rampitsch et al., 2013). While a role for this protein in *F. graminearum*-host interaction has not been reported, its bacterial homologue, elongation factor-thermo unstable (EF-Tu), is a well-characterized elicitor of immune responses in plants (Kunze et al., 2004; Furukawa et al., 2014).

1.10 Cerato-platanin proteins

Cerato-platanin proteins (CPPs) belong to a family of fungal proteins known as the cerato-platanin (CP) family. CPPs are produced by filamentous fungi with different lifestyles including pathogens, saprophytes and plant beneficial fungi. The name CP

comes from the pathogen where this family was originally identified: *Ceratocystis platani*, responsible for canker stain disease of European plane trees. Members of the CP family share certain characteristics: they possess N-terminal signal peptide sequences targeting secretory pathways; they are small (120-140 amino acids) with a single domain known as CP domain; they contain four conserved cysteine residues that have been shown to form two disulphide bridges; they exhibit moderate to strong hydrophobicity and no catalytic activity (Pazzagli et al., 1999).

CPPs possess structural similarities to expansins, and also exhibit expansin-like properties. In plants, expansins mediate cell wall extension in a non-catalytic manner and are implicated in various physiological and developmental processes which involve cell wall modifications (Sampedro and Cosgrove, 2005; Yennawar et al., 2006). Some members of the CP family possess expansin-like cellulose/cell wall weakening abilities (Barsottini et al., 2013; Baccelli et al., 2014; Quarantin et al., 2019). An aspartate residue (D77) was found to be crucial for the expansin and elicitor-like activities of *C. platani* CP as its mutation (D77A) affected these activities by this protein (Luti et al., 2017). The corresponding aspartate residue is conserved in different fungal CPPs (Luti et al., 2017) (Figure 1.4). Interestingly, mutations of a specific aspartate residue (D82) in the expansin, EXLX1 of *Bacillus subtilis*, also affected its cell wall loosening activity (Georgelis et al., 2011).

CPPs from a few fungi have been shown to possess chitin binding capabilities (Barsottini et al., 2013; Frischmann et al., 2013; Baccelli et al., 2014). The ability to bind chitin suggests possible localization of CPPs to the fungal cell wall, which is primarily composed of chitin and glucans. Accordingly, CPPs have been shown to be localized to

fungus cell walls (Boddi et al., 2004; Frias et al., 2014) where they may disrupt non-covalent interactions between fungus cell wall components, as hypothesized for expansins. It is likely that CPPs are involved in hyphal elongation, conidia germination and other developmental processes which require cell wall remodeling and enlargement. In fact, MpCP2 was found to promote germination of basidiospores in *Moniliophthora perniciosa* (Barsottini et al., 2013). Since they are localized in fungus cell walls, CPPs may also have a protective role for cell walls against degradation enzymes during interaction with plants. It has been shown that deletion of CPPs in *F. graminearum* and *Verticillium dahliae* resulted in hypersensitivity of the mutants to fungus cell wall degrading enzyme chitinase, compared with their wild-type counterparts (Quarantin et al., 2016; Zhang et al., 2017c).

CPPs have also been shown to bind chitin oligomers known as N-acetyl glucosamine (de Oliveira et al., 2011; Barsottini et al., 2013). Chitin oligomers are released from the fungus cell wall by the action of host-encoded chitinase enzymes during fungus-plant interactions, and the released chitin fragments are known to act as PAMPs which can trigger PTI responses in plants (Gao et al., 2019). CPPs in fungi may act as aggressiveness factors thanks to their ability to bind and scavenge chitin oligomers thereby preventing initiation of PTI responses by plants. Interestingly, MpCP5 of *M. perniciosa* has been shown to block defence responses in tobacco presumably by binding to chitin oligomers and preventing their perception by plant receptors (Barsottini et al., 2013). Different CPPs may have different roles in aggressiveness partly due to their varied affinity toward chitin oligomers.

CPPs of several fungal species elicit defence responses in plants (Scala et al., 2004; Djonovic et al., 2006; Seidl et al., 2006; Yang et al., 2009; Frias et al., 2011; Wang et al., 2016; Hong et al., 2017; Zhang et al., 2017c; Yang et al., 2018; Liu et al., 2019b; Quarantin et al., 2019). Two motifs required for the eliciting activity of BcSpl1 in *Botrytis cinerea* (Frias et al., 2014) are conserved in the CPPs of several fungal species (Figure 1.4). This agrees with previous reports that the sequence responsible for the eliciting activities in the microbial proteins are conserved in the corresponding protein families such as bacterial flagellin (Felix et al., 1999).

Consistent with the presence of a signal peptide for secretion, CPPs have been detected from the culture filtrates of several fungal species (Pazzagli et al., 1999; Wilson et al., 2002; Jeong et al., 2007; Frias et al., 2011; Rampitsch et al., 2013; Lu and Edwards, 2016; Yang et al., 2018). Notably, BcSpl1 secreted by *B. cinerea* is one of the most abundant proteins found in the secretome of this pathogen (Frias et al., 2011). These observations show that CPPs in these fungi are likely secreted outside the fungal cell during infection and could therefore play roles in plant infection.

CPPs of different fungi are expressed during *in vitro* growth (Djonovic et al., 2006; Yang et al., 2009; Frias et al., 2011; Baccelli et al., 2012; Barsottini et al., 2013; Frischmann et al., 2013; Quarantin et al., 2016; Zhang et al., 2017c; Pan et al., 2018), indicating a potential involvement of CPPs in fungal growth and development. Additionally, CPPs of some fungal species are also expressed during interaction with their host plants (Wilson et al., 2002; Frias et al., 2011; Quarantin et al., 2016; Wang et al., 2016; Zhang et al., 2017c; Pan et al., 2018; Liu et al., 2019b), which suggests that CPPs play a role in infection. Indeed, deletion of specific CPPs in some of these fungi

including, *B. cinerea*, *Sclerotinia sclerotiorum*, *V. dahliae* and *Fusarium oxysporum* f.sp. *cubense*, resulted in reduced aggressiveness (Frias et al., 2011; Zhang et al., 2017c; Yang et al., 2018; Liu et al., 2019b).

Despite their expression during growth or plant interaction, deletion of CPPs from several fungi did not alter their phenotype related to growth and development (Jeong et al., 2007; Frias et al., 2011; Frischmann et al., 2013; Quarantin et al., 2016; Zhang et al., 2017b; Yang et al., 2018) or aggressiveness (Wilson et al., 2002; Quarantin et al., 2016). The genomes of some fungal species have been reported to code for other expansin-like proteins (Bacelli, 2014). It is possible that gene redundancy due to other CPPs and overlapping functions with expansin-like proteins might be compensating for the deletion of specific CPPs in these fungi.

Since CPPs are most often detected in fungal secretomes, but also occur in the fungal cell walls, it is likely that CPPs may have a role in fungal development and/or during interaction with plant hosts. Some fungal CPPs are involved in plant infection as exemplified by the reduced aggressiveness of CPP deletion mutants. CPPs may contribute to plant infection by one or more of the following mechanisms: (a) expansin-like cellulose weakening, which may facilitate host colonization; (b) binding and sequestering of chitin oligomers, which prevents elicitation of host immunity; and/or (c) protection of fungal cell wall from host enzymes during infection, which may contribute to cell wall integrity. While CPPs elicit plant immunity responses, a receptor has not yet been identified for these proteins. It is also possible that CPPs are not directly recognized by plant receptors, rather the defense signaling is activated upon the perception of structural changes in the cell wall due to expansin-like activity of CPPs. The finding that the

mutation of the aspartate residue of *C. platani* CP affected its elicitor and expansin-like activities supports this hypothesis.



Figure 1.4: Alignment of amino acid sequences of fungal CPPs (without signal peptide) known to elicit immune response in plants. The alignment includes CPPs from *C. platani*, *B. cinerea*, *S. sclerotiorum*, *F. graminearum*, *Magnaporthe grisea*, *V. dahliae*, *F. graminearum*, *Trichoderma virens* and *T. atroviride* in the order shown in the alignment. The conserved regions corresponding to two peptide motifs, PepA and PepB proved to be essential for the eliciting activity of BcSpl1 are highlighted in yellow. Four conserved cysteine residues are highlighted in cyan. The cysteine residues on two peptide motives form a disulfide bond connecting the two motives. CPPs contain conserved aspartate residue (highlighted in grey), which might be essential for the expansin-like activity of fungal CPPs, when they occur alone or in combination with other residues. The alignment was created using the Clustal Omega Multiple Sequence Alignment software from EMBL-EBI.

1.11 CFEM domain-containing proteins

CFEM is a fungal-specific domain containing eight conserved cysteines commonly found in the extracellular membrane proteins of fungi. CFEM domains can occur in tandem in fungal membrane proteins, with at least one copy typically found at the N-terminus of the protein (Kulkarni et al., 2003). The number of CFEM-containing proteins vary greatly among fungi, from 1 in *Saccharomyces cerevisiae* to 20 in *M. grisea* (Zhang et al., 2015). The expansion of CFEM-containing proteins is likely due to gene duplication *via* recombination (Zhang et al., 2015). Domain duplication also is believed to have occurred in some fungal species giving rise to proteins carrying more than one CFEM domains (Zhang et al., 2015). For example, CSA1 protein from *Candida albicans*, a human fungal pathogen, possesses five CFEM domains. Even though both pathogenic and non-pathogenic fungi contain CFEM-containing proteins, more of them have been reported from pathogenic species (Zhang et al., 2015).

CFEM domain-containing proteins from different fungal pathogens have been studied to understand their potential role in host infection. Among human fungal pathogens, the best characterized CFEM-containing proteins are from *C. albicans*. Biofilm formation and iron acquisition from the host are linked to infection in this pathogen (Baillie and Douglas, 1999; Saville et al., 2003; Weissman and Kornitzer, 2004), and remarkably, CFEM-domain containing proteins play key roles in these processes. While CFEM protein encoding genes *RBT5*, *RBT51* and *CSA1* are involved in biofilm formation (Perez et al., 2006), single, double and triple deletions of these genes did not affect aggressiveness in *C. albicans* (Perez et al., 2011). Deletion of *RBT5* significantly reduced the ability of *C. albicans* to acquire iron from haemin and

haemoglobin; however, the deletion mutant showed similar aggressiveness as the WT (Weissman and Kornitzer, 2004). It cannot be completely dismissed that other CFEM proteins could compensate for the loss of the above-mentioned genes as there are at least five CFEM-containing proteins in *C. albicans* (PGA7, RBT5, RBT51, CSA1 and CSA2) (Ding et al., 2011).

The best studied CFEM-containing proteins in phytopathogenic fungi are from the rice blast pathogen, *M. grisea*. AC11 is a CFEM domain-containing glycosylphosphatidylinositol (GPI)-anchored protein in *M. grisea*. The *AC11* expression is upregulated under appressorium-inducing conditions (Kulkarni and Dean, 2004). *AC11* deletion mutant showed a significant but small delay in appressorium formation compared with the WT, although no difference was observed for aggressiveness in rice or barley. In addition, the mutant showed no differences for mycelial growth, conidiation, conidia germination, water wettability and salt tolerance (Deng and Dean, 2008).

PTH11 is a G-protein-coupled receptor (GPCR) from *M. grisea* with a CFEM domain and seven transmembrane helices. Deletion of the *PTH11* gene affected appressorium formation and aggressiveness of *M. grisea* (DeZwaan et al., 1999; Kou et al., 2017). Similarly, deletion of CFEM domain or C63A and C65A mutations within the CFEM domain of PTH11 led to delayed appressorium formation and reduced aggressiveness. These cysteine to alanine mutations likely disrupted intramolecular disulfide bonds in the CFEM domain, thereby affecting its function. These results show the importance of the CFEM domain and its conserved cysteine residues in appressorium development and aggressiveness in *M. grisea* (Kou et al., 2017). Meanwhile, *M. grisea* strain constitutively expressing CFEM domain of PTH11 formed precocious and

defective appressoria. It could be that constitutive expression of CFEM domain affects the surface characteristics of the germ tubes which differentiate to form appressorium (Kou et al., 2017).

Sabnam and Barman (2017) reported a PTH11-like CFEM-containing GPCR from *M. grisea* which they designated as WISH because it was found to be involved in Water wettability, Infection, Surface sensing and Hyper-conidiation in *M. grisea*. Like PTH11, WISH also possesses a transmembrane region with seven helices. The *M. grisea* mutants in which *WISH* is deleted were unable to infect rice due to defects in sensing inductive surfaces and appressorium differentiation. Loss of *WISH* caused a wettable phenotype and also led to excessive conidiation (Sabnam and Barman, 2017).

Three PTH11-like CFEM-containing GPCRs (FGRRES_16221, FGRRES_02155 and FGRRES_07839) are important for infection by *F. graminearum*. FGRRES_16221 promotes symptomless infection and its absence results in enhanced wheat defense responses which include rachis browning, increased expression of genes involved in chitinase and plant cell wall polysaccharide biosynthesis and in apoplastic and vascular occlusions (Dilks et al., 2019).

A CFEM-domain containing protein from *B. cinerea* (BcCFEM1) with a putative GPI anchor site was recently characterized (Zhu et al., 2017). Expression of *BcCFEM1* was much higher during early stages of infection on bean leaves compared to growth in culture medium, indicating a role of this protein during early stages of interaction with the host. Deletion of *BcCFEM1* caused reduced aggressiveness on bean leaves, however, the overexpression strain caused similar disease as the WT. The reduced aggressiveness of the *BcCFEM1* deletion mutant may be due to its increased sensitivity to plant-produced

reactive oxygen species (ROS), since the mutant exhibited hypersensitivity to H₂O₂ during *in vitro* studies (Zhu et al., 2017).

It appears that CFEM domain-containing proteins perform specific functions in fungi. Some of them are GPI anchored or are GPCRs with transmembrane helices and may function in fungal extracellular membranes, whereas others lack the GPI anchor or transmembrane helices and may be secreted outside the fungal cell (Kulkarni and Dean, 2004; Kulkarni et al., 2005; Lu and Edwards, 2016; Sabnam and Barman, 2017; Zhu et al., 2017). It also seems that the CFEM domain in each protein plays a unique role. For example, the CFEM domain of *CSAI* in *C. albicans* was unable to compensate for the deletion of CFEM domain of *PTH11* in *M. grisea* (Kou et al., 2017). This could be partly due to sequence variation that exists in the CFEM domain apart from the pattern of conserved cysteines in the domain (Kulkarni et al., 2003). Finally, CFEM domain-containing proteins are involved in host infection by fungal pathogens. While CFEM proteins in *C. albicans* are involved in biofilm formation and iron acquisition from the host, in *M. grisea*, they act in host surface sensing and penetration.

1.12 An elongation factor protein from the *F. graminearum* secretome

In bacteria, the EF-Tu protein involved in protein synthesis is a well-studied PAMP, having been shown to elicit plant immunity responses; two different EF-Tu epitopes, elf18 and EFa50, can activate defense responses in Arabidopsis and rice, respectively (Kunze et al., 2004; Furukawa et al., 2014). While fungal elongation factors have not been reported to elicit similar host responses, elongation factor 1A, the homologue of EF-Tu, was detected in the secretome of *F. graminearum* under mycotoxin- (DON-) inducing conditions *in vitro*. Moreover, the abundance of this protein

was decreased in the secretomes of two non-pathogenic mutants (*Δtri6* and *Δtri10*) compared to the WT secretome (Rampitsch et al., 2013). It is not known what role, if any, this protein may have in the *F. graminearum*-host interaction, but its secretion during conditions of pathogenicity suggests a potential role during infection.

1.13 Conclusion and thesis objectives

FHB is a devastating disease of cereals worldwide. *F. graminearum* is the most important species of *Fusarium* that causes FHB disease in North America. To facilitate infection, the pathogen secretes secondary metabolites and proteins into host plants. DON is an example of a secreted secondary metabolite and is a known aggressiveness factor in *F. graminearum*. While a series of aggressiveness factors have been identified and characterized in *F. graminearum*, most of the proteins found in the secretome of this pathogen are uncharacterized and their role in FHB disease is not yet clear. To date, the best characterized protein from the *F. graminearum* secretome is a lipase encoded by *FGL1*.

Rampitsch et al. (2013) compared the secretomes of wild-type *F. graminearum* and two of its DON-deficient non-pathogenic mutants (*ΔTri6* and *ΔTri10*). This comparative secretome analysis revealed that the abundance of 29 proteins were affected in the secretome of the mutants compared to that of the WT. These include a cerato-platanin protein (FGSG_10212), two CFEM-domain containing proteins (FGSG_02077 and FGSG_08554) and the elongation factor 1A protein (FGSG_08811). Their reduced abundance in the secretome of the non-pathogenic mutants suggests a role during infection for these proteins. Additionally, FGSG_10212, FGSG_02077 and FGSG_08554 genes were expressed during infection of wheat spikes by *F. graminearum*. FGSG_02077

and FGSG_08554 peptides were also detected in a minimal medium-based *in vitro* secretome of *F. graminearum* (Lu and Edwards, 2016), showing that they are potential candidate proteins involved in plant infection. Furthermore, as discussed in sections 1.10 and 1.11, cerato-platanin and CFEM proteins of other fungal species have been shown to participate in infection-related processes in their respective host species.

The major objective of this study was to characterize three cysteine-rich proteins (FGSG_10212, FGSG_02077 and FGSG_08554) and the elongation factor 1A protein (FGSG_08811) from the secretome of *F. graminearum*. As a first step, I developed gene disruption and overexpression transformants of these proteins. The roles of these proteins in fungal development and host plant infection were investigated as described in the following chapters. This study was aimed at gaining better insights into infection strategies used by *F. graminearum*, which is an important step towards the development of control strategies for FHB disease.

Chapter 2: Overexpression of a cerato-platanin-encoding gene leads to a small increase in *Fusarium graminearum* aggressiveness

2.1 Introduction

Fusarium graminearum is an ascomycete fungal pathogen primarily responsible for Fusarium head blight (FHB) disease of cereals in North America. The disease causes significant economic losses due to reduction in grain yield as well as contamination of grains with trichothecene mycotoxins (Goswami and Kistler, 2004). Deoxynivalenol (DON) is the major trichothecene mycotoxin produced by *F. graminearum* and has been implicated in the aggressiveness of this pathogen (Proctor et al., 1995; Bai et al., 2002). *F. graminearum* secretes cell wall degrading enzymes and the importance of pectinase, cellulase and xylanase in infection of wheat spikes has been previously demonstrated (Mary Wanjiru et al., 2002). *F. graminearum* also secretes small cysteine-rich non-catalytic proteins called cerato-platanin proteins (CPPs) (Rampitsch et al., 2013; Lu and Edwards, 2016).

CPPs show structural similarities with expansin proteins (de Oliveira et al., 2011) which consists of two domains: D1 domain containing a double $\phi\beta$ -barrel fold and D2 domain with a β -sandwich fold (Sampedro and Cosgrove, 2005). In plants, expansins mediate cell wall extension, and are involved in various physiological and developmental processes in which cell wall modifications occur (Sampedro and Cosgrove, 2005). Expansins also possess cellulose weakening properties; an expansin-like protein from *Aspergillus fumigatus* caused fragmentation of crystalline cellulose into smaller particles (Chen et al., 2010). The mechanism behind the cell wall/cellulose loosening activity of expansins is not yet understood, and like CPPs, no enzymatic activity has been reported

for expansins. It is believed that they break non-covalent interactions between cell wall polysaccharides which results in cell wall loosening (Yennawar et al., 2006).

CPPs possess a single domain known as the cerato-platanin domain, which forms a double $\phi\beta$ -barrel fold similar to the D1 domain in expansins (de Oliveira et al., 2011; Barsottini et al., 2013). Interestingly, some fungal CPPs possess cellulose/cell wall weakening ability similar to expansin proteins (Barsottini et al., 2013; Baccelli et al., 2014; Luti et al., 2017). Two *F. graminearum* CPPs, FgCPP1 and FgCPP2, were found to enhance the activity of a fungal cellulase (β -1,4-glucanase) on various cellulosic substrates such as carboxymethylcellulose (CMC), filter paper and wheat cell walls (Quarantin et al., 2019). Moreover, fungal CPPs, and at least one bacterial expansin EXLX1, carry a conserved aspartate residue. Substitution of this aspartate residue in EXLX1 (D82) to alanine or asparagine eliminated the wall loosening activity of EXLX1 in *Bacillus subtilis* showing that this residue is essential for the cell wall loosening capabilities of this protein (Georgelis et al., 2011). Similarly, a D77A in the CP of *Ceratocystis platani* affected expansin-like activities in this fungus (Luti et al., 2017). Given these similarities between CPPs and expansins, it can be hypothesized that some fungal CPPs can act as expansin proteins during interaction with plant hosts by loosening the host cell wall and favouring increased cellulase activity to facilitate fungal colonization (Barsottini et al., 2013; Baccelli et al., 2014).

Several studies have shown that CPPs can bind chitin and N- acetylglucosamine oligomers (Barsottini et al., 2013; Frischmann et al., 2013; Baccelli et al., 2014) and its ability to bind chitin suggests possible localization of CPPs to the fungal cell wall (Boddi et al., 2004; Frias et al., 2014). Unlike other fungal CPPs and similar to expansins, two

CPPs from *F. graminearum*, FgCPP1 and FgCPP2, were found to bind cellulose and not chitin in a carbohydrate binding assay (Quarantin et al., 2019). Apart from their presence in the fungal cell wall, CPPs have also been detected in the culture filtrates of several fungal species (Pazzagli et al., 1999; Wilson et al., 2002; Jeong et al., 2007; Frias et al., 2011; Rampitsch et al., 2013; Lu and Edwards, 2016; Yang et al., 2018), indicating that they are likely secreted outside the fungal cell with potential roles in plant infection. In congruence with this observation, CPPs contain signal peptides, which also suggests that they may be secreted proteins. Moreover, genes encoding CPPs are upregulated in some fungal species during infection of their host plants. This suggests that CPPs in these fungi are involved in plant infection. Indeed, deletion of CPP-encoding genes in these fungi resulted in reduced aggressiveness (reviewed in section 1.10).

The genome of *F. graminearum* codes for two CPPs (FGSG_10212 and FGSG_11205) (Lu and Edwards, 2016). These two CPPs (FgCPPs) were recently characterized by Quarantin et al. (2016), in their analysis of single and double *FgCPP* knockout mutants (*Δfgcpp1* and *ΔΔfgcpp1,2*, respectively). While neither *Δfgcpp1* nor *ΔΔfgcpp1,2* showed altered aggressiveness in point inoculated wheat spikes (Quarantin et al., 2016), their involvement in plant infection cannot be completely ruled out. A previous proteomic study had shown that these two proteins are secreted during wheat spike infection (Paper et al., 2007), and transcriptomic analysis showed that FGSG_10212 (described herein as *FgCPPI*) expression is significantly upregulated in the early stages of wheat spike infection (Quarantin et al., 2016). In addition, the abundance of FgCPP1 was reduced in the secretomes of two non-pathogenic mutants of GZ3639 compared to the secretome of the WT (Rampitsch et al., 2013), suggesting a role for *FgCPPI* in host

plant infection. In order to better understand the function of *FgCPP1*, I developed *FgCPP1* disruption (*Δcpp1*) and overexpression (*CPP1-OX*) transformants of *F. graminearum* and screened them for various growth and infection related phenotypes. In the *Δcpp1* mutant, the *FgCPP1* gene was replaced by an *hygromycin phosphotransferase* (*hph*) selection marker cassette. The *CPP1-OX* strain was designed for *in locus* overexpression using a strong constitutive *glyceraldehyde-3-phosphate dehydrogenase* (*GPDA*) promoter from *Aspergillus nidulans*, and also carries an *hph* selection marker cassette.

2.2 Materials and Methods

2.2.1 *F. graminearum* strain and growth parameters

F. graminearum strain GZ3639 was used throughout this study. To produce macroconidia, 100 mL of CMC (1.5% carboxymethylcellulose, 0.1% NH₄NO₃, 0.1% KH₂PO₄, 0.05% MgSO₄·7H₂O, 0.1% yeast extract) in 250 mL conical flask was inoculated with a plug of mycelia collected from the actively growing region on 90 mm petri plates containing potato dextrose agar (PDA). The flask was incubated on a rotary shaker (180 rpm) at 27°C for 5 days. Macroconidia were separated from mycelia by filtration through an autoclaved paper towel (WYPALL* catalog # 3540102) followed by three washes in sterile distilled water. Macroconidial concentration was determined using a haemocytometer and adjusted to working concentrations (defined below for each activity) in sterile distilled water.

2.2.2 Bioinformatic analyses of FgCPP1

To determine the evolutionary relationships of FgCPP1 with other characterized fungal CPPs, amino acid sequences of CPPs from ascomycete fungi were aligned by ClustalW and a phylogenetic tree was constructed by the Neighbor-Joining method using MEGA-X software. The presence of signal peptide and its cleavage site were predicted using SignalP 4.0 (Petersen et al., 2011). Protein domains were identified using SMART database (Letunic et al., 2015).

2.2.3 Generation of *FgCPP1* disruption and overexpression transformants

2.2.3.1 Generation of *FgCPP1* disruption and overexpression constructs

FgCPP1 disruption and overexpression constructs (pRF-HU2::*Δcpp1* and pRF-HU2E::*CPP1-OX*, respectively) were developed according to the method of Frandsen et al. (2008). Refer to Figure 2.1 for a schematic description of the steps involved; details are provided below, and all primer sequences are available in Table 2.1.

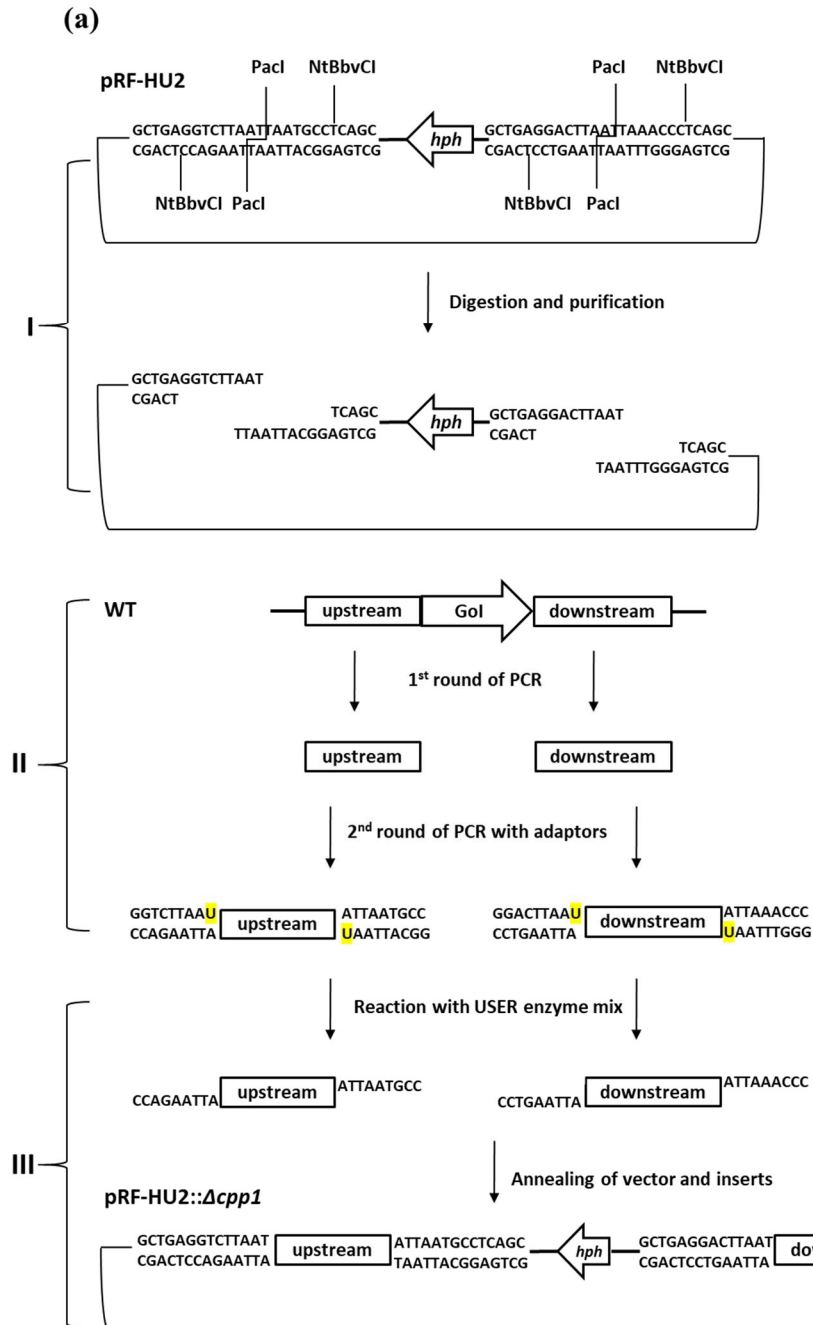
The vectors were prepared by digestion (Figure 2.1 a & b, part I) with PacI and Nt.BbvCI (both from NEW ENGLAND BioLabs® Inc.). The digestion reaction (100 µL) contained 5 µg of pRF-HU2/pRF-HU2E, 10 µL of 10X NE Buffer 4, 1 µL of 100X (10 mg ml⁻¹) BSA and 2.5 µL of PacI incubated at 37°C. After 16 h, 1 µL more of PacI and 2 µL of Nt.BbvCI were added and incubated at 37°C for 2 h. The two fragments resulting from each vector were gel purified using QIAquick® Gel Extraction Kit (Figure 2.1 a & b part I).

GZ3639 genomic DNA was isolated using QIAGEN's DNeasy Plant Mini Kit from 100 mg of mycelia harvested from potato dextrose broth. The inserts were prepared

by two rounds of polymerase chain reactions (PCRs) (Figure 2.1 a & b, part II). The first round of PCR was performed to amplify the initial 613 bp of *FgCPPI*, 843 bp upstream of its transcriptional start site and 822 bp of downstream region (primer pairs 1, 2 & 3, respectively, Table 2.1). A 10 μ L PCR reaction consisted of 2 μ L of 5X HF Phusion Buffer, 1.6 μ L of 1.25 mM dNTPs, 0.2 μ L each of 10 μ M forward and reverse primers, 0.1 μ L of 2 U μ L⁻¹ Phusion Hotstart II DNA polymerase (Thermo Scientific™) and 1 μ L of 25 ng μ L⁻¹ GZ3639 genomic DNA. PCR was carried out with an initial step of 98°C (30 s), followed by 35 cycles of 98°C (10 s), primer-specific annealing (see Table 2.1) (30 s), 72°C (90 s), and a final extension step of 72°C (10 min). This PCR product was isolated as a gel plug from 1% agarose gel with a sterile Pasteur pipet and diluted in 50 μ L Optima water (Thermo Scientific™) and used as the template for second PCR to incorporate adaptor sequences with a deoxy-uridine base at the 5' and 3' ends of the amplicons (primer pairs 4, 5 & 6 for *FgCPPI* gene, upstream and downstream, respectively). A 50 μ L reaction for this PCR consisted of 5 μ L of 10X PfuTurbo C_x Buffer, 8 μ L of 1.25 mM dNTPs, 1 μ L each of 10 μ M forward and reverse primers, 1 μ L of 2.5 U μ L⁻¹ PfuTurbo C_x Hotstart DNA polymerase (designed to overcome uracil sensitivity, Agilent Technologies) and 2.5 μ L of water from gel plug. Thermocycling conditions were as follows: an initial step of 95°C (2 min), followed by 30 cycles of 95°C (30 s), primer-specific annealing (see Table 2.1) (30 s), 72°C (60 s), and a final extension step of 72°C (10 min).

The amplicons from the second PCR were extracted from 1% agarose gels (QIAquick® Gel Extraction Kit) and cloned into the digested pRF-HU2/pRF-HU2E vector fragments using a USER (Uracil-specific excision reagent) enzyme mix (NEW

ENGLAND BioLabs® Inc.) (Figure 2.1 a & b part III). For each vector, the cloning reaction contained 250 ng each of two amplicons, 100 ng of digested vector fragments, 3 μ L of 10X PfuTurbo Buffer and 1 μ L of USER enzyme mix in 30 μ L reaction volume. The cloning reaction was transformed into DH5 α chemically competent cells (Thermo Scientific™) and plated on to Luria-Bertani (LB) plates containing 50 μ g mL⁻¹ kanamycin (LB Kan₅₀). Colony PCR was carried out using the same primers as used for preparation of the constructs (primer pairs 5 & 6 for pRF-HU2::*Acpp1* and 4 & 5 for pRF-HU2E::*CPPI-OX*) and a 10 μ L PCR reaction consisted of 5 μ L of 2X HotStarTaq Plus Master Mix (Qiagen), 1 μ L of 10X Coral Load and 0.2 μ L each of 10 μ M forward and reverse primers. Thermocycling conditions were as follows: an initial step of 95°C (15 min), followed by 35 cycles of 95°C (30 s), primer-specific annealing (see Table 2.1) (30 s), 72°C (60 s), and a final extension step of 72°C (10 min).



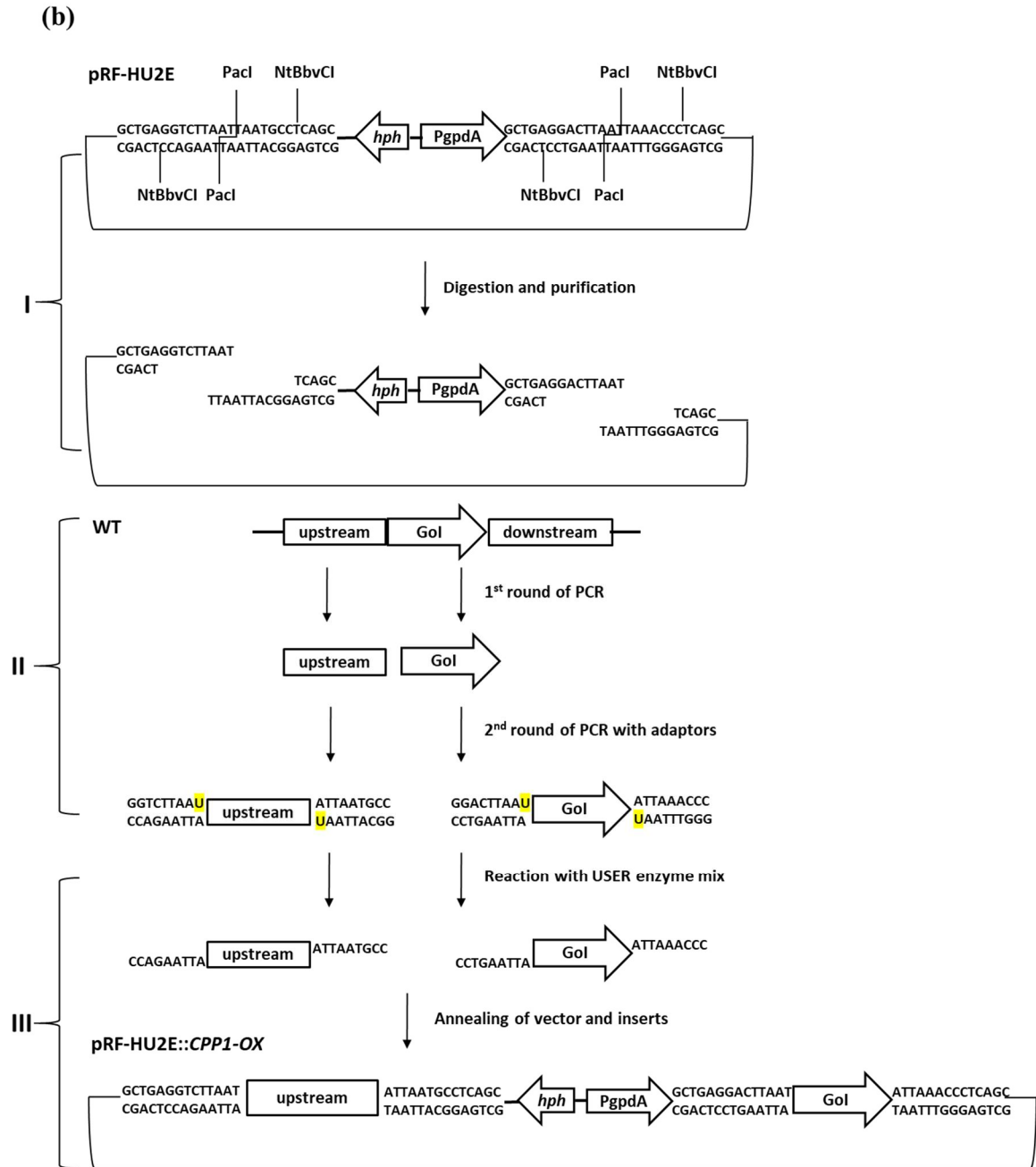


Figure 2.1: Preparation of (a) *FgCPP1* disruption (pRF-HU2:: $\Delta cpp1$) and (b) overexpression (pRF-HU2E::*CPP1-OX*) constructs. Part I. pRF-HU2 and pRF-HU2E were both digested with PacI and NtBbvCI to generate two fragments with sticky ends from each vector. Part II. Inserts were prepared by two rounds of PCRs; *FgCPP1* gene, its upstream and downstream regions were amplified by first round of PCR, and adaptors containing deoxy-uridine base at both ends of the amplicons were attached by a second round of PCR. Part III. USER cloning of upstream and downstream amplicons into digested pRF-HU2 or upstream and gene into digested pRF-HU2E. GoI stands for gene of interest. Drawings were adapted from Frandsen et al. 2008.

2.2.3.2 Electroporation of pRF-HU2::*Δcpp1* and pRF-HU2E::*CPPI-OX* constructs into *Agrobacterium tumefaciens*

Plasmid from a PCR positive colony of pRF-HU2::*Δcpp1* or pRF-HU2E::*CPPI-OX* was transferred into *A. tumefaciens* strain LBA4404 by electroporation. Briefly, a 0.1 cm Gene pulser cuvette (BioRad) which contained 15 ng of construct and 100 μ L of LBA4404 electro-competent cells was placed in an Easyject electroporator (Equibio Ltd.), and an electric pulse was given at 1800 V, 335 R, 15 μ F. Immediately after the pulse, 450 μ L of SOC medium was added to the cuvette, which was then incubated at 28°C, 350 rpm for 90 min. The reaction was plated onto LB plates containing 100 μ g mL⁻¹ kanamycin (LB Kan₁₀₀) and incubated at 28°C for 2 days. The colonies were screened by PCR for the presence of the desired inserts using the primer pairs 5 & 6 for pRF-HU2::*Δcpp1* and 4 & 5 for pRF-HU2E::*CPPI-OX* according to method described for colony PCR in section 2.2.3.1.

2.2.3.3 *A. tumefaciens*-mediated transformation of *F. graminearum*

The disruption and overexpression cassettes were integrated into *F. graminearum* GZ3639 by an *A. tumefaciens*-mediated transformation system, as previously described (Frandsen et al., 2012). In *Δcpp1* mutants, the *FgCPPI* gene was replaced by an *hph* selection marker cassette. For *CPPI-OX*, an *hph* selection marker cassette followed by a *gpdA* promoter were inserted immediately upstream of the *FgCPPI* coding sequence (Figure 2.2).

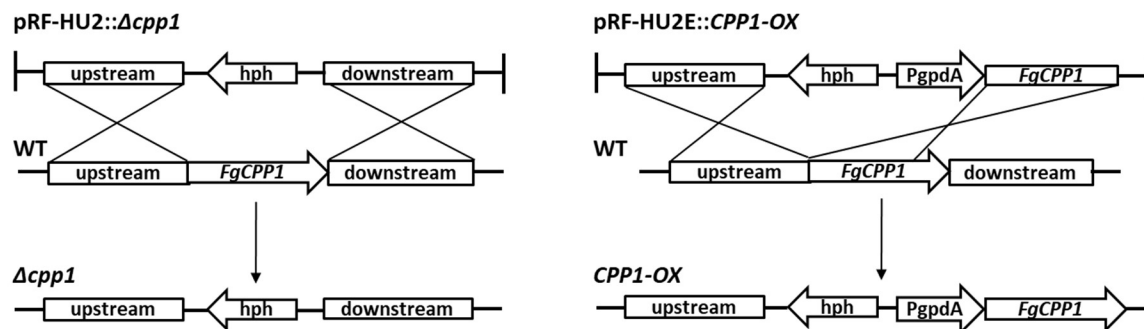


Figure 2.2: Strategy used for disruption (left) and overexpression (right) of *FgCPP1* in *F. graminearum* (Frandsen et al., 2008). Transformants were developed by a double crossover event between the construct and WT.

2.2.3.4 Verification of $\Delta cpg1$ and *CPP1-OX* transformants

DNA was isolated by boiling 2 mg of mycelia in 50 μ L of 10X TE buffer in a microwave oven for 1 min. After cooling to room temperature, the mycelia in TE buffer was centrifuged at 10,000 rpm for 5 min. PCR was carried out as described for colony PCR (section 2.2.3.1), where 1 μ L of 10 times diluted cell lysate (supernatant) was used (Tendulkar et al., 2003) as the template. The transformants were screened for the desired cross over at the left border (primer pairs 7 for $\Delta cpg1$ and 8 for *CPP1-OX*) and the right border (primer pair 9 for both $\Delta cpg1$ and *CPP1-OX*), and for the presence of *hph* gene (primer pair 10) (Figure 2.3 a). Single spores were isolated from PCR-positive transformants and single-spored transformants were re-verified by PCR, as described above.

Copy number of *FgCPP1* disruption and overexpression cassette in $\Delta cpg1$ and *CPP1-OX* transformants, respectively was determined by Southern blotting. Genomic DNA was isolated with QIAGEN's DNeasy Plant Maxi Kit from 800 mg mycelia of WT, $\Delta cpg1$ and *CPP1-OX* transformants collected from potato dextrose broth. Ten micrograms of DNA digested overnight at 37°C with EcoRI and NcoI (both from NEW

ENGLAND BioLabs® Inc.) was run on 0.8% agarose gel. The DNA was then transferred from the gel to a positively charged nylon membrane (Sigma-Aldrich). For hybridization, a probe synthesized by PCR (primer pair 11) with digoxigenin (DIG)-labeled dUTP was used (PCR DIG Probe Synthesis Kit, Sigma-Aldrich). Hybridization was performed overnight at 47°C in DIG Easy Hyb buffer (Sigma-Aldrich). Hybridized DNA fragments were detected with an Anti-DIG antibody conjugated to alkaline phosphatase (DIG Nucleic Acid Detection Kit, Sigma-Aldrich). Restriction enzyme cutting sites and probe binding sites are indicated in Figure 2.3 b.

FgCPPI gene was amplified from *CPPI-OX* using a high fidelity Phusion Hotstart II DNA polymerase (Thermo Scientific™) and the purified PCR product was sequenced to confirm that there are no mutations in the *FgCPPI* sequence of the *CPPI-OX*. (primer pair 12).

Reverse transcription-quantitative PCR (RT-qPCR) was employed to determine *FgCPPI* and *FgCPP2* expression levels in *FgCPPI* transformants. Total RNA was isolated from 100 mg of mycelia collected from PDA-Hyg₁₀₀ plates using the TRIzol reagent (Life Technologies). DNA was removed from RNA samples using DNase I (Thermo Scientific™) and elimination of DNA was confirmed by PCR (primer pair 13). cDNA was synthesised from 250 ng of RNA using SuperScript^R III Reverse Transcriptase (Invitrogen) according to manufacture's instructions. For RT-qPCR, 2.5 µL cDNA was mixed with 5 µL of 2X QuantiTect SYBR GREEN (Qiagen) and 0.3 µL each of 5 µM forward and reverse primers (primer pairs 14 & 15 for *FgCPPI* and *FgCPP2*, respectively) in 10 µL reaction. Amplification was carried out using QuantStudio 6 Flex, (Applied Biosystems™) by employing the following reaction cycles: A hold stage of

50°C (2 min) followed by 95°C (10 min), a PCR stage (40 cycles) of 95°C (15 s) and 60°C (1 min) and a melt curve stage of 95°C (15 s) and 60°C (1 min) followed by 95°C (15 s).

FgCPP1 and *FgCPP2* expressions were normalized to that of *F. graminearum* β -*TUBULIN* gene (FGSG_09530) (primer pair 16).

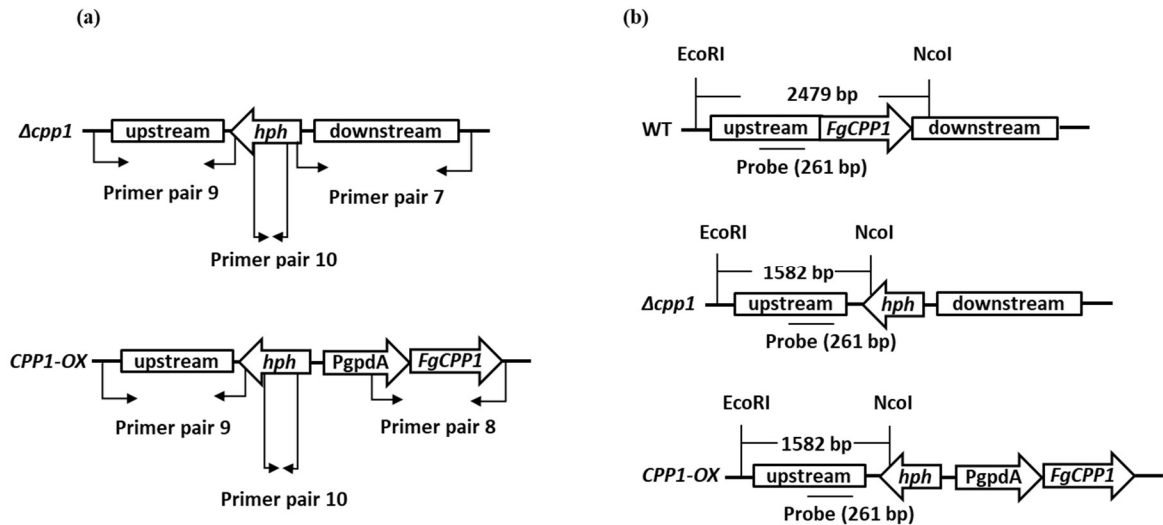


Figure 2.3: Schematic representation of (a) annealing sites of the primers used for verification of successful cross over in *Δcpp1* and *CPP1-OX*, and (b) restriction sites and probe binding positions in WT, *Δcpp1* and *CPP1-OX* transformants for Southern blotting.

2.2.4 Mycelial growth and macroconidia germination assays

For mycelial growth experiment, mycelial plugs of 10 mm diameter were collected from PDA cultures of *Δcpp1*, *CPP1-OX* or the WT using a cork borer. The mycelial plug was placed, mycelial side down, at the centre of a 90 mm petri plate containing PDA. Five PDA plates were used for each transformant and the plates were incubated at 27°C. The diameter of the colony was measured in two perpendicular directions every 24 h for 4 days. The average of the two measurements was used to calculate radial growth of mycelia.

In order to compare macroconidia germination in *Δcppi1* and *CPPI-OX* with the WT, a modified protocol from Spolti et al. (2012) was employed. A grid was drawn on the back of 90 mm petri plates containing 1.5% water agar and squares (1cm² each) were spotted with 5 μL of macroconidia (5 x 10³ macroconidia mL⁻¹). The petri plates were incubated at 27°C, and the number of germinated and non-germinated macroconidia were counted at 6 and 9 h using a microscope. There were two replications for each treatment and five squares for each replication.

2.2.5 Sensitivity to cell wall stress agents and cell wall degrading enzymes

In order to assess stress tolerance in *FgCPPI* transformants, *F. graminearum* growth was measured on PDA plates supplemented with 0.2 mg mL⁻¹ calcofluor white (CFW), 0.5 mg mL⁻¹ congo red (CR), 0.01% sodium dodecyl sulfate (SDS) and 1M NaCl. The concentrations tested for SDS and NaCl were selected based on previous studies (Chen et al., 2014; Quarantin et al., 2016). The concentration for CFW and CR were selected by first screening the effects of 0.05, 0.1, 0.15 or 0.2 mg mL⁻¹ CFW and 0.3, 0.4 or 0.5 mg mL⁻¹ CR on WT *F. graminearum*, where 0.2 and 0.5 mg mL⁻¹ for CFW and CR were respectively found to be the minimum inhibitory concentrations for mycelial growth (data not shown). Cell growth inhibition was assessed by spot inoculating PDA plates (supplemented with or without the cell wall stress agents) with 5 μL of ten-fold dilutions of *Δcppi1*, *CPPI-OX* or the WT macroconidia starting at 6 x 10⁵ macroconidia mL⁻¹. Pictures were taken after 40 h of growth at 25°C in the dark. The experiment was repeated two times, each with three replicates.

In order to assess sensitivity of *FgCPPI* transformants to cell wall degrading enzymes, *F. graminearum* macroconidia germination was monitored in yeast mannitol

agar (YMA) liquid medium (0.4 % sucrose, 0.4 % yeast extract and 0.4 % malt extract) containing 1.4 or 1.6 mg mL⁻¹ Glucanex using a modified protocol from Rittenour and Harris (2013). These two concentrations were selected by first screening the effects of 0.5-1.7 mg mL⁻¹ Glucanex on WT *F. graminearum*. While 1.4 mg mL⁻¹ slightly affected macroconidia germination, 1.6 mg mL⁻¹ almost completely inhibited it (data not shown). The effects of these two Glucanex concentrations on the macroconidia germination of *FgCPPI* transformants were assessed by incubating *Δcpp1*, *CPPI-OX* or WT macroconidia (25 μL from 10⁶ macroconidia mL⁻¹) in YMA with or without Glucanex at 28°C for 14 h. The germinating conidia were observed using EVOS FL Auto Imaging System (Thermo Scientific™) under 20X magnification and photographed. The experiment was repeated two times, each with three replicates.

2.2.6 Plant infection assays on wheat spikes by spray and point inoculations

Spray and point inoculations were used to assess Type I resistance and Type II resistance (Schroeder and Christensen, 1963), respectively. Canadian wheat cultivars (cvs.) Roblin, Penhold, Awesome and Tenacious were used for infection assays because they show different levels of Type I and Type II resistance and susceptibility to FHB. The major resistance mechanisms of these cultivars are provided in Table 2.2. The wheat plants were grown in 1-gallon pots with Cornell mix in a greenhouse at 25/18°C day/night and 16 h photoperiod. Pots were watered daily and fertilized biweekly. Prophylactic sprays were given at 5-7 leaf stage with Nova (Dow AgroSciences Canada) to prevent powdery mildew.

Plants were inoculated with *Δcpp1*, *CPPI-OX* or WT at anthesis. Wheat cvs. Roblin, Penhold, and Awesome were sprayed with an atomized hand sprayer which was

used to disperse macroconidia (10^5 macroconidia mL^{-1} with 0.05% Tween 20) on individual wheat spikes (10 sprays equivalent to 1 mL on each spike). Wheat cvs. Roblin, Penhold, and Tenacious were point inoculated by pipetting 10 μL of macroconidia (10^5 macroconidia mL^{-1}) between the lemma and palea of a spikelet located approximately at one third of the length of spike from the top. Following inoculations, plants were kept in a mist chamber with 95% relative humidity (90% for point inoculation) and 25°C day/night. After 3 days, plants were returned to the greenhouse. Disease severity was evaluated as percentage of spikelets per spike exhibiting symptoms at 3, 6, 9 and 18 days-post inoculation (dpi) for spray inoculated plants. The number of diseased spikelets below the inoculated spikelet, including the inoculated spikelet, was counted at 7, 12 and 18 dpi for point inoculated plants. For both inoculation types, there were five replications per treatment consisting of five spikes from five different plants. The experiments were repeated three times.

2.2.7 Fungal biomass estimation in wheat spikes

Fungal biomass was estimated in wheat spikes following inoculation with *Δcppl*, *CPPI-OX* or WT. Spikes of cv. Penhold were spray-inoculated as described in section 2.2.6. Five spikes per treatment from each of the experimental repetitions were harvested together at 3 dpi, flash frozen in liquid nitrogen and stored at -80°C.

The spikes were ground in liquid nitrogen and DNA was isolated from 100 mg of homogenized tissue with QIAGEN's DNeasy Plant Mini Kit. For qPCR, 2.5 μL of 10 ng μL^{-1} DNA, 5 μL of 2X PerfeCTa SYBR Green SuperMix Low ROX (Quanta BiosciencesTM) and 0.3 μL each of 5 μM forward and reverse primers (primer pair 13) were used in a 10 μL reaction. Amplification was performed in a QuantStudioTM 6 Flex

Real-Time PCR System, (Applied Biosystems™) using the following program: a hold stage of 50°C (2 min) followed by 95°C (10 min), a PCR stage (40 cycles) of 95°C (15 s) and 58°C (45 s), and a melt curve stage of 95°C (15 s) and 60°C (1 min) followed by 95°C (15 s). The amount of fungal DNA in wheat samples was calculated from a standard curve generated using 10-fold dilution series of *F. graminearum* genomic DNA (primer pair 13). The results were expressed as picogram (pg) of fungal DNA from 25 ng of total wheat and fungal DNA (Rossi et al., 2007).

2.2.8 Cellophane penetration experiment

Penetration of *FgCPP1* transformants was studied by inoculating 10 µL from 2×10^6 macroconidia mL⁻¹ of *Δcpp1*, *CPP1-OX* or WT on a cellophane sheet (Cellophane Membrane Backing, Biorad Laboratories) laid on top of minimal medium. Formulation of the minimal medium is as follows: 3% sucrose, 0.2% NaNO₃, 0.1% KH₂PO₄, 0.05% MgSO₄·7H₂O, 0.05% KCl, 0.02% trace elements solution and 2% agar. The trace elements solution consisted of the following: 5% citric acid, 5% ZnSO₄·7H₂O, 4.75% FeSO₄·7H₂O, 1% Fe(NH₄)₂(SO₄)₂·6H₂O, 0.25% CuSO₄·5H₂O, 0.05% MnSO₄·H₂O, 0.05% H₃BO₃ and 0.05% Na₂MoO₄·2H₂O (Puhalla and Spieth, 1983). After 4 days of incubation at 28°C in the dark, the cellophane sheets were removed and the plates returned to the incubator for 2 days, allowing growth of penetrated mycelia (Wang et al., 2014). The experiment was repeated two times, each time with five replications (plates) per strain.

2.2.9 DON production in axenic culture

To induce deoxynivalenol (DON) synthesis in axenic culture, a modified protocol from Miller and Blackwell (1986) was used. A 6-well Clear Multiwell Plate (Falcon®),

catalogue # 353046) with a sterile 100 μm nylon net filter (NY1H type from Millipore Ref# NY1H02500) and 4 mL of first stage medium (0.3% NH_4Cl , 0.2% $\text{MgSO}_4 \cdot 7\text{H}_2\text{O}$, 0.02% $\text{FeSO}_4 \cdot 7\text{H}_2\text{O}$, 0.2% KH_2PO_4 , 0.2% peptone, 0.2% yeast extract, 0.2% malt extract and 2% glucose, pH 7.0) per well was inoculated with $10 \mu\text{L}$ of 2×10^4 macroconidia mL^{-1} of *Δcpp1* , *CPP1-OX* or WT. The culture plates were sealed with parafilm and incubated in the dark at 27°C , 170 rpm for 24 h, after which, the medium was removed using a sterile transfer pipette without disturbing the mycelia, which were washed two times with sterile distilled water. The nylon filter with mycelia was re-suspended in 4 mL of second stage medium (0.1% putricine di-HCl, 0.3% KH_2PO_4 , 0.02% $\text{MgSO}_4 \cdot 7\text{H}_2\text{O}$, 0.5% NaCl, 4% sucrose and 1% glycerol, pH 4.0). After 48 h of incubation in the dark at 27°C , 170 rpm, 450 μL of the supernatant filtered through a 0.2-micron membrane was sent to a collaborator's lab (Dr. Rajagopal Subramaniam, AAFC, Ottawa) for DON analysis. The filtered supernatant was mixed with 150 μL of MeOH for HPLC analysis using a Shimadzu prominence LC-20AD (Mandel) equipped with a Shimadzu SIL-20A HT prominence auto sampler. One hundred microliters of sample were loaded onto an Restek Pinnacle DB C18 Column (5 μm , 150x4.6mm Cat#9414565) with a 22.5% isocratic MeOH: H_2O flow over 20 minutes at a rate of 1 mL min^{-1} . DON was monitored by UV at 220 nm.

DON content was normalized against the mycelial dry weight. The nylon filter collected from each well was dried in a fume hood for 24 h before weighing, and a nylon filter without mycelia was used as a blank to calculate mycelial weight.

2.2.10 DON production in planta

DON production by *FgCPPI* transformants during infection was estimated from spikes of cv. Penhold, that were spray or point inoculated with *Δcppi*, *CPPI-OX* or WT. Plants were inoculated as described in section 2.2.6. For point inoculation, two spikelets on the opposite sides of a rachis were inoculated. Five spikes and 10 spikelets from spray and point inoculated treatments, respectively from each of the experimental repetitions were harvested together at 1, 2 and 3 dpi and flash frozen in liquid nitrogen. Amount of DON in inoculated wheat tissues was estimated in a collaborator's lab using ELISA (Dr. Rajagopal Subramaniam, AAFC, Ottawa) as previously described (Sinha et al., 1995).

2.2.11 TRI gene expression in planta

TRI5 and *TRI6* expressions were determined at 3 dpi from spikes of cv. Penhold spray-inoculated with *Δcppi*, *CPPI-OX* or WT by RT-qPCR. Total RNA was isolated from 100 mg of ground tissue saved from fungal biomass estimation experiment (section 2.2.7) using QIAGEN's RNeasy Plant Mini Kit. cDNA was synthesised from 800 ng of RNA using SuperScript^R III Reverse Transcriptase (Thermo ScientificTM) according to manufacture's instructions. For RT-qPCR, 2.5 μL cDNA was mixed with 5 μL of 2X PerfeCTa SYBR Green SuperMix Low ROX (Quanta BiosciencesTM) and 0.4 μL each of 5 μM forward and reverse primers (primer pairs 17 for *TRI5* and 18 for *TRI6*) in a 10 μL reaction. Amplification was carried out using QuantStudio 6 Flex Real-Time PCR System (Applied BiosystemsTM) by employing the following reaction cycles. A hold stage of 50°C (2 min) followed by 95°C (10 min), a PCR stage (40 cycles) of 95°C (15 s) and 57°C (45 s) and a melt curve stage of 95°C (15 s) and 60°C (1 min) followed by 95°C (15

s). *TRI5* and *TRI6* expression was normalized using *F. graminearum* β -*TUBULIN* (FGSG_09530) and *EF1A* (FGSG_08811) genes (primer pairs 16 and 13, respectively).

2.2.12 Statistical analyses

RT-qPCR data were analyzed using REST© software (Pfaffl et al., 2002) to obtain relative expression of genes in *FgCPP1* transformants compared to the WT. Data from the remaining experiments were analyzed using one-way analysis of variance (ANOVA) at $p < 0.05$. The means between treatments were separated by Fisher's least significant difference (LSD).

2.3 Results

2.3.1 Bioinformatic analyses of FgCPP1

A phylogenetic tree was constructed with the amino acid sequence of FgCPP1 and CPPs from other ascomycete fungal species. The phylogenetic analysis showed that FgCPP1 was closely related to CPPs from *Fusarium pseudograminearum* and *Fusarium poae*. Among the characterized fungal CPPs, FgCPP1 was closest to BcSpl1 and SsCP1, which are important for aggressiveness in *Botrytis cinerea* and *Sclerotinia sclerotiorum*, respectively (Frias et al., 2011; Yang et al., 2018). FgCPP2 was distant from FgCPP1 in the phylogenetic tree and appeared to be closer to FocCP1 (Figure 2.4), which was found to be required for *Fusarium oxysporum* f.sp. *cubense* aggressiveness in banana (Liu et al., 2019b).

FgCPP1 is a secreted protein and the first 18 amino acids constitute the signal peptide responsible for its secretion. The remaining residues (19-137) encode the CP domain in this protein (predicted by SignalP 4.0 and SMART database, respectively).

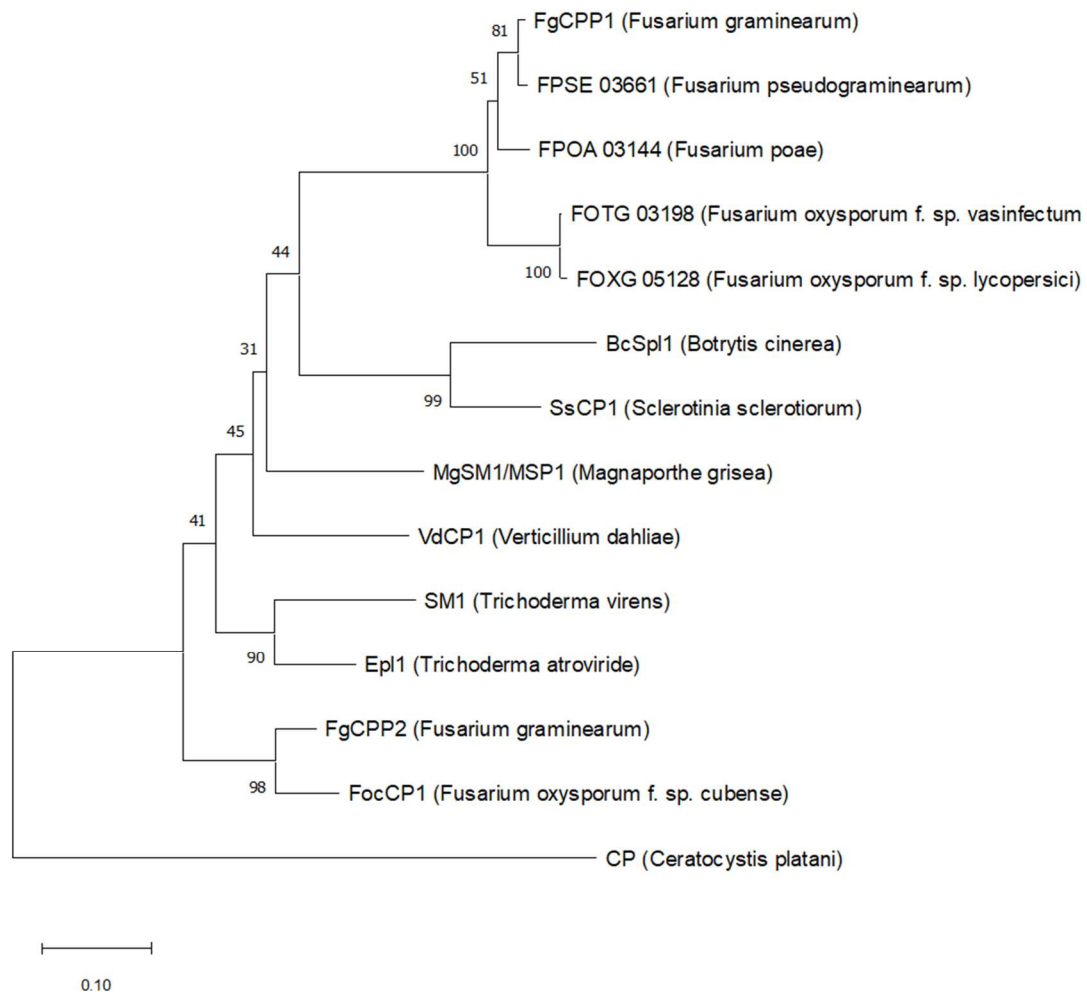


Figure 2.4: Phylogenetic analysis of CPPs from a group of ascomycete fungi. The Neighbor-Joining phylogenetic tree was constructed with the bootstrap method (500 replicates) using MEGA-X software.

2.3.2 Targeted deletion and *in locus* overexpression of *FgCPP1* in *F. graminearum*

A targeted approach was used to generate $\Delta cpp1$ and *CPP1-OX* transformants (Frandsen et al., 2008) of *FgCPP1* resulting in the disruption of the gene or modified expression of the gene *in locus*, respectively. Amplification using primers that anneal to

the genome of the transformants outside of the homologous recombination site confirms the success of the targeted approach used in this study (Figure 2.3 a & 2.5 a). Southern blotting results showed that a single copy of *FgCPP1* disruption and overexpression construct was integrated in $\Delta cpp1$ and *CPP1-OX* transformants, respectively (Figure 2.3 b & Figure 2.5 b). As expected, no *FgCPP1* transcripts were detected from $\Delta cpp1$ in the RT-qPCR experiment, whereas *FgCPP1* expression was approximately 12-fold higher in *CPP1-OX* compared to its expression in WT (Figure 2.5 c). Expression analysis by RT-qPCR showed no significant change in expression of the other cerato-platanin, *FgCPP2* in $\Delta cpp1$ or *CPP1-OX* transformant compared to WT (Figure 2.5 d).

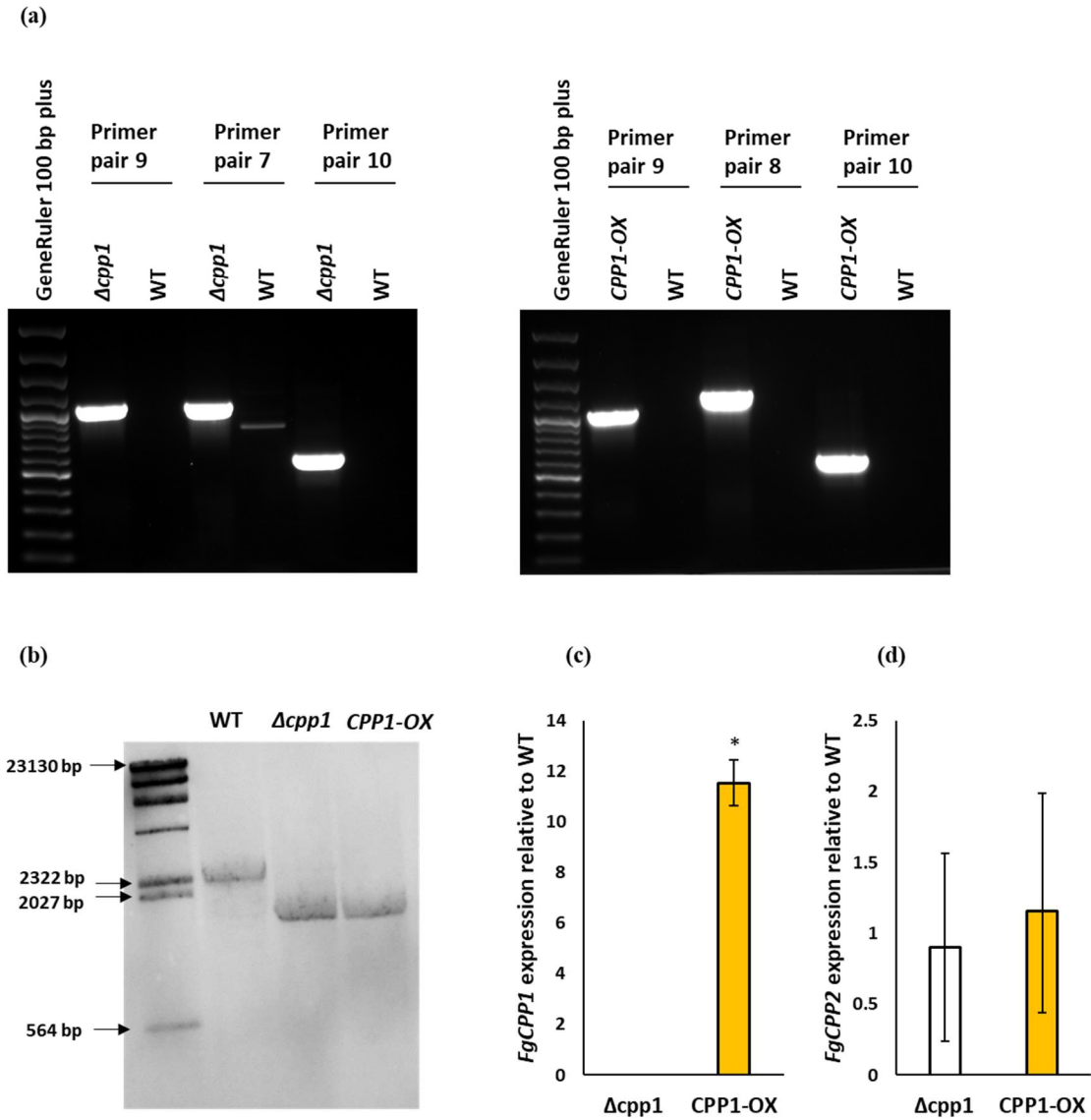


Figure 2.5: Verification of $\Delta cpp1$ and $CPP1-OX$ transformants. (a) Amplification using primers that bind outside the homologous recombination sites were used for verification of crossover at desired sites in the genome of the transformants. (b) Southern blot showing a single band of 2479 bp for WT and 1582 bp for $\Delta cpp1$ and $CPP1-OX$ transformants indicating single copy integration of $FgCPP1$ disruption and overexpression construct in $\Delta cpp1$ and $CPP1-OX$, respectively. (c) $FgCPP1$ expression in $\Delta cpp1$ and $CPP1-OX$ compared to WT as determined by RT-qPCR. *F. graminearum* β -*TUBULIN* gene was used for normalization. Bars represent standard error from three replicates, each performed in triplicate. Asterisk indicates statistically significant difference compared with the WT ($p < 0.05$). (d) $FgCPP2$ expression in $\Delta cpp1$ and $CPP1-OX$ compared to WT as determined by RT-qPCR. *F. graminearum* β -*TUBULIN* gene was used for normalization. Bars represent standard error from three replicates, each performed in triplicate.

2.3.3 *FgCPPI* disruption or overexpression has no effect on general fitness of *F. graminearum*

To determine the effect of *FgCPPI* disruption or overexpression on *F. graminearum* fitness, macroconidia germination and mycelial growth of *FgCPPI* transformants were monitored. Macroconidia of $\Delta cpp1$ or *CPPI-OX* incubated on water agar did not show significant difference in germination at 6 or 9 h after incubation compared to WT (nearly 75% and 100% germination for the three strains at 6 and 9 h after incubation, respectively) (Figure 2.6 a). Similarly, there was no change in mycelial growth of the transformants compared to WT over a 4-day period of growth on PDA (Figure 2.6 b). These results indicate that *FgCPPI* does not have a role in macroconidia germination or mycelial growth in *F. graminearum*.

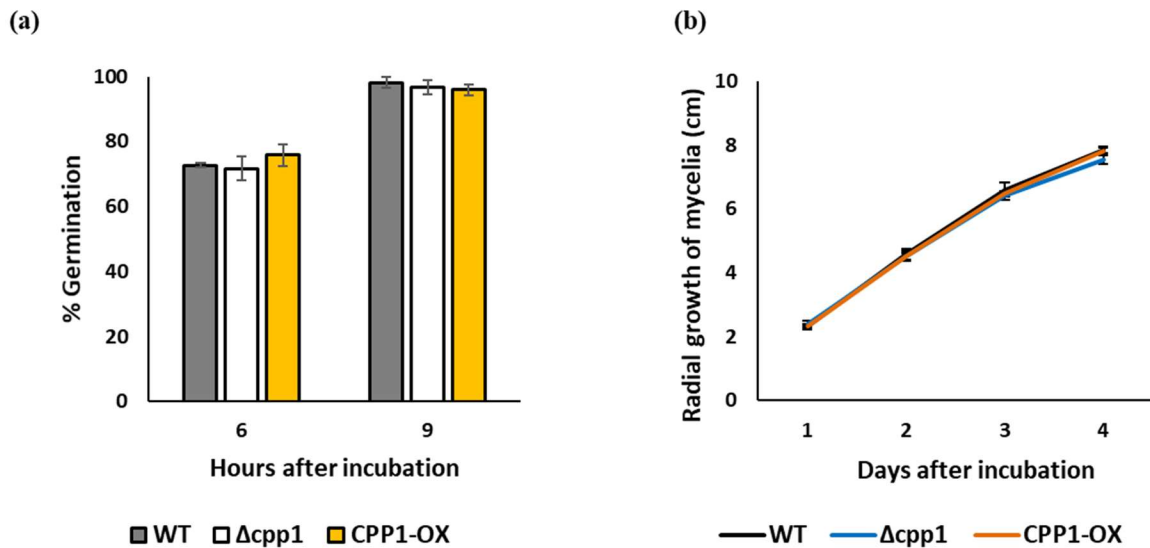


Figure 2.6: (a) Percentage germination of macroconidia of *FgCPPI* transformants and WT on water agar after 6 and 9 h incubation at 27°C. Bars represent standard error from two independent experiments, each with five replicates. (b) Radial mycelial growth of *FgCPPI* transformants and WT over 4 days of growth on PDA at 27°C. Bars represent standard error from five replicates.

2.3.4 *FgCPPI* is not likely involved in *F. graminearum* cell wall protection

Since CPPs from some fungal species have been suggested to have a protective role against cell wall stress agents (Pan et al., 2018) or cell wall degrading enzymes (Quarantin et al., 2016; Zhang et al., 2017c), experiments to assess a similar role for *FgCPPI* in protecting *F. graminearum* cell wall were performed.

In order to assess sensitivity to stress agents, different macroconidial dilutions of *FgCPPI* transformants were incubated on PDA plates with various stress agents, and then mycelial growth was observed. CFW and CR were used to assess the cell wall integrity and SDS was used to check the cell membrane integrity of the transformants; NaCl was used as an osmotic stress agent. The transformants exhibited similar growth pattern as the WT on PDA plates with different stress agents (Figure 2.7 a).

To test if the altered expression of *FgCPPI* leads to a change in sensitivity of *F. graminearum* to cell wall degrading enzymes, the macroconidia of the transformants were incubated with Glucanex (a commercial mixture of β -glucanase, cellulase and chitinase) and macroconidia germination was monitored. The two concentrations used in this experiment affected macroconidia germination, however, the transformants and the WT showed similar sensitivity to Glucanex (Figure 2.7 b), suggesting that *FgCPPI* is not involved in cell wall protection in *F. graminearum*.

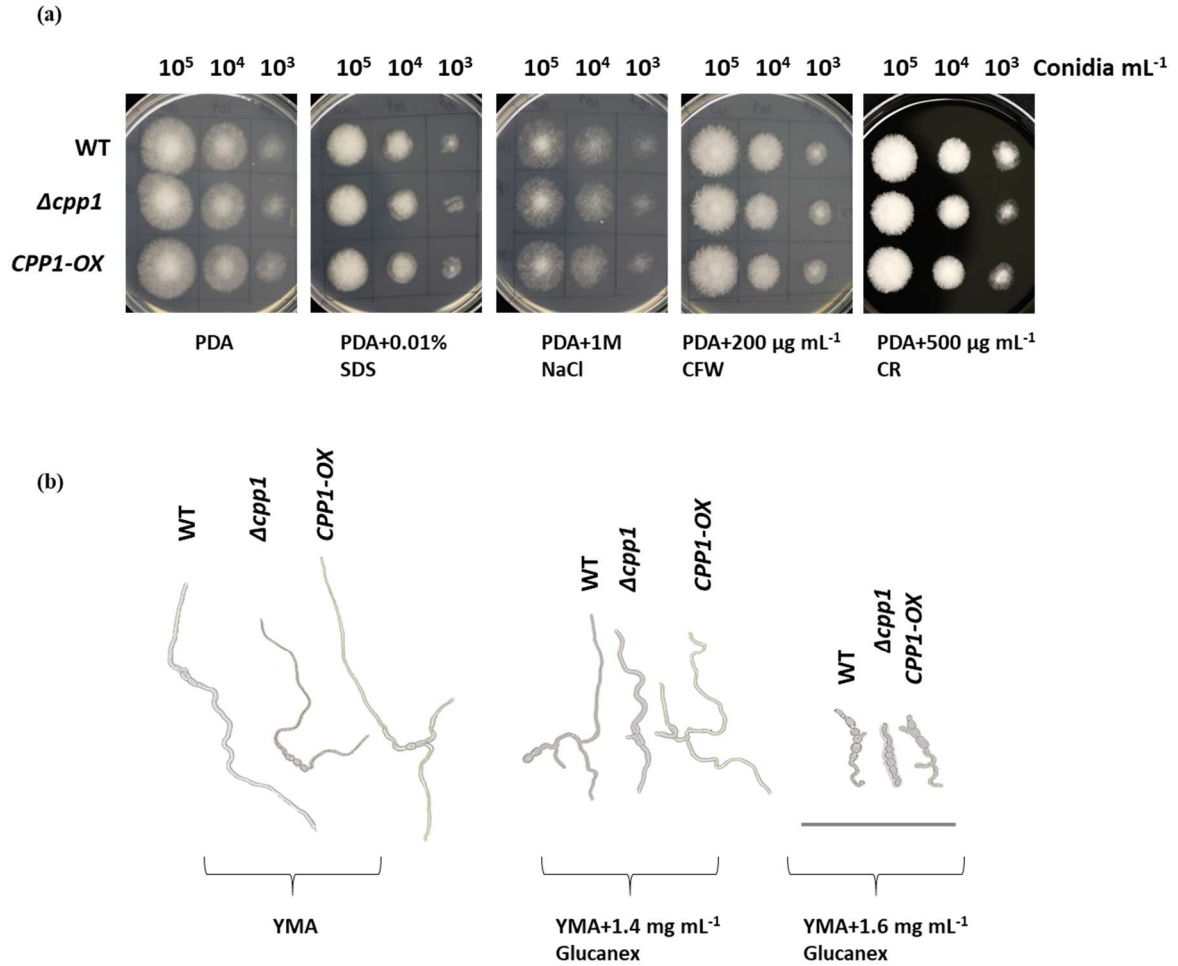


Figure 2.7: Sensitivity of *FgCPP1* transformants to chemicals targeting fungal cell wall/membranes. (a) Mycelial growth from different macroconidia dilutions of *FgCPP1* transformants and WT on PDA containing cell wall/membrane stress agents. SDS= sodium dodecyl sulfate, CFW= calcofluor white and CR= congo red. Images were taken after 40 h of growth at 25°C. Images are representative of two independent experiments, each with three replicates. (b) Macroconidia of *FgCPP1* transformants and WT germinating in YMA containing cell wall degrading enzyme, Glucanex. Images were taken after 14 h of incubation at 28°C. Scale bar = 200 μ m. Images are representative of two independent experiments, each with three replicates.

2.3.5 *FgCPP1* overexpression leads to increase in initial infection, but no effect on disease spread

To determine the involvement of *FgCPP1* in disease interaction, spray and point inoculations were performed with *FgCPP1* transformants and compared with the WT.

Spray inoculation results showed 1.4, 1.7 and 1.6 times increase in initial infection by *CPPI-OX* as early as 3 dpi in cvs. Roblin, Penhold and Awesome, respectively compared to the WT (Figure 2.8 a), whereas initial infection by $\Delta cppi1$ was comparable to infection levels caused by the WT in all three wheat cultivars (Figure 2.8 a). Meanwhile, cvs. Roblin, Penhold and Awesome point inoculated with *CPPI-OX* or $\Delta cppi1$ exhibited similar disease spread as the WT (Figure 2.8 b). These results suggest a possible minor role of *FgCPPI* in initial infection without any measurable effect on disease spread.

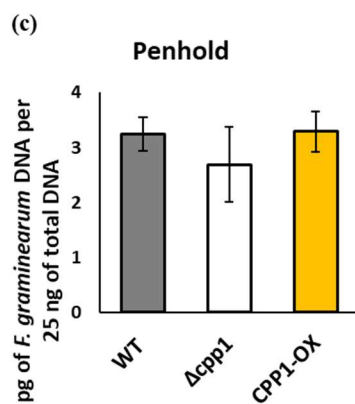
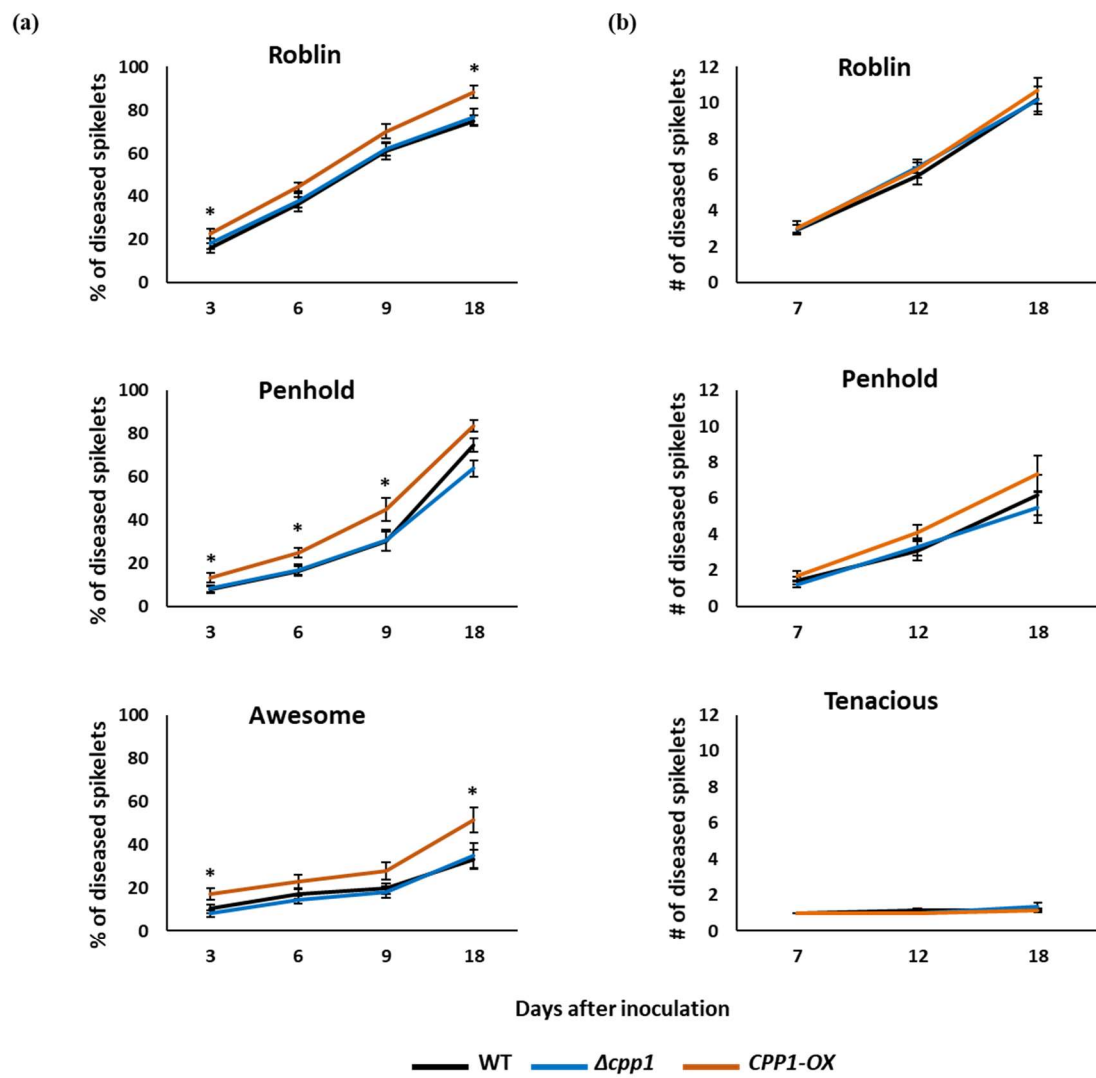


Figure 2.8: Disease severity of *FgCPPI* transformants on wheat. (a) Percentage of diseased spikelets of susceptible wheat cultivar Roblin, moderately susceptible Penhold and moderately resistant Awesome 3, 6, 9 and 18 days after spray inoculation with $\Delta cppi1$, *CPPI-OX* or WT. Bars represent standard error from three independent experiments, each with five replicates (b) Number of diseased spikelets of Roblin, Penhold and resistant wheat cultivar Tenacious 7, 12 and 18 days after point inoculation with $\Delta cppi1$, *CPPI-OX* or WT. Bars represent standard error from three independent experiments, each with five replicates (c) Quantity of $\Delta cppi1$, *CPPI-OX* or WT in spikes of Penhold 3 days after spray inoculation as determined by qPCR. Bars represent standard error from three replicates, each performed in triplicate. Asterisks indicate statistically significant difference compared with the WT ($p < 0.05$).

2.3.6 *FgCPPI* seems to have no role in cell wall penetration

Since *CPPI-OX* strain caused increased initial infection on wheat spikes, the role of *FgCPPI* in cell wall penetration was assessed. Cellophane penetration is routinely used as a qualitative assay to predict penetration of plant cells by fungal species (Lopez-Berges et al., 2010; Gu et al., 2014; Li et al., 2019b). Deletion of *FocCPI* in *F. oxysporum* f.sp. *cubense* negatively affected cellophane penetration by this pathogen (Liu et al., 2019b). The penetration ability of *FgCPPI* transformants was evaluated by inoculating macroconidia of the transformants on cellophane sheets overlaid on minimal medium. *FgCPPI* transformants herein grew from minimal medium after removal of the cellophane (Figure 2.9) showing that the transformants were not compromised in their ability to penetrate cellophane membrane.

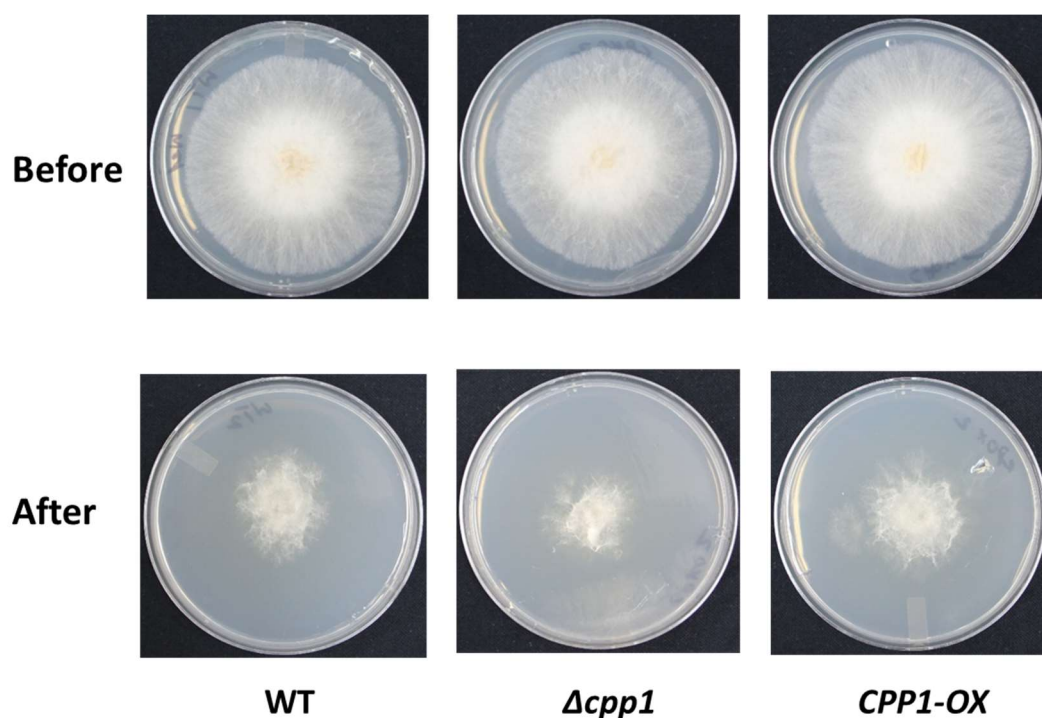


Figure 2.9: Cellophane penetration experiment. Before: *FgCPP1* transformants and WT grown on cellophane sheet placed over minimal medium for 4 days at 28°C in dark. After: The cellophane sheets were removed and the plates were incubated at 28°C for 2 days allowing penetrated hyphae to grow from the medium. Images are representative of two independent experiments, each with five replicates.

2.3.7 *FgCPP1* overexpression increases DON production in axenic culture

In order to study whether *FgCPP1* disruption or overexpression influences DON synthesis, the amount of DON produced by *FgCPP1* transformants in axenic cultures was determined. While DON production by *Δcpp1* did not differ significantly from the WT, *CPP1-OX* accumulated 1.3 times higher amount of DON in axenic culture compared to the WT (Figure 2.10).

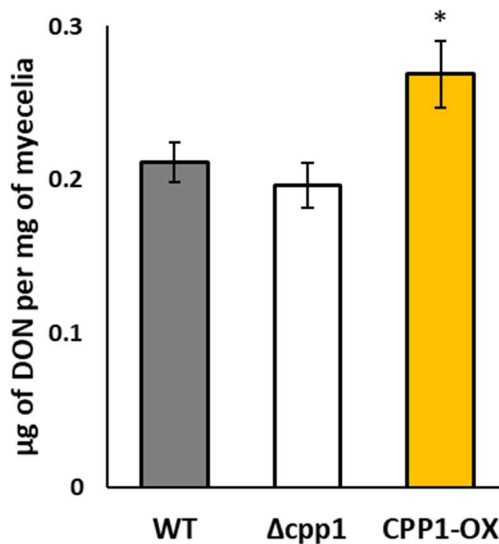


Figure 2.10: DON production by *FgCPP1* transformants or WT in axenic cultures under DON-inducing conditions. Bars represent standard error from six replicates. Asterisk indicates statistically significant difference compared with the WT ($p < 0.05$).

2.3.8 *FgCPP1* disruption or overexpression likely affects DON production during interaction with host

DON synthesis by *FgCPP1* transformants was determined during infection of Penhold wheat spikes. In spray inoculated wheat spikes, DON production by *CPP1-OX* was comparable to WT at 1 and 2 dpi, whereas it was 2.6 times higher than WT at 3 dpi. In the meantime, DON produced by *Δcpp1* did not significantly differ from WT at any sampling days (Figure 2.11 a). DON levels from point inoculated spikelets showed a different pattern than spray-inoculates spikes. While DON accumulation at 1 and 3 dpi did not differ in *Δcpp1* or *CPP1-OX* compared to WT, DON levels were 2.1 times and 1.97 times lower for *Δcpp1* and *CPP1-OX*, respectively compared to WT at 2 dpi (Figure 2.11 b).

Expression of trichothecene biosynthesis pathway genes were also analyzed from Penhold spikes spray inoculated with *FgCPP1* transformants. *TRI5* and *TRI6* expression in wheat spikes sampled 3 days after inoculations did not show significant difference between *FgCPP1* transformants and WT (Figure 2.11 c).

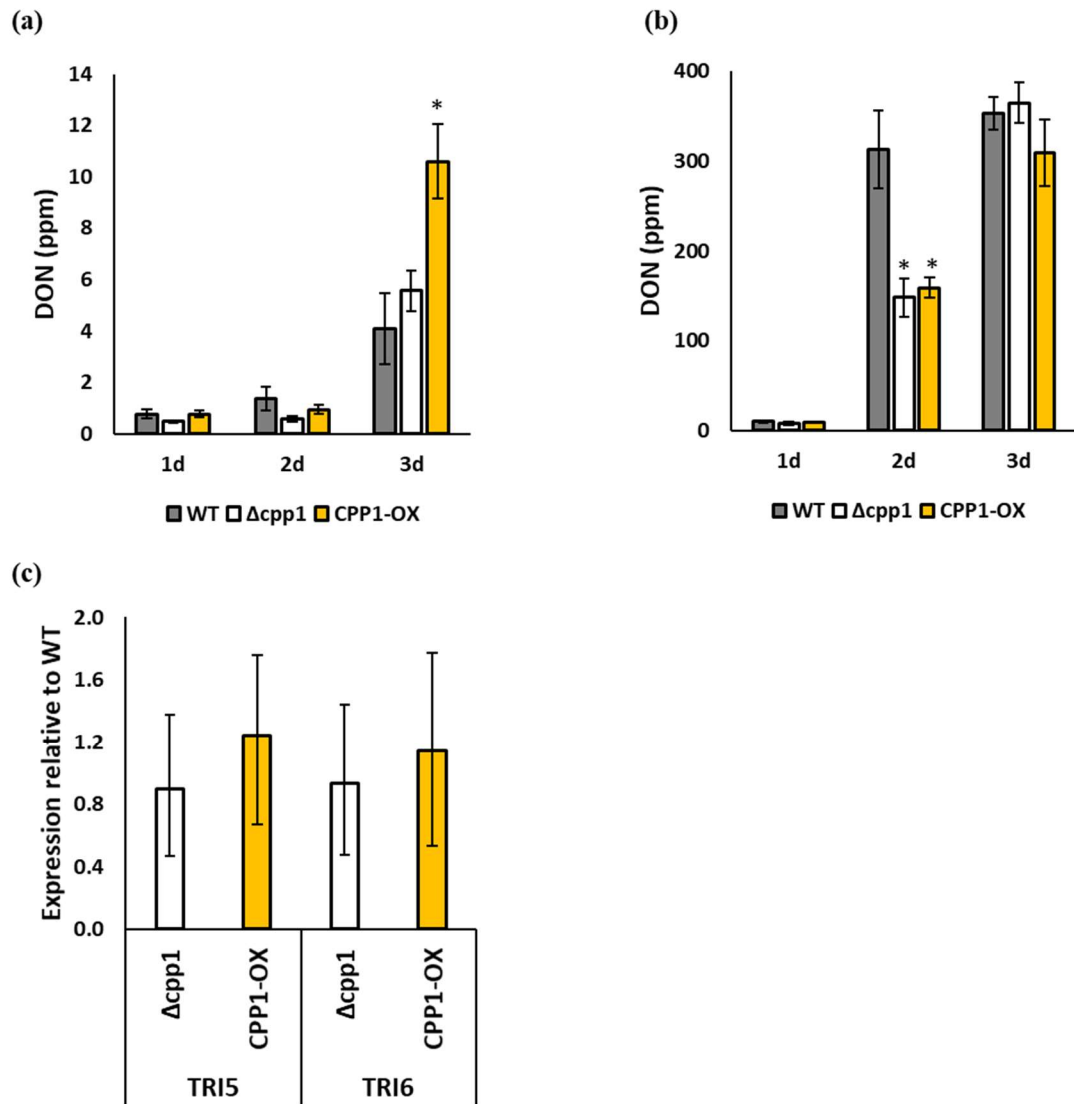


Figure 2.11: DON production by *FgCPP1* transformants or WT during interaction with wheat spikes. (a) DON production in spray inoculated Penhold spikes at 1, 2 and 3 dpi with *FgCPP1* transformants or WT. Bars represent standard error from three replicates. (b) DON production in point inoculated Penhold spikelets at 1, 2 and 3 dpi with *FgCPP1* transformants or WT. Bars represent standard error from three replicates. (c) Expression of *TRI5* and *TRI6* by *FgCPP1* transformants compared to WT 3 days after spray

inoculation of Penhold spikes. *F. graminearum* β -TUBULIN and *EF1A* genes were used for normalization. Bars represent standard error from three replicates, each performed in triplicate. Asterisks indicate statistically significant difference compared with the WT ($p < 0.05$).

2.4 Discussion

Targeted disruption and *in locus* overexpression transformants of *FgCPP1* were generated to study the role of FgCPP1 protein in fungal growth and plant infection.

Disruption or overexpression of *FgCPP1* did not influence macroconidia germination or mycelial growth in *F. graminearum* (Figure 2.6 a & b). This is consistent with a previous study in which mycelial growth of $\Delta fgcpp1$ or $\Delta\Delta fgcpp1,2$ mutants did not differ from WT (Quarantin et al., 2016). Furthermore, deletion of genes encoding CPPs from other fungal species, despite their expression during *in vitro* growth, did not alter their phenotype related to growth and development (Jeong et al., 2007; Frias et al., 2011; Frischmann et al., 2013; Zhang et al., 2017b; Yang et al., 2018).

CPPs have been previously shown to be localized to the fungal cell wall (Boddi et al., 2004; Frias et al., 2014) and some fungal CPPs also bind chitin (Barsottini et al., 2013; Frischmann et al., 2013; Baccelli et al., 2014), suggesting a potential role for CPPs in protecting the fungal cell wall from host defense responses. Indeed, CP deletion mutants of *Verticillium dahliae* and *F. graminearum* ($\Delta vdcp1$ and $\Delta\Delta fgcpp1,2$, respectively) showed increased sensitivity to the cell wall degrading enzyme, chitinase (Quarantin et al., 2016; Zhang et al., 2017c), and RNAi-directed silencing of *SM1* in *Sclerotinia sclerotiorum* resulted in its hypersensitivity to cell wall stress agents (Pan et al., 2018). Therefore, it was surprising that $\Delta cpp1$ or *CPP1-OX* strains used in this study did not show, in comparison to WT, an altered sensitivity to cell wall stress agents or cell

wall degrading enzymes. This discrepancy could be explained by differences in experimental approaches. In this study, macroconidia of *Δcpl1* mutant were incubated with Glucanex (β-glucanase, cellulase and chitinase activities) and the hyphal growth was examined using a microscope. On the other hand, Quarantin et al. (2016) incubated macroconidia of the double mutant (*ΔΔfgcpl1,2*) with chitinase alone, and used absorbance of resazurin dye to determine the effect of the enzyme on fungal growth. However, this protective role of FgCPPs against chitinase in Quarantin et al. (2016) was not observed when purified FgCPPs were incubated with a chitin solution in the presence of chitinase (Quarantin et al., 2019). Importantly, the authors (Quarantin et al., 2019) determined that, unlike many other fungal CPPs, which have been shown to bind chitin *in vitro* (Barsottini et al., 2013; Frischmann et al., 2013; Baccelli et al., 2014), FgCPP1 and FgCPP2 are not able to bind chitin. The lack of sensitivity in *Δcpl1* or *CPPI-OX* transformants to cell wall stress agents or cell wall degrading enzymes (Figure 2.7 a & b) may be explained by the inability of FgCPP1 to bind chitin, and hence to the fungal cell wall. It should also be noted that the localization of FgCPP1 to the cell wall has not been reported in *F. graminearum*.

Previous studies show that fungal CPPs possess cellulose weakening abilities (Barsottini et al., 2013; Baccelli et al., 2014), a property shared by expansins (Chen et al., 2010; Georgelis et al., 2011). A recent study demonstrated a synergistic effect of two FgCPPs on the activity of fungal cellulase (β-1,4-glucanase) on various cellulosic substrates such as CMC, filter paper and wheat cell walls. Incubation of CMC or wheat cell wall with β-1,4-glucanase released more reducing sugars in the presence of FgCPPs than in their absence (Quarantin et al., 2019). The expansin-like cellulose loosening

activity of FgCPPs is likely responsible for the improved β -1,4-glucanase activity on these cellulosic materials (Quarantin et al., 2019). This synergistic effect of FgCPPs on fungal cellulase may facilitate advancement of fungal hyphae into the plant tissue. A similar synergistic effect on cellulose hydrolysis activity has also been reported for an expansin-like protein, EXLX1 from *B. subtilis* (Yan, 2012). Deletion of EXLX1 affected the ability of this bacterium to colonize maize roots (Kerff et al., 2008). Furthermore, overexpression of an expansin-like protein, swollenin, improved the ability of *Trichoderma asperellum* to colonize cucumber roots (Brotman et al., 2008). In this study, overexpression of a cerato-platanin-encoding gene (*FgCPPI*) resulted in 1.4-1.7 times increase in initial infection in different wheat cultivars. It is possible that FgCPP1 acts as an expansin causing loosening of plant cell wall during infection. Despite the observed increase in initial infection by *CPPI-OX* in wheat spikes, fungal biomass estimated from *CPPI-OX*-inoculated wheat spikes was not significantly higher than that from WT-inoculated spikes. This is probably due to a minor effect of *FgCPPI* on infection and the small difference in infection between *CPPI-OX* and the WT.

Since a slight increase was observed in initial infection, a cellophane penetration assay was conducted to study whether *FgCPPI* is involved in cell wall penetration. No change in cellophane penetration ability between *FgCPPI* transformants and WT was observed. Cellophane is not an absolute substitute for plant cell wall; however, cellophane does mimic plant cell walls to some extent and is commonly used to assess penetration of fungal strains *in vitro* (Lopez-Berges et al., 2010; Gu et al., 2014; Li et al., 2019b).

Deletion of *FgCPPI* ($\Delta cppi$) had no effect on initial infection of wheat spikes by *F. graminearum*. Quarantin et al. (2019) reported a significantly higher cellulase activity

for their $\Delta\Delta fgcpp1,2$ mutant compared to WT. It therefore seems likely that the increased cellulase activity by $\Delta cpp1$ could compensate for the loss of expansin-like activity of *FgCPP1* in this mutant, thus explaining the lack of difference in initial infection compared to the WT. $\Delta cpp1$ and *CPP1-OX* transformants were also screened by point inoculation for their change in ability to cause disease spread in wheat spikes. Neither *FgCPP1* disruption nor overexpression was found to have an effect on disease spread by *F. graminearum* in the rachis of wheat spikes. Quarantin et al. (2016) observed similar results when comparing $\Delta fgcpp1$ or $\Delta\Delta fgcpp1,2$ with WT in point inoculated wheat spikes. This lack of difference in disease spread between *FgCPP1* transformants and the WT could be due to a larger effect on disease spread of other effectors secreted by *F. graminearum*. For example, DON secreted by *F. graminearum* during infection is required for its spread as evidenced by the inability of DON non-producing mutants to spread through wheat rachis (Proctor et al., 1995; Bai et al., 2002). Therefore, it could be considered that any possible role for *FgCPP1* in disease spread is masked by such a large effect of DON and/or other effectors influencing disease spread.

DON analysis from point inoculated Penhold spikelets showed no differences in the amount of DON produced by *FgCPP1* transformants and the WT at 1 and 3 dpi. Meanwhile both $\Delta cpp1$ and *CPP1-OX* accumulated less DON at 2 dpi. These observed changes in DON production by *FgCPP1* transformants do not correlate with their aggressiveness.

In summary, overexpression of *FgCPP1* gene led to a small increase in *F. graminearum* aggressiveness. Given the structural and functional similarities between FgCPPs and expansins, it can be hypothesized that FgCPPs, by virtue of their cell wall

loosening ability, would facilitate infection of wheat spikes by *F. graminearum*. As a future direction, it would be interesting to determine whether co-inoculation of purified FgCPP proteins along with *F. graminearum* has any effect on the aggressiveness of this pathogen.

Table 2.1: Primers used for various experiments in this chapter

Primer pair	Primer name	Primer sequence (Tm °C)	Purpose
1	Fg10212-F1	ATGAAGTTCACTGGTATCCTC (51.6)	Amplification of <i>FgCPP1</i> gene
	Fg10212-R613	ATAGTCTAAACGCCAGCCAG (54.5)	
2	Fg10212-f 1133(+)	TTCCACGATACATTGCAGCA (54.7)	Amplification of upstream of <i>FgCPP1</i>
	Fg10212-r290(+)	TCCAAATCGAGAAAGTGACTGG (54.8)	
3	Fg10212-f721(-)	TGCTCTGCTTGATCGAATTGG (55.6)	Amplification of downstream of <i>FgCPP1</i>
	Fg10212-r1543(-)	CTGTCTTGAGGGCTCCAGAT (56.4)	
4	Fg10212-F1OX	ggacttaauATGAAGTTCACTGGTATC (53.3)	Amplification of <i>FgCPP1</i> with adaptors
	Fg10212-R613OX	gggttaauATAGTCTAAACGCCAG (53.4)	
5	Fg10212-f1133(+)KO	ggcttaauTTCCACGATACATTGC (54.4)	Amplification of upstream of <i>FgCPP1</i> with adaptors
	Fg10212-r290(+)KO	ggcattaauTCCAAATCGAGAAAGTG (54.9)	
6	Fg10212-f721(-)KO	ggacttaauTGCTCTGCTTGATC (54.0)	Amplification of downstream of <i>FgCPP1</i> with adaptors
	Fg10212-r1543(-)KO	gggttaauCTGTCTTGAGGGCT (56.8)	
7	RF-1	AAATTTTGTGCTCACCGCCTGGAC (60.5)	Verification of cross over in $\Delta cpp1$
	Fg10212-M-1	CAAAGGCGAAACGGGACTCTTTTA (57.6)	
8	RF-3	TTGCGTCAGTCCAACATTTGTTGCCA (61.7)	Verification of cross over in <i>CPP1-OX</i>
	Fg10212-M-3	GATGACACTCTTGATTGGGACGAAA (57.1)	
9	Fg10212-M-2	AAAGCTCAGACCATTGCCATGTTG (58.3)	Verification of cross over in $\Delta cpp1$ and <i>CPP1-OX</i>
	RF-2	TCTCCTTGCGATGCACCATTCTTG (59.8)	
10	Hyg588U	AGCTGCGCCGATGGTTTCTACAA (61.3)	Amplification of <i>hph</i> gene from transformants
	Hyg588L	GCGCGTCTGCTGCTCCATACAA (62.3)	
11	CP-SB-F1	GGTTCTCCCCCAAAGCTAC (55.6)	Probe synthesis for Southern blotting
	CP-SB-R1	AGCTCAGCTTAGTGCCCGTA (58.3)	
12	CPOX-seq-F	CATCTTCCCATCCAAGAACC (53.1)	Amplification and sequencing of <i>FgCPP1</i> gene from <i>CPP1-OX</i>
	CPOX-seq-R	CCAGCCATTGCCAAGTATTA (52.9)	
13	FgEF-F	CCTCGCTACTATGTCACCGT (56.2)	PCR confirmation of DNA elimination from RNA and normalization of <i>TRI5</i> and <i>TRI6</i> transcripts
	FgEF-R	CAAGGGTGTAGGCAAGGAGA (56.6)	
14	Fg10212-F2	CGTCTCTTGCTCTGATGGCT (57.0)	Expression analyses of <i>FgCPP1</i> in $\Delta cpp1$ and <i>CPP1-OX</i> by RT-qPCR
	Fg10212-R2	CGATGATGTTGACACCACCG (56.2)	
15	Fg11205-F1	CCTACAAGGGCAAGAGCATC (55.7)	Expression analyses of <i>FgCPP2</i> in $\Delta cpp1$ and <i>CPP1-OX</i> by RT-qPCR
	Fg11205-R1	CCTGAGTAGCAGTCGCATCA (56.7)	
16	B-tub-F	GTTCTGGACGTTGCGCATCTG (59.0)	Normalization of <i>FgCPP1</i> , <i>FgCPP2</i> , <i>TRI5</i> and <i>TRI6</i> transcripts
	B-tub-R	TGATGGCCGCTTCTGACTTCC (59.7)	
17	TRI5-F2	GGGATGTTGGATTGAGCAGT (55.1)	Expression analysis of <i>TRI5</i> from Penhold spikes inoculated with <i>FgCPP1</i> transformants
	TRI5-R2	AGAAGCCCCAACACAATGAC (55.6)	
18	TRI6-F2	GGCATTACCGGCAACACTTCAA (58.4)	Expression analysis of <i>TRI6</i> from Penhold spikes inoculated with <i>FgCPP1</i> transformants
	TRI6-R2	CATGTTATCCACCCTGCTAAAGACC (57.4)	

Table 2.2: Major resistance mechanisms of wheat cultivars used in this study

Wheat cultivars	Type I resistance	References	Type II resistance	References
Roblin	Susceptible	(Campbell and Czarnecki, 1987)	Susceptible	(Campbell and Czarnecki, 1987)
Penhold	Moderately resistant	(Cuthbert et al., 2017)	Moderately susceptible	Raman Dhariwal, AAFC
Awesome	Moderately resistant	Raman Dhariwal, AAFC	Moderately resistant	Raman Dhariwal, AAFC
Tenacious	Resistant	(Brown et al., 2015)	Resistant	Raman Dhariwal, AAFC

Chapter 3: Roles of two secreted CFEM domain-containing proteins in growth and aggressiveness of *Fusarium graminearum*

3.1 Introduction

Fusarium graminearum is the primary cause of Fusarium head blight (FHB) disease of cereals (Goswami and Kistler, 2004). During infection, the fungus secretes secondary metabolites and proteins into the host plant (Paper et al., 2007; Oide et al., 2014). Most of the proteins found in the *F. graminearum* secretome are uncharacterized and their role in FHB disease is unclear. *F. graminearum* encodes six putatively secreted proteins containing a fungal-specific domain called common in fungal extracellular membrane (CFEM) domain (Lu and Edwards, 2016). Not all CFEM domain-containing proteins are secreted, in fact, this domain is also commonly found in the extracellular membrane proteins of fungi (Kulkarni et al., 2003; Zhang et al., 2015). The *F. graminearum* genome encodes at least 12 CFEM domain-containing proteins in addition to those that have been observed in the secretome (Jiang et al., 2019).

These cysteine-rich proteins with eight conserved cysteine residues within the CFEM domain, secreted or otherwise, are found in both pathogenic and non-pathogenic fungi. However, pathogenic fungi were reported to have more CFEM-containing proteins compared with non-pathogenic species, which suggests a potential role for CFEM-containing proteins in fungal infection (Zhang et al., 2015). CFEM domain-containing proteins have been implicated in several infection-related functions of fungal pathogens. For example, CFEM-containing proteins in the human pathogen, *Candida albicans*, are associated with biofilm formation and heme uptake from host cells, whereas in the plant

pathogen, *Magnaporthe grisea*, they are involved in host surface sensing, appressorium formation and penetration (reviewed in section 1.11).

CFEM-containing proteins may also have a role in the maintenance of fungal cell wall integrity. For instance, deletion of *RBT51*, a gene encoding a CFEM-containing protein in *C. albicans*, led to increased sensitivity of the fungus to cell wall perturbing agents such as calcofluor white (CFW) and congo red (CR) and cell membrane stress agent sodium dodecyl sulfate (SDS) (Perez et al., 2006). This sensitivity could be due to structural alterations which were observed at the cell surface of the mutant (Perez et al., 2011). Similarly, *BcCFEM1* deletion resulted in hypersensitivity of *Botrytis cinerea* to CFW, CR and SDS (Zhu et al., 2017) and deletion of a CFEM protein-encoding gene, *WISH*, caused decreased tolerance of *M. grisea* towards fungal cell wall degrading enzymes (Sabnam and Barman, 2017).

Of the six putatively secreted CFEM-containing proteins of *F. graminearum*, FGSG_02077 and FGSG_08554 were detected from a minimal medium-based *in vitro* secretome. Moreover, these same proteins were also found to be expressed during infection of wheat spikes (Lu and Edwards, 2016).

Some CFEM-containing proteins are glycosylphosphatidylinositol (GPI)-anchored (Kulkarni and Dean, 2004; Zhu et al., 2017), while others are G-protein-coupled receptors (GPCRs) with transmembrane helices (Kulkarni et al., 2005; Sabnam and Barman, 2017; Dilks et al., 2019). FGSG_02077 and FGSG_08554, the two CFEM proteins detected from the *in vitro* secretome of *F. graminearum*, lack a GPI-anchor motif or transmembrane helices (Lu and Edwards, 2016), meaning that they may be secreted outside the fungal cell. These two proteins also had a reduced abundance in the

secretomes of non-pathogenic mutants of *F. graminearum* compared to the secretome of the WT (Rampitsch et al., 2013), which suggests that they may be involved in host plant infection. An *FGSG_02077* deletion mutant of *F. graminearum* was reported to have reduced aggressiveness on wheat coleoptiles (Zhang et al., 2012) and wheat spikes (Dufresne et al., 2008).

To gain more insights into the roles of *FGSG_02077* and *FGSG_08554* (described herein as *FgCFEM1* and *FgCFEM2*, respectively) in growth and aggressiveness of *F. graminearum*, I developed disruption and overexpression transformants for the corresponding genes in this fungus and screened them for traits related to growth, cell wall integrity, DON synthesis and infection.

3.2 Materials and Methods

3.2.1 Bioinformatic analyses of FgCFEM1 and FgCFEM2

To determine the evolutionary relationships of FgCFEM1 and FgCFEM2 with other characterized fungal CFEM proteins, amino acid sequences of CFEM proteins from ascomycetes and saccharomycetes were aligned by ClustalW and a phylogenetic tree was constructed by the Neighbor-Joining method in MEGA-X software. Additionally, a multiple sequence alignment of CFEM domains of six putatively secreted *F. graminearum* CFEM proteins was created using the Clustal Omega Multiple Sequence Alignment software from EMBL-EBI. Presence of the signal peptides and their cleavage site in FgCFEM1 and FgCFEM2 were predicted using SignalP 4.0 (Petersen et al., 2011). CFEM domains in these proteins were identified using SMART database (Letunic et al., 2015).

3.2.2 Generation of disruption and overexpression transformants of *FgCFEM1* and *FgCFEM2*

The disruption and overexpression transformants of *FgCFEM1* and *FgCFEM2* ($\Delta cfem1$, *CFEM1-OX*, $\Delta cfem2$ and *CFEM2-OX*, respectively) were developed utilizing the vectors and protocol used to generate *FgCPP1* transformants (Frandsen et al., 2008). Figure 2.1 in Chapter two provides a schematic representation of the protocol, and vectors were prepared as detailed in section 2.2.3.1. The inserts were prepared by two rounds of PCR, as described in section 2.2.3.1, using primers presented in Table 3.1. For the first PCR, primer pairs 1, 2 and 3 were used to amplify the initial 778 bp of *FgCFEM1*, 807 bp upstream of its transcriptional start site and 700 bp of downstream region, respectively. Primer pairs 4, 5 and 6 were used to amplify the first 732 bp of *FgCFEM2*, 812 bp upstream of transcriptional start site and 723 bp of downstream region from *F. graminearum* GZ3639 genomic DNA, respectively. The second PCR to add adapter sequences was employed with primer pairs 7, 8, 9, 10, 11 & 12 (see Table 3.1 for details). The inserts were cloned into pRF-HU2 or pRF-HU2E vectors (section 2.2.3.1), transformed into *Agrobacterium tumefaciens* strain LBA4404 (section 2.2.3.2), which was then used for transformation of *F. graminearum* strain GZ3639 (section 2.2.3.3).

3.2.3 Verification of *FgCFEM1* and *FgCFEM2* transformants

Homologous recombination at the desired site in the fungal genome was verified by PCR using genomic DNA from the transformants. Primer pairs used for verification and primer binding sites in the transformants are shown in Figure 3.1 a & b. DNA isolation, PCR reaction and thermocycling conditions were same as described in section 2.2.3.1.

Copy number estimation in *FgCFEM1* and *FgCFEM2* transformants was performed by Southern blotting. Genomic DNA from $\Delta cfem1$ and *CFEM1-OX* was digested with SacI and ScaI, and that from $\Delta cfem2$ and *CFEM2-OX* was digested with PvuII and ScaI (all enzymes are from NEW ENGLAND BioLabs® Inc.). Primer pairs 20 and 21 were used for probe synthesis for *FgCFEM1* and *FgCFEM2* transformants, respectively. The remaining part of the experiment was performed as described in section 2.2.3.4. Restriction enzyme cutting sites and probe binding sites are indicated in Figure 3.1 c & d.

FgCFEM1 and *FgCFEM2* sequences from *CFEM1-OX* and *CFEM2-OX* were amplified (primer pairs 22 & 23, respectively) using a high fidelity Phusion Hotstart II DNA polymerase (Thermo Scientific) and purified PCR products were sequenced to confirm that there were no mutations in protein coding sequences.

FgCFEM1 and *FgCFEM2* expression levels in *FgCFEM1* and *FgCFEM2* transformants were determined by RT-qPCR (primer pairs 24 & 25, respectively). Total RNA was isolated from 100 mg of dry weight of mycelia collected from potato dextrose broth using QIAGEN's RNeasy Plant Mini Kit. cDNA synthesis and RT-qPCR were performed as discussed in section 2.2.3.4. *F. graminearum* β -TUBULIN (FGSG_09530) was used for normalization (primer pair 26).

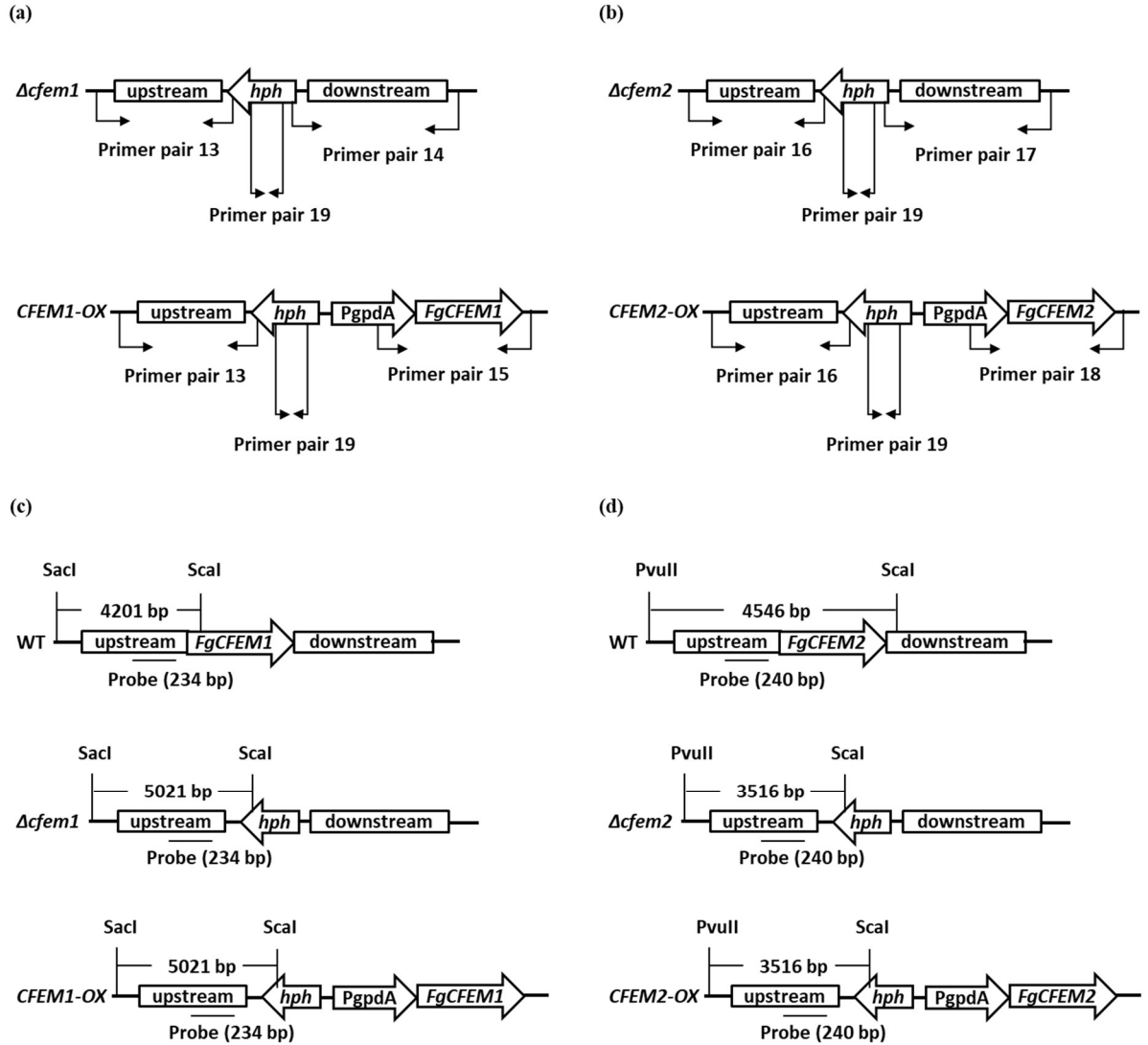


Figure 3.1: Schematics showing annealing position of primer pairs used for the verification of crossover in (a) *FgCFEM1* and (b) *FgCFEM2* transformants, and restriction enzyme cutting sites and probe binding positions in (c) WT, $\Delta cfem1$ and *CFEM1-OX* and (d) WT, $\Delta cfem2$ and *CFEM2-OX* for Southern blotting.

3.2.4 *In vitro* characterization and plant infection assays

FgCFEM1 and *FgCFEM2* transformants were tested for mycelial growth, macroconidia germination, sensitivity to chemicals targeting cell wall, *in vitro* DON

accumulation, cellophane penetration ability and aggressiveness in wheat as detailed in the respective sections of Chapter two.

3.2.5 Statistical analyses

Relative expression of *FgCFEM1* and *FgCFEM2* in the corresponding transformants were determined using REST© software (Pfaffl et al., 2002). Data from other experiments were analyzed using one-way ANOVA, with significant differences indicated by $p < 0.05$. Treatment means were separated by Fisher's least significant difference (LSD).

3.3 Results

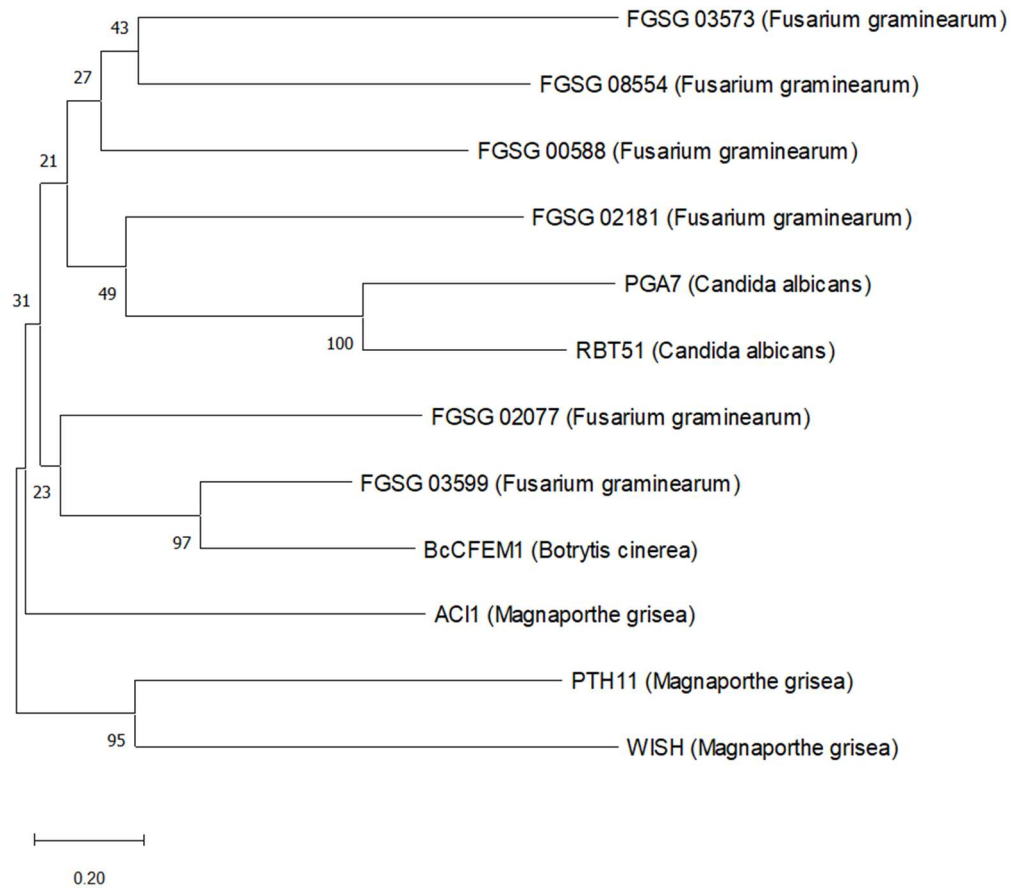
3.3.1 Bioinformatic analyses of FgCFEM1 and FgCFEM2

A phylogenetic tree was constructed using amino acid sequences of the six putatively secreted *F. graminearum* CFEM proteins along with other characterized fungal CFEM proteins from ascomycetes and saccharomycetes. Phylogenetic analysis showed that FgCFEM1 (FGSG_02077) and FgCFEM2 (FGSG_08554) were separated into two different clades. FgCFEM1 and a putatively secreted FGSG_03599 were closely related to BcCFEM1 which is important for infection by *B. cinerea* (Zhu et al., 2017), whereas FgCFEM2 appeared to be distant from any of the characterized CFEM proteins included in the analysis (Figure 3.2 a). Multiple sequence alignment of CFEM domains of six putatively secreted *F. graminearum* CFEM proteins revealed eight highly conserved cysteine residues in CFEM domains (Figure 3.2 b).

FgCFEM1 and FgCFEM2 are secreted proteins. The signal peptides responsible for their secretion were predicted by SignalP 4.0 and the CFEM domains in these proteins

were determined by SMART database. The first 17 amino acids of FgCFEM1 encode the signal peptide and residues 19-86 encode a CFEM domain. In FgCFEM2, the signal peptide is coded in the first 15 residues and a CFEM domain is found between residues 17-84.

(a)



(b)

FGSG_00588	---KLPKCAQPCVDQYTTGGGVAGCGQLDIKCICSNKNFLS----GIAACCLEKECDAQGK
FGSG_03573	-LDWVPECVGTCTVERAVAA---QCDDPNLQECYCGRGFFDP---WYACVSQ-ACSREDL
FGSG_02181	LASQVPNCVAVCLRNHES---IGCDVGDIVCLCKSKASL--ISKVGLCVVGSQCDFEDA
FGSG_08554	-LSGQPECALKCLKEFIPK---AGCELDNTACQCEASFQTKLAPIITPCLTE-ACQVDDL
FGSG_02077	-LADVPKCAIPCLDKAIAS--ETSCDKTDLACVCKGFSAV--RSKATSCVID-ECGTDVA
FGSG_03599	-TSAIPTCGAPCITSAAAAAG---C--TDIACQCASSEVI--QASALGCVVG-NCGIPVA
FGSG_00588	ETAVKYA-KQICATAG
FGSG_03573	PNGYIWG-FTRCDPKT
FGSG_02181	SSSTDIV-RDMCDLVA
FGSG_08554	LKAQKAA-ADACKAYA
FGSG_02077	INEVLPATENLCKNPP
FGSG_03599	LSVQAAA-AAVCTACA

Figure 3.2: **(a)** Phylogenetic analysis of CFEM proteins from ascomycetes and saccharomycetes. The Neighbor-Joining phylogenetic tree was constructed with the bootstrap method (500 replicates) using MEGA-X software. **(b)** Multiple sequence alignment of CFEM domains of FGSG_02077 and FGSG_08554 along with four other putatively secreted *F. graminearum* CFEM proteins. The alignment was created using the Clustal Omega Multiple Sequence Alignment software from EMBL-EBI. Eight highly conserved cysteine residues of CFEM domains are highlighted in cyan.

3.3.2 Targeted disruption and *in locus* overexpression of *FgCFEM1* or *FgCFEM2* in

F. graminearum

The disruption and overexpression of *FgCFEM1* and *FgCFEM2* were obtained by homologous recombination between the respective construct and *F. graminearum* genome. The recombination at desired sites in the genome was verified by PCR (Figure 3.3 a; see Figure 3.1 a & b for primer annealing sites in the transformants) and the recombination led to the integration of a single copy of disruption and overexpression constructs in *FgCFEM1* and *FgCFEM2* transformants, as estimated by Southern blotting (Figure 3.3 b). *FgCFEM1* and *FgCFEM2* expression levels in the transformants were determined by RT-qPCR. As anticipated, no transcripts of *FgCFEM1* and *FgCFEM2* were detected from *Δcfem1* and *Δcfem2*, respectively, whereas transcription of these two genes were upregulated 5- and 11-fold in *CFEM1-OX* and *CFEM2-OX* respectively, compared to WT (Figure 3.3 c).

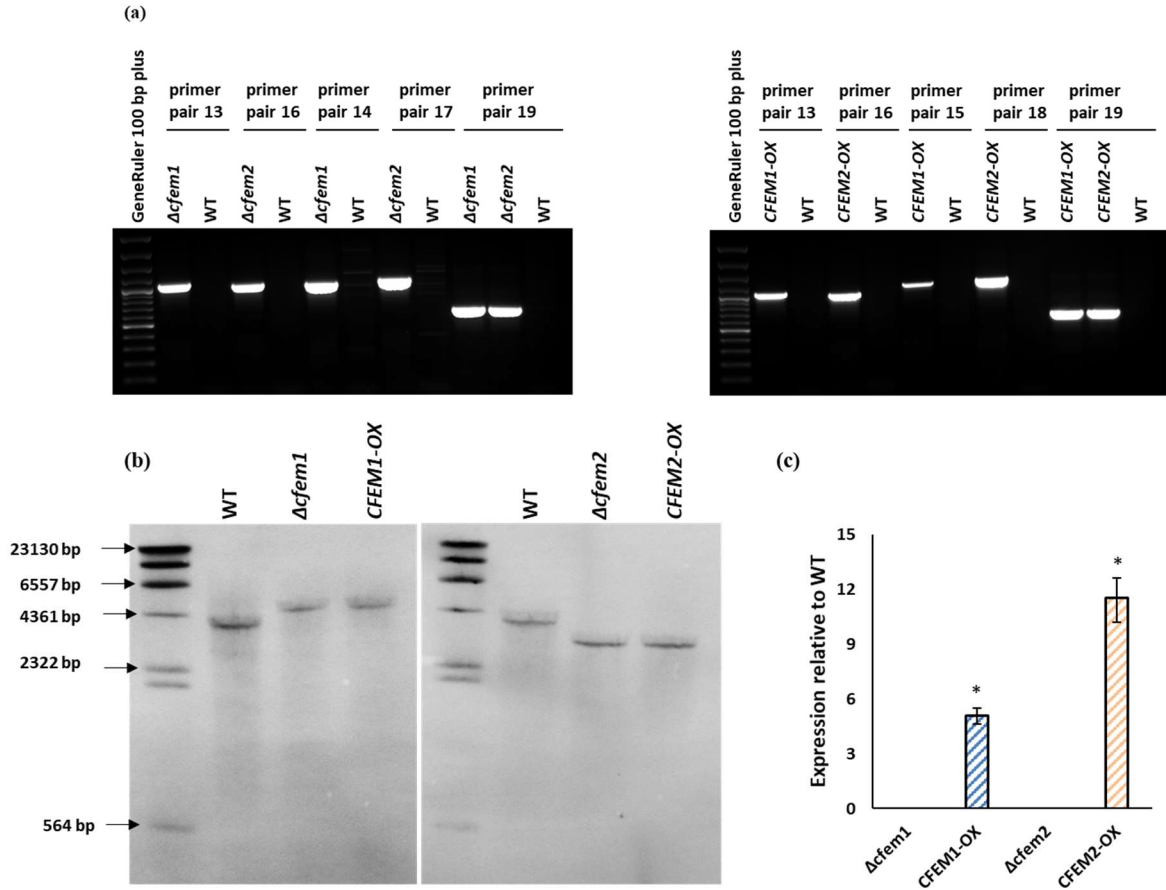


Figure 3.3: Verification of *FgCFEM1* and *FgCFEM2* disruption and overexpression transformants. (a) Amplification using primers that bind outside the homologous recombination sites was performed for verification of cross over at desired sites in the genome of the transformants. (b) Southern blot showing a single band of 4201 bp for WT and 5021 bp for *Δcfem1* and *CFEM1-OX* indicating single copy integration of *FgCFEM1* disruption and overexpression construct in *Δcfem1* and *CFEM1-OX*, respectively. A single band of 4546 bp for WT and 3516 bp for *Δcfem2* and *CFEM2-OX* transformants indicates single copy integration of *FgCFEM2* disruption and overexpression construct in *Δcfem2* and *CFEM2-OX*, respectively. (c) Transcript levels of *FgCFEM1* and *FgCFEM2* in the transformants compared to the WT estimated by RT-qPCR. *F. graminearum* β -*TUBULIN* was used for normalization. Bars represent standard error from three replicates, each performed in triplicate. Asterisks indicate statistically significant difference compared with the WT ($p < 0.05$).

3.3.3 Neither *FgCFEM1* nor *FgCFEM2* seems to have a major influence on fungal fitness

FgCFEM1 and *FgCFEM2* transformants were tested for macroconidia germination and mycelial growth. A higher percentage of germination was detected for *CFEM1-OX* at 6 hour after incubation (hai) on water agar (87% versus 73% in WT), whereas germination percentage was similar for *CFEM1-OX* and WT at 9 hai (100% and 98%, respectively). None of $\Delta cfem1$, $\Delta cfem2$ or *CFEM2-OX* showed differences in germination compared with the WT at either time point (Figure 3.4 a). Similarly, there was no difference in mycelial growth of the transformants compared with WT when cultured on PDA medium (Figure 3.3 b).

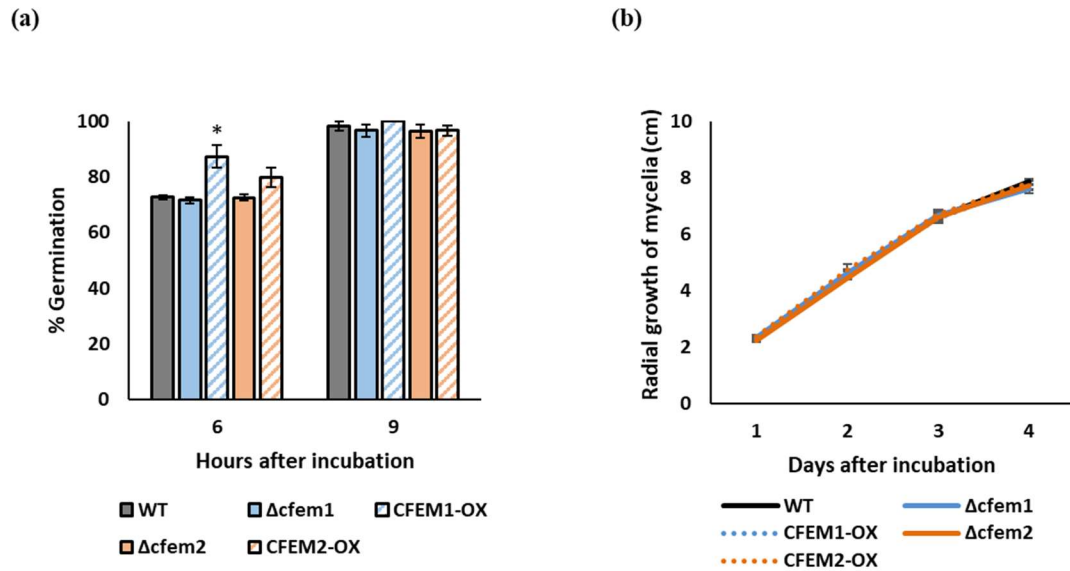


Figure 3.4: (a) Percentage of macroconidia germination in *FgCFEM1* and *FgCFEM2* transformants and the WT after 6 and 9 h of incubation on water agar at 27°C. Bars represent standard error from two independent experiments, each with five replicates. Asterisk indicates statistically significant difference compared with the WT at $p < 0.05$. (b) Radial mycelial growth of *FgCFEM1* and *FgCFEM2* transformants as well as the WT over 4 days of growth on PDA at 27°C. Bars represent standard error from five replicates.

3.3.4 Disruption or overexpression of *FgCFEM1* or *FgCFEM2* does not affect stress tolerance in *F. graminearum*

CFEM deletion mutants in other fungal species have shown higher sensitivity to cell wall stress agents (Perez et al., 2006; Zhu et al., 2017) or cell wall degrading enzymes (Sabnam and Barman, 2017). To determine if *FgCFEM1* and *FgCFEM2* have a similar role in cell wall/membrane integrity, *FgCFEM1* and *FgCFEM2* transformants were grown on PDA with stress agents targeting cell wall/membrane. The transformants did not differ from the WT in their tolerance to the tested agents (Figure 3.5 a). When tested for their sensitivity to cell wall degrading enzyme, Glucanex, the transformants and the WT showed a similar dose-dependent sensitivity to Glucanex. (Figure 3.5 b).

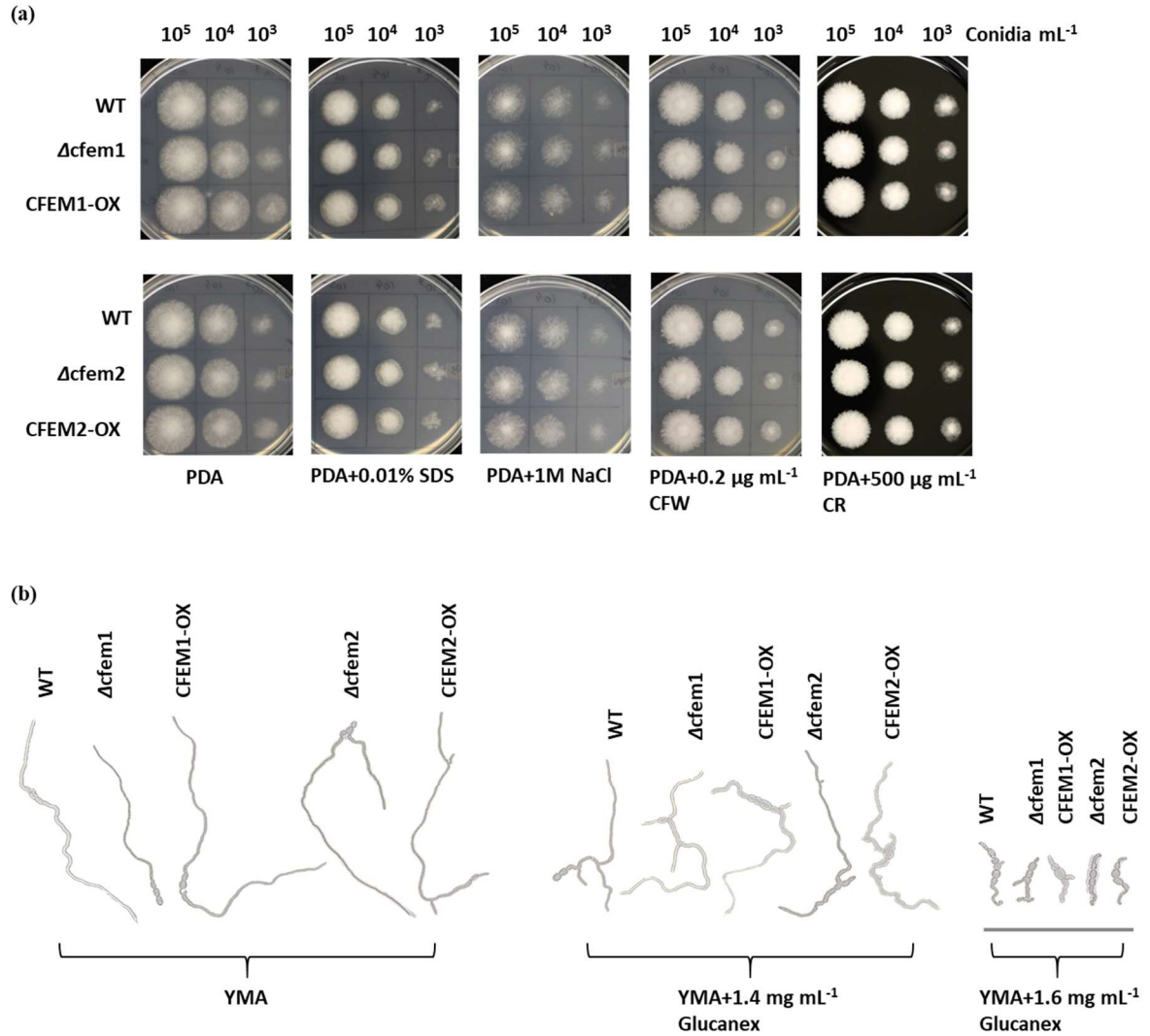


Figure 3.5: Stress tolerance of *FgCFEM1* and *FgCFEM2* transformants. (a) Mycelial growth following inoculation with different macroconidia dilutions of *FgCFEM1* and *FgCFEM2* transformants and the WT on PDA containing various stress agents. Images were taken after 40 h of growth at 25°C. Images are representative of two independent experiments, each with three replicates. (b) Germination of macroconidia of *FgCFEM1* and *FgCFEM2* transformants and the WT in YMA containing the cell wall degrading enzyme, Glucanex. Images were taken after 14 h of incubation at 28°C. Scale bar = 200 μm. Images are representative of two independent experiments, each with three replicates.

3.3.5 *FgCFEM1* or *FgCFEM2* overexpression affects DON production by *F. graminearum* in axenic cultures

To determine whether disruption or overexpression of *FgCFEM1* or *FgCFEM2* affects DON production, the transformants were grown in a DON-inducing medium. While *CFEM1-OX* transformant produced less DON compared to the WT, *CFEM2-OX* accumulated higher levels of DON in axenic cultures. Meanwhile, DON produced by $\Delta cfem1$ or $\Delta cfem2$ did not significantly differ from the WT (Figure 3.6).

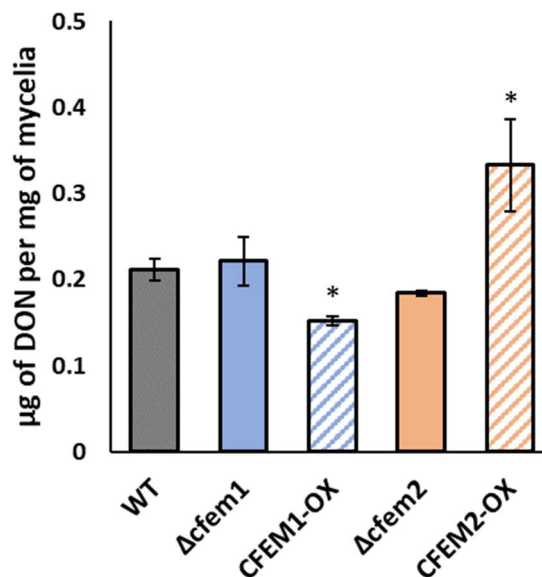


Figure 3.6: Amount of DON produced by *FgCFEM1* and *FgCFEM2* transformants as well as the WT in axenic culture. Bars represent standard error from six replicates. Asterisks indicate statistically significant difference compared with the WT at $p < 0.05$.

3.3.6 Neither *FgCFEM1* nor *FgCFEM2* is involved in cell wall penetration

Penetration by *FgCFEM1* and *FgCFEM2* transformants were compared to WT on cellophane sheets laid over minimal medium. Cellophane mimics plant cell walls, to some extent, and has been previously used to assess penetration by fungal strains (Lopez-Berges et al., 2010; Gu et al., 2014; Li et al., 2019b). No differences in cellophane

penetration were observed between transformants and WT (Figure 3.7), suggesting that *FgCFEM1* or *FgCFEM2* are not involved in cell wall penetration.

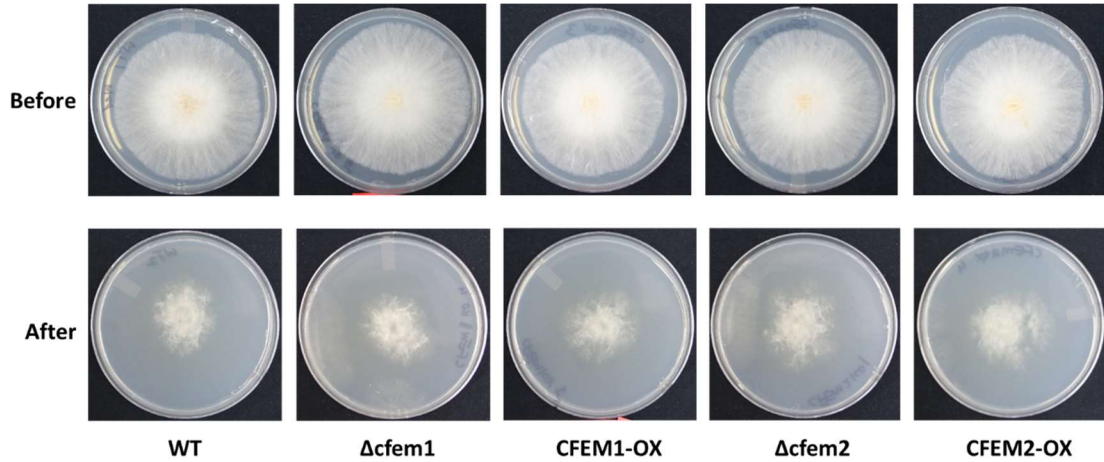


Figure 3.7: Cellophane penetration experiment. Before: *FgCFEM1* and *FgCFEM2* transformants and WT grown on cellophane sheet placed over minimal medium for 4 days at 28°C in dark. After: The cellophane sheets were removed, and the plates were returned to the incubator for 2 more days allowing penetrated hyphae to grow through the medium. Images are representative of two independent experiments, each with five replicates.

3.3.7 *FgCFEM1* overexpression leads to increased disease spread

To elucidate the potential involvement of *FgCFEM1* or *FgCFEM2* in infection, disease assays were carried out in different wheat cultivars with varying levels of resistance or susceptibility to FHB by point and spray inoculations (wheat cultivars used for infection assays and their major resistance mechanisms are available in Table 2.2). Contrary to previous studies which reported reduced disease severity for *FgCFEM1* disruption mutants in Fg820 and PH-1 (Dufresne et al., 2008; Zhang et al., 2012), disease spread by $\Delta cfem1$ in GZ3639 was comparable to WT in wheat cultivars (cvs.) Roblin (susceptible), Penhold (moderately susceptible) and Tenacious (resistant) (Figure 3.8 a). Meanwhile, *CFEM1-OX* caused 1.6 times and 1.5 times increase in disease spread in

Penhold at 12 and 18 dpi compared to WT, whereas no significant change in disease spread was observed for this strain in Roblin or Tenacious (Figure 3.8 a). Similarly, *Δcfem2* and *CFEM2-OX* transformants did not show significant difference in disease spread compared to WT (Figure 3.8 a). *FgCFEM1* and *FgCFEM2* transformants were also screened by spray inoculations. The transformants did not differ from the WT in their ability to cause initial infection in the wheat cultivars tested (Figure 3.8 b).

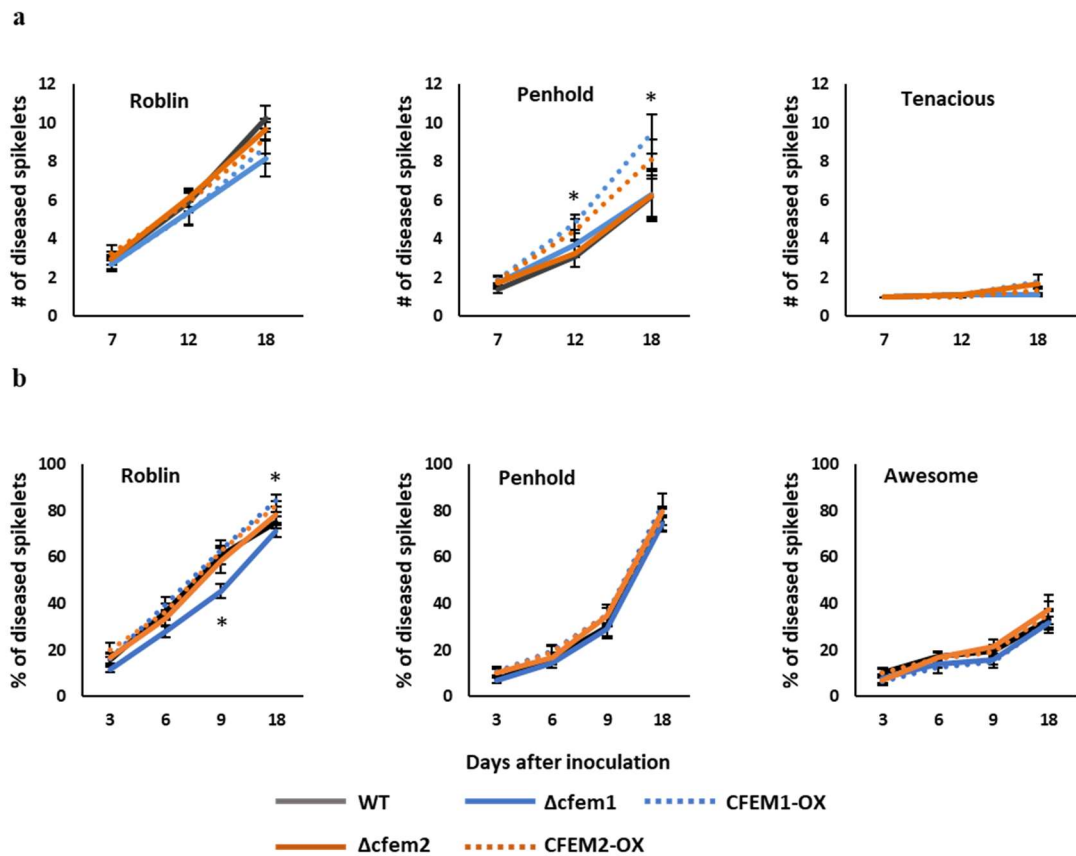


Figure 3.8: Disease severity of *FgCFEM1* and *FgCFEM2* transformants following point or spray inoculation on susceptible (Roblin), moderately susceptible (Penhold), moderately resistant (Awesome) and resistant (Tenacious) wheat cultivars. (a) Number of diseased spikelets of Roblin, Penhold and Tenacious at 7, 12 and 18 days after point inoculation with the transformants or WT. Bars represent standard error from three independent experiments, each with five replicates. Asterisks indicate statistically significant difference compared with the WT ($p < 0.05$). (b) Percentage of diseased spikelets of Roblin, Penhold and Awesome at 3, 6, 9 and 18 days after spray inoculation with the transformants or WT. Bars represent standard error from three independent

experiments, each with five replicates. Asterisks indicate statistically significant difference compared with the WT ($p < 0.05$).

3.4 Discussion

F. graminearum codes for six putatively secreted CFEM-domain containing proteins (Lu and Edwards, 2016). Two CFEM-containing proteins (FgCFEM1 and FgCFEM2) whose relative abundance was decreased in the secretomes of non-pathogenic mutants of GZ3639 (Rampitsch et al., 2013) were characterized in this study. FgCFEM1 and FgCFEM2 contain N-terminal signal peptide sequences with no transmembrane helices (Lu and Edwards, 2016), suggesting that they are secreted proteins. Moreover, these two CFEM-containing proteins have been detected from a minimal medium-based *in vitro* secretome of *F. graminearum* (Lu and Edwards, 2016).

To understand the involvement of *FgCFEM1* and *FgCFEM2* in the growth and infection of *F. graminearum*, disruption and overexpression transformants for the corresponding genes were developed in this fungus. The transformants were screened for various phenotypes including mycelial growth and macroconidia germination. Mycelial growth of the transformants was similar to WT in PDA medium, which suggests that *FgCFEM1* and *FgCFEM2* are dispensable for growth of *F. graminearum*. This is consistent with a previous study in which deletion of *FgCFEM1* did not affect mycelial growth in *F. graminearum* (Dufresne et al., 2008). Similar findings have been made for CFEM-containing proteins from other fungal species (Deng and Dean, 2008; Zhu et al., 2017).

Overexpression of *FgCFEM1* resulted in a small increase in macroconidia germination percentage in *CFEM1-OX* at 6 hai. At 9 hai, the germination percentage was

similar in *CFEM1-OX* and WT (100% and 98%, respectively) (Figure 3.4 a). However, deletion (Deng and Dean, 2008; Zhu et al., 2017) or overexpression (Zhu et al., 2017) of CFEM protein-encoding genes did not affect spore germination in other fungal species. It could be hypothesized that *FgCFEM1* expression is induced during macroconidia germination in the WT and its constitutive overexpression in *CFEM1-OX* leads to increased germination in this transformant.

FgCFEM1 or *FgCFEM2* transformants did not show an altered sensitivity to cell wall stress agents or cell wall degrading enzymes used in this study. Deletion of genes encoding CFEM proteins in some fungal species led to hypersensitivity of the mutants to stress agents or enzymes targeting the cell wall (Perez et al., 2006; Sabnam and Barman, 2017; Zhu et al., 2017). It should be considered that not all CFEM-containing proteins belong to the same category. Some of them are GPCRs with transmembrane helices (for example, PTH11 and WISH), some are GPI-anchored (BcCFEM1 and AC11), while others lack a GPI anchor site or transmembrane helices (*FgCFEM1* and *FgCFEM2*) (Kulkarni and Dean, 2004; Kulkarni et al., 2005; Lu and Edwards, 2016; Sabnam and Barman, 2017; Zhu et al., 2017). These CFEM domain-containing proteins may have different functions in the extracellular membranes of the respective fungal species.

Involvement of *FgCFEM1* and *FgCFEM2* in cell wall penetration was assessed using cellophane membranes, which mimic plant cell walls to some extent. Disruption or overexpression of *FgCFEM1* or *FgCFEM2* did not affect cellophane breaching ability of the transformants, suggesting that neither *FgCFEM1* nor *FgCFEM2* is necessary for cell wall penetration. An *M. grisea* mutant lacking *WISH*, a CFEM protein-encoding gene, was able to cause blast disease on wounded rice leaves but not on intact leaves (Sabnam

and Barman, 2017), showing the importance of this CFEM protein in host penetration. It cannot be ignored that other CFEM proteins could compensate for the loss of *FgCFEM1* or *FgCFEM2* as there are at least six putatively secreted CFEM-containing proteins in *F. graminearum* (Lu and Edwards, 2016).

CFEM1-OX accumulated less DON in axenic culture compared with the WT and also caused slightly increased disease spread in a moderately susceptible wheat cv., Penhold. While DON is required for disease spread in wheat (Proctor et al., 1995; Bai et al., 2002), the correlation between DON accumulation levels and disease spread is not clearly understood. Some studies showed an association between DON accumulation and *F. graminearum* aggressiveness in terms of disease spread in some wheat genotypes (Foroud et al., 2012), whereas others did not detect such an association (Gilbert et al., 2010). Additionally, it has not yet been determined whether DON accumulation in axenic culture by *CFEM1-OX* reflects its DON production *in planta*. A small but significant difference in disease spread was only observed in the moderately susceptible cv. Penhold, but not in susceptible cv. Roblin or resistant cv. Tenacious. It is possible that the contribution of *FgCFEM1* to *F. graminearum* aggressiveness is too small to detect the difference in disease spread between *CFEM1-OX* and WT in resistant wheat cultivars, where the disease is mostly confined to inoculated spikelet, or susceptible ones, where disease spread occurs too fast.

FgCFEM1 disruption ($\Delta cfem1$) did not have a major effect on the aggressiveness of *F. graminearum* in wheat spikes, probably due to a minor role, if any, of *FgCFEM1* in *F. graminearum* aggressiveness. Contrary to this, two separate studies have shown a reduced aggressiveness for *FgCFEM1* deletion mutants in wheat spikes (Dufresne et al.,

2008) and wheat coleoptiles (Zhang et al., 2012). All the transformants in the present study, including *Δcfem1*, were developed in the GZ3639 strain of *F. graminearum*, whereas *FgCFEM1* deletion mutants in the previous studies were developed using other strains; strain Fg820 in Dufresne et al. (2008) and PH-1 in Zhang et al. (2012). It is unknown whether *FgCFEM1* from different *F. graminearum* strains contribute differently to aggressiveness. However, CFEM mutants (*Δpth11*) generated in different strains of *M. grisea* varied in aggressiveness and in their ability to differentiate into appressoria on barley leaves (DeZwaan et al., 1999). Furthermore, a cerato-platanin encoding gene, *MSPI*, had different roles in infection by two different *M. grisea* strains. While deletion of this gene in *M. grisea* strain Guy 11 did not affect its aggressiveness in rice (Wang et al., 2016), deletion of the same gene in strain 70-15 led to reduced aggressiveness (Jeong et al., 2007).

Characterization of *FgCFEM1* and *FgCFEM2* herein shows that two CFEM-containing proteins from the same species may have different roles in fungal growth and infection. While overexpression of *FgCFEM1* had a small effect on macroconidia germination and disease spread, overexpression of *FgCFEM2* did not show any phenotype for these traits (Figures 3.4 a & 3.8 a). In addition, *CFEM1-OX* produced less DON in axenic culture, whereas *CFEM2-OX* produced more DON compared to the WT (Figure 3.6). CFEM domains of different proteins, apart from the pattern of conserved cysteines, exhibit considerable sequence diversity (Kulkarni et al., 2003; Zhang et al., 2015). Moreover, CFEM proteins from a same fungus may have varying expression patterns (Vaknin et al., 2014) or could be localized to different locations which might explain different functions of CFEM proteins from the same fungal species.

Table 3.1: Primers used for various experiments in this chapter

Primer pair	Primer name	Primer sequence (5'-3') (Tm °C)	Purpose
1	Fg02077-F1	ATGAAGTACTCCGTCGCTT (53.4)	Amplification of <i>FgCFEM1</i>
	Fg02077-R778	CGATAGCGTTTCCAATTCTCA (52.9)	
2	Fg02077-f1094(+)	CTGAGCATCGAGTGGAACA (54.9)	Amplification of upstream of <i>FgCFEM1</i>
	Fg02077-r287 (+)	CAATTGCATGAGGTGTGGTC (54.3)	
3	Fg02077-f1149(-)	AAAGGCCCTTCTTTGTTGGT (55.0)	Amplification of downstream of <i>FgCFEM1</i>
	Fg02077-r1850(-)	TCTGCGAGGAGAATTGGAGT (55.7)	
4	Fg08554-5'UTR55	CATCAATCGCTCAAGCAAAA (51.7)	Amplification of <i>FgCFEM2</i>
	Fg08554-R677	AGCAATAATGGCGAGGAGAC (54.9)	
5	Fg08554-f1069(+)	CAAAATCAAGAGGGCTGGTG (54.1)	Amplification of upstream of <i>FgCFEM2</i>
	Fg08554-r257(+)	CTCCATGCCATACCTGTTCT (54.4)	
6	Fg08554-f1830(-)	GTCTCTCCAGCCCGTAATCA (56.3)	Amplification of downstream of <i>FgCFEM2</i>
	Fg08554-r2553(-)	GTCGAGACGGTTGTTTGTGTT (55.5)	
7	Fg02077-F1OX	ggacttaauATGAAGTACTCCGTC (52.5)	Amplification of <i>FgCFEM1</i> with adaptors
	Fg02077-R778OX	gggttaauCGATAGCGTTTCCAAT (55.6)	
8	Fg02077-f1094(+)KO	ggtcttaauCTGAGCATCGAGTG (55.1)	Amplification of upstream of <i>FgCFEM1</i> with adaptors
	Fg02077-r287(+)KO	ggcattaauCAATTGCATGAGGTG (55.1)	
9	Fg02077-f1149(-)KO	ggacttaauAAAGGCCCTTCTTTG (53.9)	Amplification of downstream of <i>FgCFEM1</i> with adaptors
	Fg02077-r1850(-)KO	gggttaauTCTGCGAGGAGAATTG (56.2)	
10	Fg08554-F1OX	ggacttaauATGAAGGCTACCCTC (54.5)	Amplification of <i>FgCFEM2</i> with adaptors
	Fg08554-R677OX	gggttaauAGCAATAATGGCGAG (54.2)	
11	Fg08554-f1069(+)KO	ggtcttaauCAAAATCAAGAGGGC (54.1)	Amplification of upstream of <i>FgCFEM2</i> with adaptors
	Fg08554-r257(+)KO	ggcattaauCTCCATGCCATACC (56.0)	
12	Fg08554-f1830(-)KO	ggacttaauGTCCTCCAGCCC (57.4)	Amplification of downstream of <i>FgCFEM2</i> with adaptors
	Fg08554-r2553(-)KO	gggttaauGTCGAGACGGTT (57.2)	
13	Fg02077-M2	TTCAATATCTTCAGCTAGCAAGAGG (54.6)	Verification of cross over in $\Delta cfem1$ and <i>CFEM1-OX</i>
	RF-2	TCTCCTTGCATGCACCATTCCTTG (59.8)	
14	RF-1	AAATTTTGTGCTCACCGCCTGGAC (60.5)	Verification of cross over in $\Delta cfem1$
	Fg2077-M1	TACTAAGTGTAGCCAGCGTTTCG (56.5)	
15	RF-3	TTGCGTCAGTCCAACATTTGTTGCCA (61.7)	Verification of cross over in <i>CFEM1-OX</i>
	Fg2077-M3	AAACGAAAGAGGGAGAGAAGTAAGGT (57.5)	
16	Fg08554-M2	GGTTATCCGTTGGTTCAATTAAGGT (55.4)	Verification of cross over in $\Delta cfem2$ and <i>CFEM2-OX</i>
	RF-2	TCTCCTTGCATGCACCATTCCTTG (59.8)	
17	RF-1	AAATTTTGTGCTCACCGCCTGGAC (60.5)	Verification of cross over in $\Delta cfem2$
	Fg08554-M1	ATATTTGGGCTCCTGGTCTGTTTG (57.3)	
18	RF-3	TTGCGTCAGTCCAACATTTGTTGCCA (61.7)	Verification of cross over in <i>CFEM2-OX</i>
	Fg08554-M3	GAAGAATAGAGACGCGGGCTTGTAT (58.6)	

Primer pair	Primer name	Primer sequence (5'-3') (Tm °C)	Purpose
19	Hyg588U Hyg588L	AGCTGCGCCGATGGTTTCTACAA (61.3) GCGCGTCTGCTGCTCCATACAA (62.3)	Amplification of <i>hph</i> gene from transformants
20	CFEM1-SB-F1 CFEM1-SB-R1	TTTCAATCTCTGCGCTGTTG (53.7) CGCTTCTGGCCTGTCTATTC (55.6)	Probe synthesis for <i>FgCFEM1</i> transformants for Southern blotting
21	CFEM2-SB-F1 CFEM2-SB-R1	CATGTCCCGAGAATCAATCC (53.1) CCCGTGGTTAACTTTTTGGA (53.1)	Probe synthesis for <i>FgCFEM2</i> transformants for Southern blotting
22	CFEM1OX-seq-F CFEM1OX-seq-R	TCTTCCCATCCAAGAACCTTT (53.9) CGATAGCGTTTCCAATTCTCA (52.9)	Amplification and sequencing of <i>FgCFEM1</i> gene from <i>CFEM1-OX</i>
23	CFEM2OX-seq-F CFEM2OX-seq-R	TTCCCATCCCTTATTCCTTTG (52.3) AATGGCAACCTGTTGTGTTTC (54.3)	Amplification and sequencing of <i>FgCFEM2</i> gene from <i>CFEM2-OX</i>
24	Fg02077-F1 Fg02077-R1	ATTGACGAGTGTGGTACCGAC (56.8) GACTTGGCCTCAGACTCCTTG (57.5)	Expression analyses of <i>FgCFEM1</i> in $\Delta cfem1$ and <i>CFEM1-OX</i> by RT-qPCR
25	Fg08554-F1 Fg08554-R1	GCCATCTTCTCAAGCATCCCT (57.2) GATCCACCTCCCTCAGTCATG (56.9)	Expression analyses of <i>FgCFEM2</i> in $\Delta cfem2$ and <i>CFEM2-OX</i> by RT-qPCR
26	B-tub-F B-tub-R	GTTCTGGACGTTGCGCATCTG (59.0) TGATGGCCGCTTCTGACTTCC (59.7)	Normalization of <i>FgCFEM1</i> and <i>FgCFEM2</i> transcript levels

Chapter 4: Expression of the elongation factor 1A gene under the strong constitutive *GPDA* promoter affects fungal fitness, DON production and aggressiveness in *Fusarium graminearum*

4.1 Introduction

Translation elongation factor 1A (EF1A) is one of the most abundant proteins found in eukaryotic cells (Merrick, 1992). It is a G-protein involved in protein synthesis and its canonical function is to deliver aminoacyl-tRNAs (aa-tRNAs) to the ribosome during translation elongation. EF1A in its GTP-bound state binds aa-tRNA (Carvalho et al., 1984). A correct pairing of messenger RNA (mRNA) and cognate aa-tRNA triggers GTPase activity of EF1A, leading to the conversion of EF1A-GTP to EF1A-GDP and the release of aa-tRNA to the A-site of the ribosome (Taylor et al., 2007). The GDP bound to EF1A is exchanged for a GTP by a guanidine nucleotide exchange factor (GEF) and the resulting EF1A-GTP takes part in another round of translation elongation (Janssen and Moller, 1988) (Figure 4.1). In yeast, the GEF consists of two subunits, α and γ , also called EF1B and EF1G, respectively. In higher eukaryotes, the GEF complex contains a third subunit, β (in plants) or δ (in metazoans); this subunit is also called EF1D (reviewed in: Sasikumar et al., 2012; Li et al., 2013).

Besides its canonical role in translation, EF1A is also involved in several moonlighting functions. (reviewed in: Thornton et al., 2003; Sasikumar et al., 2012). EF1A was proposed to play a role in nuclear export of tRNAs (Grosshans et al., 2000). EF1A also participates in proteolysis by directing misfolded or damaged proteins to proteasome (Chuang et al., 2005). In higher eukaryotes, EF1A occurs in two different isoforms, EF1A1 and EF1A2. While the former functions as a proapoptotic factor, the

latter was reported to be antiapoptotic (Ruest et al., 2002) and a human oncogene (reviewed in Thornton et al., 2003). Another role of EF1A is in viral propagation through its interaction with viral proteins including RNA-dependent RNA polymerase (Yamaji et al., 2006). EF1A also binds and bundles actin filaments in yeast and other organisms (Kurasawa et al., 1992; Munshi et al., 2001). Competitive binding experiments showed that binding of EF1A to F-actin and aa-tRNA is mutually exclusive and also suggest that their binding sites in EF1A may overlap. Affinity of EF-1A to F-actin is pH-dependent; as pH increases, EF1A affinity for F-actin decreases which shifts binding of EF-1A from F-actin to aa-tRNA (Liu et al., 1996).

Consistent with the role of EF1A in actin binding, alterations in EF1A levels can lead to organizational changes in the actin cytoskeleton (Munshi et al., 2001), and disruption of actin filaments affects protein synthesis (Stapulionis et al., 1997), suggesting a reciprocal regulation of two separate cellular processes (Sasikumar et al., 2012). The actin cytoskeleton could serve as a scaffold for cellular translation machineries facilitating a spatial ordering of translation components and their co-ordinated interactions leading to efficient translation (Sasikumar et al., 2012). Overexpression of *EF1A* in *Saccharomyces cerevisiae* resulted in reduced budding, but no discernible effect on protein synthesis was observed (Munshi et al., 2001). Similarly, elevated EF1A levels affected growth and nuclear organization in human and yeast cells. Its overexpression also affected metabolism and amino acid homeostasis in yeast (Tarrant et al., 2016).

EF-Tu, the prokaryotic homologue of the eukaryotic EF1A, is responsible for the transport of aa-tRNA to the ribosome during translation elongation (Sprinzl, 1994). It is also one of the highly conserved and most abundant proteins in bacteria (Jeppesen et al.,

2005). In addition to its role in protein synthesis, EF-Tu also acts as elicitor of plant innate immunity. In fact, EF-Tu is a well-studied pathogen-associated molecular pattern (PAMP) which triggers defense responses in Arabidopsis and other Brassicaceae species (Kunze et al., 2004). Arabidopsis plants recognize the N-terminus of EF-Tu from *E. coli*; an N-acetylated epitope of this protein comprising the first 18 amino acids (elf18) was found to be sufficient for the full eliciting activity of EF-Tu in Arabidopsis. Arabidopsis leaves treated with elf18 showed increased biosynthesis of ethylene and production of reactive oxygen species. This treatment also triggered resistance to subsequent infections by pathogenic bacteria (Kunze et al., 2004).

EF-Tu is recognized by a receptor kinase known as EF-Tu receptor (EFR) (Zipfel et al., 2006), located in the plasma membrane of the plant cells. *Nicotiana benthamiana* is naturally unable to perceive EF-Tu or elf18; however, transient expression in *N. benthamiana* of Arabidopsis *EFR* made the plant responsive to EF-Tu. Moreover, Arabidopsis plants mutated for EFR became non-responsive to EF-Tu, suggesting that EF-Tu is recognized by the Arabidopsis EFR (Zipfel et al., 2006). EF-Tu is a cytoplasmic bacterial protein, whereas EFR, which is able to perceive EF-Tu is localized at the plasma membrane of plant cells. This interaction is likely made possible by the secretion of EF-Tu during host plant infection; the protein has been detected in the secretomes of *Xanthomonas campestris*, *Pseudomonas fluorescens* and *Erwinia chrysanthemi* (Kazemi-Pour et al., 2004; Singh et al., 2004; Watt et al., 2005).

EF-Tu is also recognized by rice plants, but a different sequence is required for this recognition: rather than the N-terminal peptide recognized by AtEFR, a 50 residue stretch within the EF-Tu sequence (amino acids from 176 to 225; EFa50) is required for

PAMP activation in rice (Furukawa et al., 2014). EF-Tu-treated rice leaves showed callose deposition, H₂O₂ synthesis and resistance to co-inoculation with pathogenic bacteria (Furukawa et al., 2014). The requirement of distinct EF-Tu epitopes for elicitation of immune responses in Arabidopsis and rice indicates that different plant species evolved to recognize different regions of EF-Tu.

Fungal elongation factors have not been reported as PAMPs, but the EF1A protein (FgEF1A) of *F. graminearum* has been detected in the secretome under DON-inducing conditions which, to some extent, mimics the conditions during interaction with the host. The abundance of this protein was found to be reduced in the secretome of two non-pathogenic mutants of GZ3639 strain (*Δtri6* and *Δtri10*) compared to WT secretome (Rampitsch et al., 2013), suggesting a role for FgEF1A in *F. graminearum* infection. In order to study its potential involvement in infection, I generated and characterized *FgEF1A* overexpression transformants (*GPDA:EF1A*).

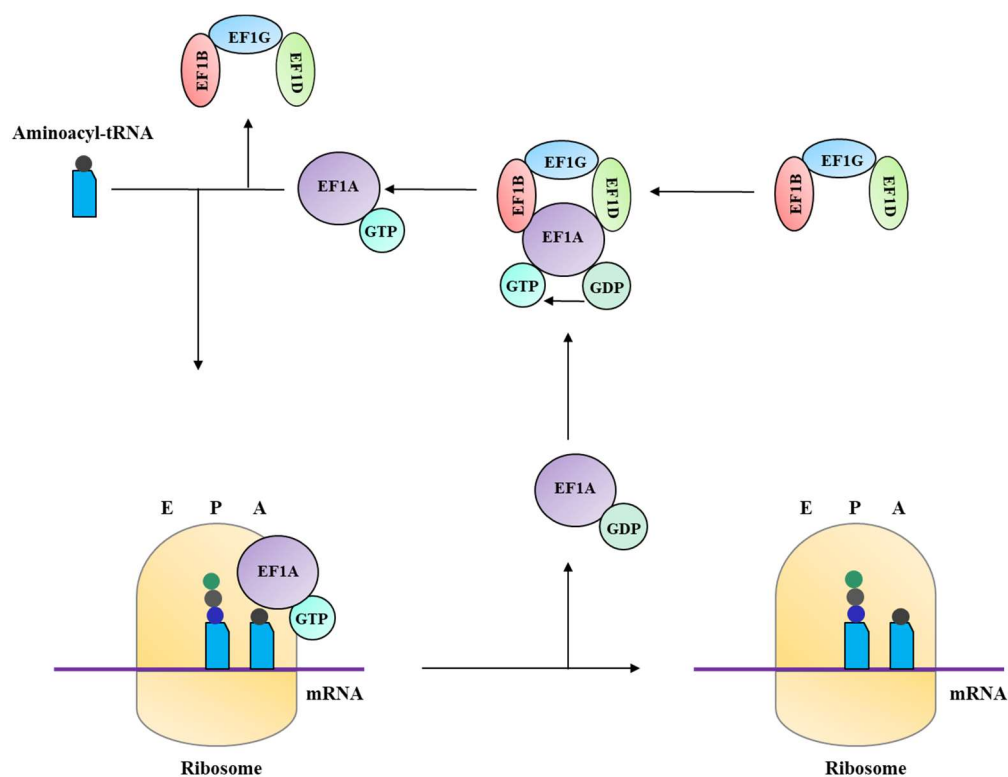


Figure 4.1: Role of EF1A in eukaryotic translation elongation. EF1A when bound to GTP transports aminoacyl-tRNA (aa-tRNA) to the A-site of ribosome. Codon-anticodon pairing stimulates the GTPase activity of EF1A leading to the hydrolysis of GTP and the release of aa-tRNA to the A-site of ribosome. The GDP bound to EF1A is exchanged for GTP by a guanine nucleotide exchange factor (GEF), which in higher eukaryotes consists of three subunits, EF1B, EF1D and EF1G. The EF1A-GTP is now ready to participate in another round of elongation. The drawing was adapted from Li et al., 2013.

4.2 Materials and Methods

4.2.1 Generation of *FgEF1A* overexpression transformants

FgEF1A overexpression construct (pRF-HU2E::*EF1A-OX*) was developed using the same vector and protocol used to generate *FgCPPI* overexpression construct. Figure 2.1 b in Chapter two provides a schematic representation of the protocol, and pRF-HU2E vector was prepared as detailed in section 2.2.3.1. The inserts were prepared by two rounds of PCR, as described in section 2.2.3.1, using primers presented in Table 4.1. For the first PCR, primer pairs 1 and 2 were used to amplify the first 837 bp of *FgEF1A* and

773 bp region upstream of its transcriptional start site from *F. graminearum* GZ3639 genomic DNA, respectively. The second PCR to add adaptor sequences was employed with primer pairs 3 and 4 (see Table 4.1 for details). The inserts were cloned into pRF-HU2E vector (section 2.2.3.1), transformed into *Agrobacterium tumefaciens* strain LBA4404 (section 2.2.3.2), which was then used for transformation of *F. graminearum* strain GZ3639 (section 2.2.3.3).

Four *GPDA:EF1A* transformants (*GPDA:EF1A-C1* to *GPDA:EF1A-C4*) were developed from two independent transformation experiments. *GPDA:EF1A-C1* was obtained from the first round of *A. tumefaciens*-mediated transformation of *F. graminearum* and the remaining were generated in the second round of transformation using the same overexpression construct.

4.2.2 Verification of *FgEF1A* overexpression transformants

GPDA:EF1A transformants were verified by PCR using genomic DNA of the transformants. DNA isolation, PCR reaction and thermocycling conditions were same as described in section 2.2.3.1. To ensure that the overexpression construct had integrated at the desired site of the *F. graminearum* genome, PCR using primer pairs 5 and 6 was performed. Primer pair 7 was used to amplify *hygromycin phosphotransferase* gene (*hph*) from the transformants. Primer pairs used for verification and primer binding sites in the transformants are shown in Figure 4.2 a.

Copy number of *FgEF1A* overexpression construct in *GPDA:EF1A* transformants was determined by Southern blotting. Genomic DNA from the transformants was digested with *StuI* and *NcoI* (NEW ENGLAND BioLabs® Inc.). Primer pair 8 was used for probe synthesis and hybridization with probe was performed overnight at 44°C. The

remaining part of the experiment was performed as described in section 2.2.3.4.

Restriction enzyme cutting sites and probe binding sites are indicated in Figure 4.2 b.

FgEF1A sequence from the transformants was amplified (primer pairs 9, 10, 11 and 12) using a high fidelity Phusion Hotstart II DNA polymerase (Thermo Scientific) and purified PCR products were sequenced to confirm that no mutation(s) were introduced in the *FgEF1A* sequence for the *GPDA:EF1A* transformants.

FgEF1A expression levels in *GPDA:EF1A* transformants were determined by RT-qPCR (primer pair 13). Using QIAGEN's RNeasy Plant Mini Kit, total RNA was isolated from 100 mg of mycelia collected from potato dextrose broth. cDNA synthesis and RT-qPCR were performed as discussed in section 2.2.3.4. *F. graminearum* β -TUBULIN (FGSG_09530) was used for normalization (primer pair 14).

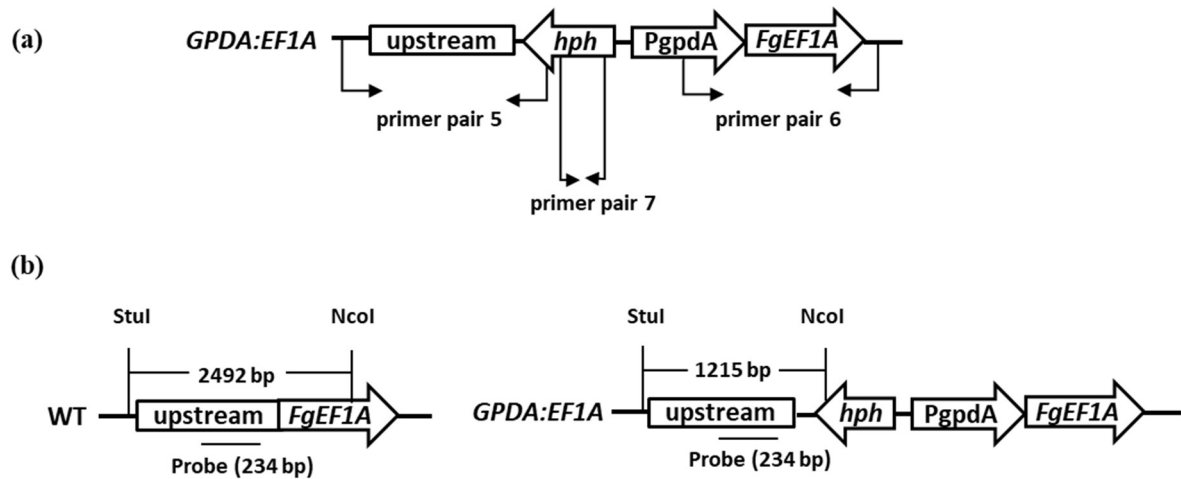


Figure 4.2: Schematics showing (a) annealing sites of the primers used for verification of successful crossover during the integration of the expression cassette for *GPDA:EF1A* transformants, and (b) restriction enzyme cutting sites and probe binding sites in WT and *GPDA:EF1A* transformants for Southern blotting.

4.2.3 *In vitro* characterization of *GPDA:EF1A* transformants

Mycelial growth and macroconidia germination in *GPDA:EF1A* transformants and DON accumulation in axenic culture by *GPDA:EF1A-C1* were performed as described in respective sections of Chapter two.

4.2.4 Infection assays on wheat spikes by spray and point inoculations

GPDA:EF1A-C1 was screened following spray and point inoculations in spikes of wheat cultivars Roblin, Penhold, Awesome and Tenacious. The major resistance mechanisms of these wheat cultivars are provided in Table 2.2. *GPDA:EF1A-C2* to *-C4* transformants were screened in separate experiment following point inoculation in Roblin. Inoculations and disease evaluations were carried out as detailed in section 2.2.6.

4.2.5 Identification of FgEF1A amino acid sequences for peptide synthesis

elf18 and EFa50 elicit immunity in Arabidopsis and rice, respectively (Kunze et al., 2004; Furukawa et al., 2014). In order to identify FgEF1A regions similar to these two EF-Tu epitopes, FgEF1A amino acid sequence (GenBank accession number XP_011319909.1) was aligned with elf18 or EFa50 sequences. Three regions were identified for peptide synthesis: peptide P1 with 53% identity to elf18 (Figure 4.3 a), and P2 and P3 with 30% and 50% identities to EFa50, respectively (Figure 4.3 b & c). A region unique to FgEF1A was also identified by aligning FgEF1A with Arabidopsis EF1A (GenBank accession number NP_200847.1) and the unique sequence was selected to synthesize the peptide P4 (Figure 4.3 d). The alignments were performed with blastp option in NCBI. The select peptides were synthesized by GenScript. P1 = N-acetylated

GKEEKTHLNVVVIG, P2 = GIDKRTIEKFEKEAAELGKG, P3 =
IEPPKRPNDKPLRLPLQDVYKIGGIG and P4 = GWEREIKSGKLS.

(a)

	Score	Expect	Identities	Positives	Gaps
	18.5 bits(36)	0.010	9/17(53%)	9/17(52%)	4/17(23%)
Query	2	KEKFERTKPHVNVGTIG	18		
		KE E T H NV IG			
Sbjct	3	KE--EKT--HLNVVVIG	15	→	P1

(b)

	Score	Expect	Method	Identities	Positives	Gaps
	11.2 bits(17)	9.8	Composition-based stats.	6/20(30%)	9/20(45%)	0/20(0%)
Query	30	AIDKPFLLPIDVFSISGRG	49			
		IDK + E + G+G				
Sbjct	34	GIDKRTIEKFEKEAAELGKG	53	→	P2	

(c)

	Score	Expect	Method	Identities	Positives	Gaps
	31.2 bits(69)	1e-06	Composition-based stats.	13/26(50%)	17/26(65%)	0/26(0%)
Query	24	IPEPERAIDKPFLLPIDVFSISGRG	49			
		I P+R DKP LP++DV+ I G G				
Sbjct	234	IEPPKRPNDKPLRLPLQDVYKIGGIG	259	→	P3	

(d)

Query	180	KVGYNPDKIPFVPISGFEGDNMIERSTNLDWYKG-----PTLLEALDQINEPK	227
		KVGYNP + FVPISGF GDNM+ STN WYKG	TLLEA+D I PK
Sbjct	179	KVGYNPKAVAFVPISGFNGDNMLTASTNCPWYKGWEREIKSGKLSGKTLLEAIDSIEPPK	238

↓

P4

Figure 4.3: Alignment of FgEF1A sequence with elf18 (a), EFa50 (b & c) or Arabidopsis EF1A (d). The amino acid sequence used for peptide synthesis are indicated as P1 (a), P2 (b), P3 (c) and P4 (d).

4.2.6 Eliciting activities of FgEF1A peptides

4.2.6.1 Callose induction in Arabidopsis

For the callose induction experiment, the protocol by Schenk and Schikora (2015) was employed with slight modifications. Sixty seeds of *A. thaliana* Col-0 were surface

sterilized in 70% ethanol for 5 min, washed three times in sterile distilled water and randomly distributed into 6 wells (10 seeds per well) of a 24-well tissue culture plate (VWR, catalogue # 10861-558) with 1 mL Murashige and Skoog (MS) medium (Murashige and Skoog, 1962). The plates were incubated at 4°C in the dark for 3 days before transferring to a growth chamber at 22°C and 16/8 h day/night cycle. The media was replaced with 1 mL fresh MS on day 7, and seedlings in each well were treated on day 9 with 10 µL of 100 µM FgEF1A peptide in sterile distilled water for 24 h. Each peptide was assessed separately. The same concentration of flg22 or water served as positive and negative controls, respectively. Seedlings were then cleared in 1:3 acetic acid/ethanol until the material was transparent (usually overnight). The cleared seedlings were washed in 150 mM K₂HPO₄ for 30 min and stained for 2 h with 0.01% aniline blue in 150 mM K₂HPO₄ in a Falcon tube wrapped with aluminum foil. Callose was visualised using EVOS FL Auto Imaging System (Thermo Scientific™) with DAPI filter.

4.2.6.2 β-1,3-glucanase assay in wheat seedlings

To study the potential eliciting activity of FgEF1A peptides, β-1,3-glucanase activity was measured from 10-day-old Roblin seedlings sprayed with FgEF1A peptides. Seedlings grown in root trainers were sprayed until run off with 1 µM of P1, P2, P3, P4, flg22 or sterile distilled water with 0.2% Tween 20. Samples from each treatment were collected at 12, 24 and 48 h after spraying and flash frozen in liquid nitrogen. The experiment was repeated twice, each with three replications (seedlings) per treatment per time point. Samples were ground in liquid nitrogen and 1.5 mL of 0.05 M sodium acetate buffer pH 5.2 was added per g of ground tissue. The homogenate was centrifuged at 10000 rpm for 20 min at 4°C and the supernatant was used for β-1,3-glucanase assay.

The total protein concentration for each sample was determined by the Bradford method (Bradford, 1976) using 0.25-1.50 mg mL⁻¹ bovine serum albumin (Sigma-Aldrich) as a standard. A β -1,3-glucanase assay was performed by incubating 10 μ L of the supernatant with 20 μ L of 0.75% laminarin (w/v of 0.05 M sodium acetate buffer pH 5.2) in PCR strip tubes (AXYGEN) at 50°C for 10 min. Afterwards, 100 μ L of 3,5-dinitrosalicylic acid (DNS) reagent was added and the samples heated at 95°C for 5 min. After the reaction was cooled to 25°C for 2 min, 100 μ L of reaction mixture was transferred to a 96-well microplate (VWR, catalogue# 10861-562) and absorbance was measured at 540 nm in a microplate reader (Synergy HT Micro-Detection Reader, Bio Tek Instruments). β -1,3-glucanase activity was determined as the amount of reducing sugar (μ mol) released per min per mg of protein using 0.1-1.0 mg mL⁻¹ glucose as a standard.

4.2.7 Statistical analyses

Relative expression of *FgEF1A* in *GPDA:EF1A* transformants was determined using REST© software (Pfaffl et al., 2002). Analyses for *in vitro* DON assay and *GPDA:EF1A-CI* infection assay were performed using unpaired t-test at $p < 0.05$. Data from the remaining experiments, including disease assays for remaining transformants, were analyzed by one-way ANOVA at $p < 0.05$. Treatment means were separated by Fisher's least significant difference (LSD).

4.3 Results

4.3.1 *FgEF1A* in locus expression from a *glyceraldehyde-3-phosphate dehydrogenase* overexpression promoter resulted in a limited increase in transcript levels

GPDA:EF1A transformants were developed by replacing *FgEF1A* native promoter with a strong constitutive *glyceraldehyde-3-phosphate dehydrogenase* (*GPDA*) promoter from *Aspergillus nidulans*, through homologous recombination. Recombination at desired sites in the genome and presence of *hph* were verified by PCR (Figure 4.4 a & b; see Figure 4.2 a for primer annealing sites in the transformants). Copy number estimation was performed by Southern blotting and the results showed single integration of the overexpression construct in *GPDA:EF1A* transformants (Figure 4.4 c; refer to Figure 4.2 b for restriction enzyme cutting and probe binding sites). *FgEF1A* expression in *GPDA:EF1A* transformants was determined by RT-qPCR. While the transcript levels of *FgEF1A* gene in *GPDA:EF1A-C1* did not significantly differ from the WT, the remaining three transformants (*GPDA:EF1A-C2*, *GPDA:EF1A-C3* and *GPDA:EF1A-C4*) did show a small but significant increase in expression (Figure 4.4 d).

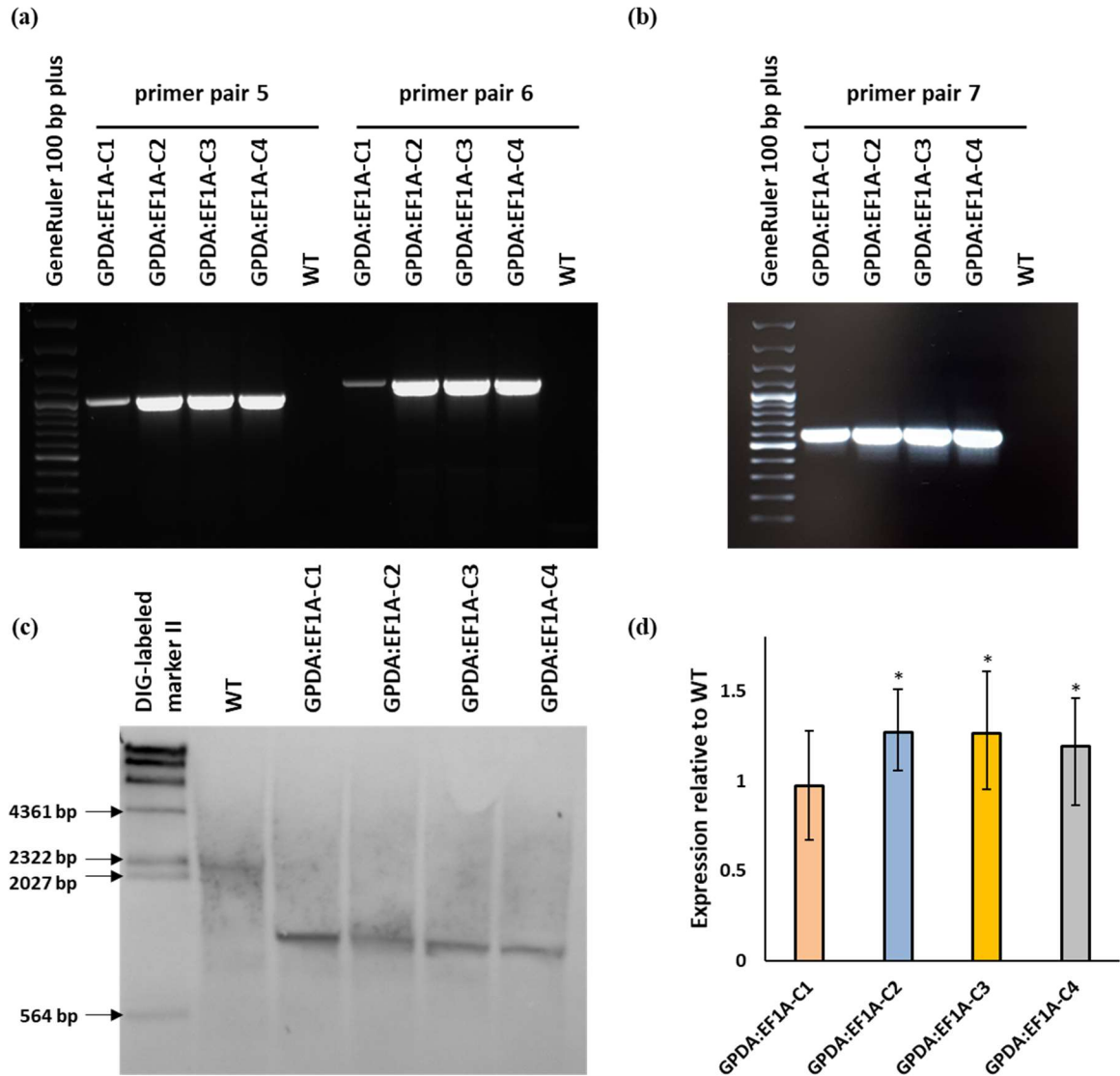


Figure 4.4: Verification of *GPDA:EF1A* transformants. (a) Amplification using primers that bind outside the homologous recombination sites was performed for verification of cross over at desired sites in the genome of the transformants. (b) Amplification of *hph* from *GPDA:EF1A* transformants. (c) Southern blot showing a single band of 2492 bp for WT and 1215 bp for *GPDA:EF1A* transformants indicating single copy integration of *FgEF1A* overexpression construct in *GPDA:EF1A* transformants. (d) Transcript levels of *FgEF1A* in *GPDA:EF1A* transformants compared to the WT estimated by RT-qPCR. *F. graminearum* β -*TUBULIN* was used for normalization. Bars represent standard error from three replicates, each performed in triplicate. Asterisks indicate statistically significant difference compared with the WT ($p < 0.05$).

4.3.2 *GPDA:EF1A* transformants exhibit reduced fitness

Macroconidia germination in *GPDA:EF1A-C1*, *GPDA:EF1A-C2*, *GPDA:EF1A-C3* and *GPDA:EF1A-C4* was studied by incubating macroconidia of the transformants and the WT in water agar. Delayed germination was observed for macroconidia of all *GPDA:EF1A* transformants. While almost 80% of WT macroconidia germinated at 6 hour after incubation (hai), the germination in *GPDA:EF1A* transformants ranged between 22-27% for this time point. By 9 hai, nearly 100% germination was observed for WT macroconidia, whereas only less than 50% of the macroconidia from the transformants had germinated (Figure 4.5 a). Mycelial growth of *GPDA:EF1A-C1*, *GPDA:EF1A-C2*, *GPDA:EF1A-C3* and *GPDA:EF1A-C4* was compared with WT by growing them on PDA for 5 days. No difference in growth was observed between the transformants and the WT at 1 day after incubation (dai). At 2 dai, *GPDA:EF1A-C1*, *GPDA:EF1A-C2* and *GPDA:EF1A-C4* showed reduced growth, whereas growth in *GPDA:EF1A-C3* did not differ from the WT. While there was no difference in mycelial growth at 3 dai, the transformants had a reduced growth at 4 and 5 dai, compared to the WT (Figure 4.5 b).

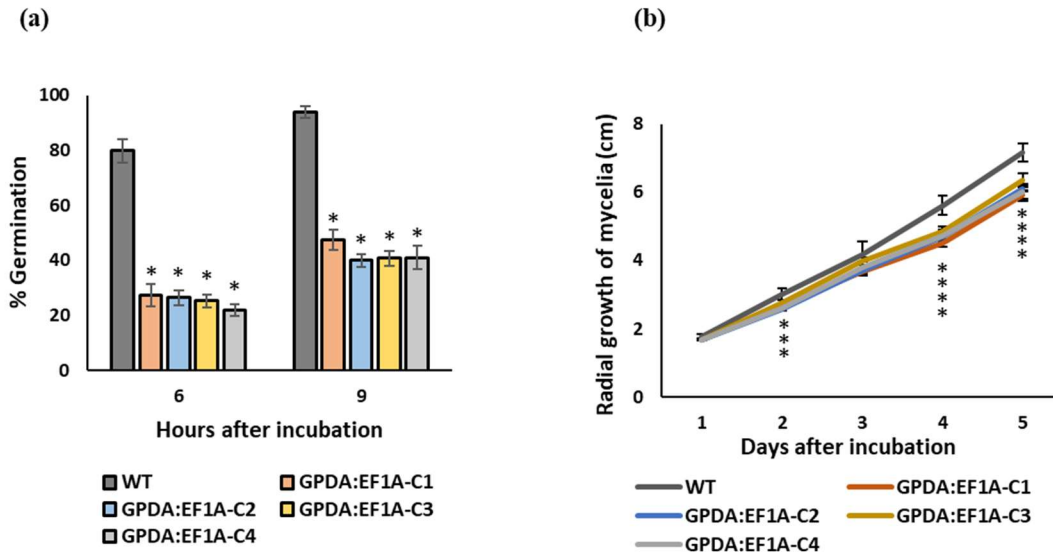


Figure 4.5: (a) Percentage macroconidia germination of WT and *GPDA:EF1A* transformants after 6 and 9 h of incubation on water agar at 27°C. Bars represent standard error from two independent experiments, each with five replicates. Asterisks indicate statistically significant difference compared with the WT ($p < 0.05$). (b) Radial mycelial growth of WT and *GPDA:EF1A* transformants over 5 days of growth on PDA at 27°C. Bars represent standard error from five replicates. Asterisks indicate statistically significant difference compared with the WT ($p < 0.05$).

4.3.3 DON production is greatly affected in *GPDA:EF1A-C1* transformant

DON synthesis in *GPDA:EF1A-C1* was tested using a two stage DON-inducing medium (Miller and Blackwell, 1986). The transformant showed significantly reduced DON production in this medium compared to the WT (Figure 4.6). It is unknown whether the reduced DON accumulation is due to a pleiotropic effect on fungal translation.

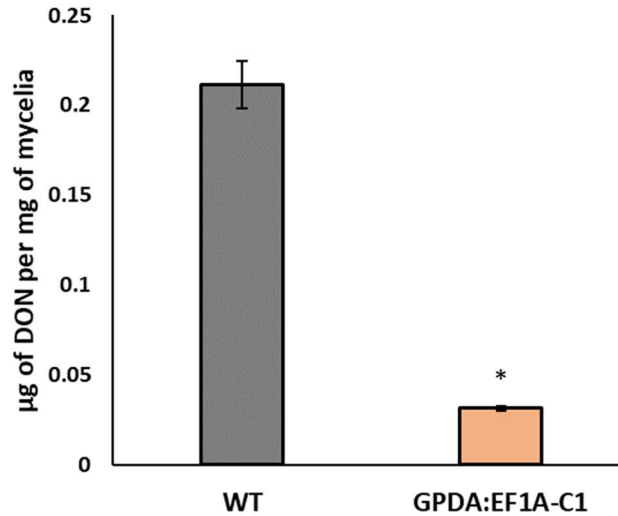
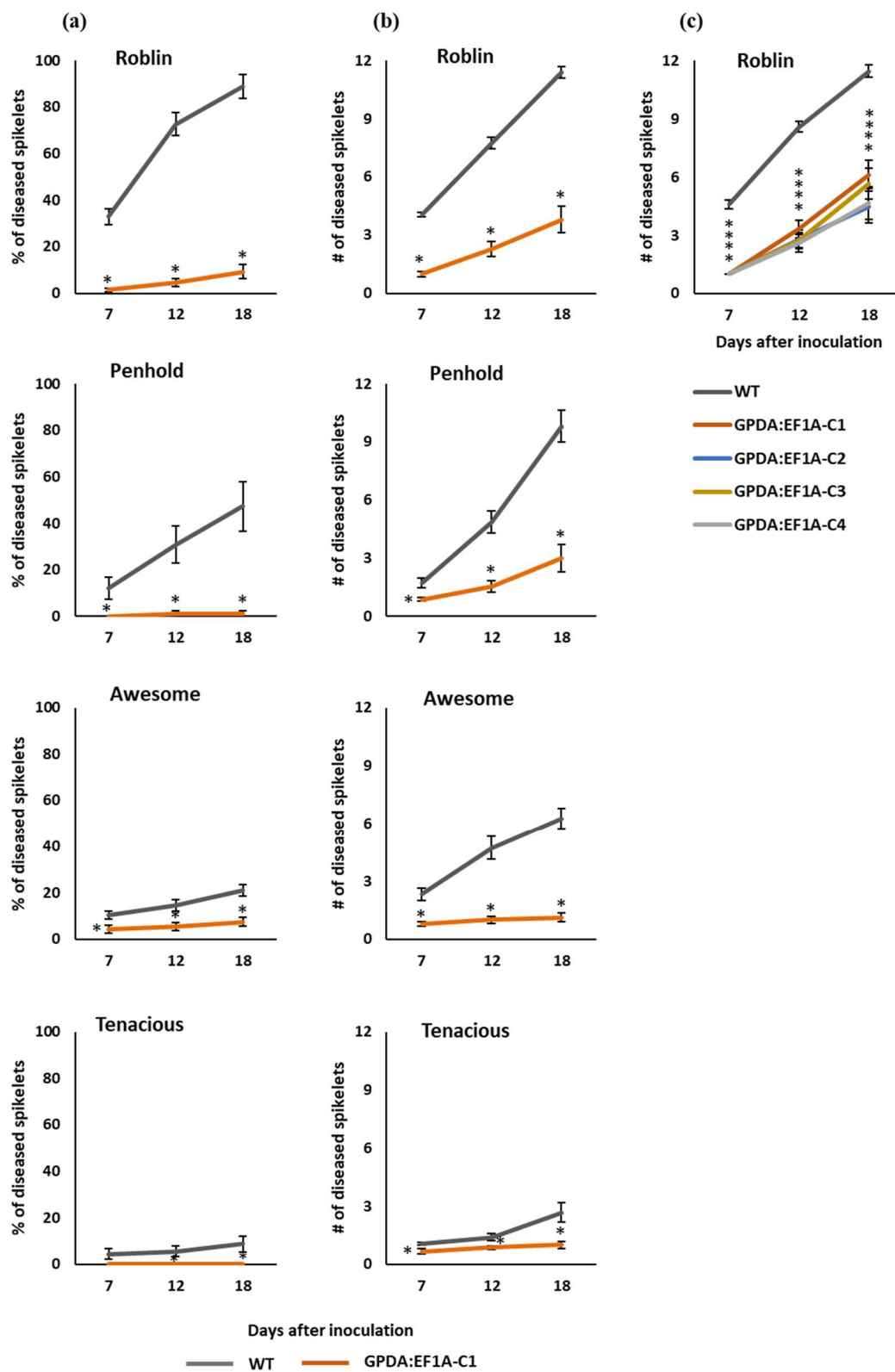


Figure 4.6: Amount of DON produced by *GPDA:EF1A-C1* transformant and the WT in axenic culture. Bars represent standard error from six replicates. Asterisks indicate statistically significant difference compared with the WT ($p < 0.05$).

4.3.4 *GPDA:EF1A* transformants are compromised in their ability to cause disease in wheat spikes

GPDA:EF1A-C1 was screened in wheat cultivars (cvs.) having different levels of resistance/susceptibility to FHB by spray and point inoculations (the resistance mechanisms of wheat cultivars are provided in Table 2.2). The transformant was found to be substantially impaired in its ability to cause initial infection and disease spread (Figure 4.7 a & b). The difference in initial infection and disease spread between the transformant and the WT was more obvious in susceptible cvs., Roblin and Penhold than in the resistant cv., Tenacious (Figure 4.7 a & b). *GPDA:EF1A-C2*, *GPDA:EF1A-C3* and *GPDA:EF1A-C4* were screened in Roblin by point inoculation. *GPDA:EF1A-C1* was included in the screening as a control. All four transformants showed significantly reduced disease spread compared to the WT (Figure 4.7 c).



(d)



WT
spray_Roblin
GPDA:EFIA-C1
spray_Roblin
WT
spray_Penhold
GPDA:EFIA-C1
spray_Penhold
WT
spray_Awesome
GPDA:EFIA-C1
spray_Awesome
WT
spray_Tenacious
GPDA:EFIA-C1
spray_Tenacious

(e)



WT
point_Roblin
GPDA:EFIA-C1
point_Roblin
WT
point_Penhold
GPDA:EFIA-C1
point_Penhold
WT
point_Awesome
GPDA:EFIA-C1
point_Awesome
WT
point_Tenacious
GPDA:EFIA-C1
point_Tenacious

Figure 4.7: Disease severity of *GPDA:EF1A* transformants following spray or point inoculation on susceptible (Roblin), moderately susceptible (Penhold), moderately resistant (Awesome) and resistant (Tenacious) wheat cultivars. (a) Percentage of diseased spikelets of Roblin, Penhold, Awesome and Tenacious at 7, 12, and 18 days after spray inoculation with *GPDA:EF1A-C1* or WT. Bars represent standard error from three independent experiments, each with five replicates. Asterisks indicate statistically significant difference compared with the WT ($p < 0.05$). (b) Number of diseased spikelets of Roblin, Penhold, Awesome and Tenacious at 7, 12 and 18 days after point inoculation with *GPDA:EF1A-C1* or WT. Bars represent standard error from three independent experiments, each with five replicates. Asterisks indicate statistically significant difference compared with the WT ($p < 0.05$). (c) Number of diseased spikelets of Roblin at 7, 12 and 18 days after point inoculation with *GPDA:EF1A-C1*, *GPDA:EF1A-C2*, *GPDA:EF1A-C3*, *GPDA:EF1A-C4* or WT. Bars represent standard error from three independent experiments, each with five replicates. Asterisks indicate statistically significant difference compared with the WT ($p < 0.05$). (d) FHB disease symptoms in Roblin, Penhold, Awesome and Tenacious at 18 days after spray inoculation with WT or *GPDA:EF1A-C1* and (e) in Roblin, Penhold, Awesome and Tenacious at 18 days after point inoculation with WT or *GPDA:EF1A-C1*.

4.3.5 FgEF1A peptides do not elicit plant immune responses

Callose deposition is commonly used as a marker of plant defense activation in response to pathogen attack or elicitor treatment (Voigt and Somerville, 2009; Luna et al., 2011). The flg22 epitope of bacterial flagellin elicits callose deposition in *Arabidopsis* (Gomez-Gomez et al., 1999; Luna et al., 2011). *Arabidopsis* seedlings treated with four synthetic peptides from FgEF1A amino acid sequence (P1, P2, P3 and P4) were observed for callose deposition. While the positive control, flg22, induced callose accumulation in *Arabidopsis* cotyledons, the same was not observed for the FgEF1A peptides evaluated (Figure 4.8 a). The peptides were also tested for their ability to induce β -1,3-glucanase activity in wheat seedlings. β -1,3-glucanase is an antifungal enzyme with hydrolytic activity on fungal cell walls and its activity is induced as a plant resistance mechanism in response to pathogen infection (Sack et al., 1990; Jutidamrongphan et al., 1991; Ignatius et al., 1994). While increased β -1,3-glucanase activity was observed in flg22-treated

wheat seedlings after 24 h, no significant change in the enzymatic activity was observed for any of the FgEF1A peptides compared with the water control treatment (Figure 4.8 b).

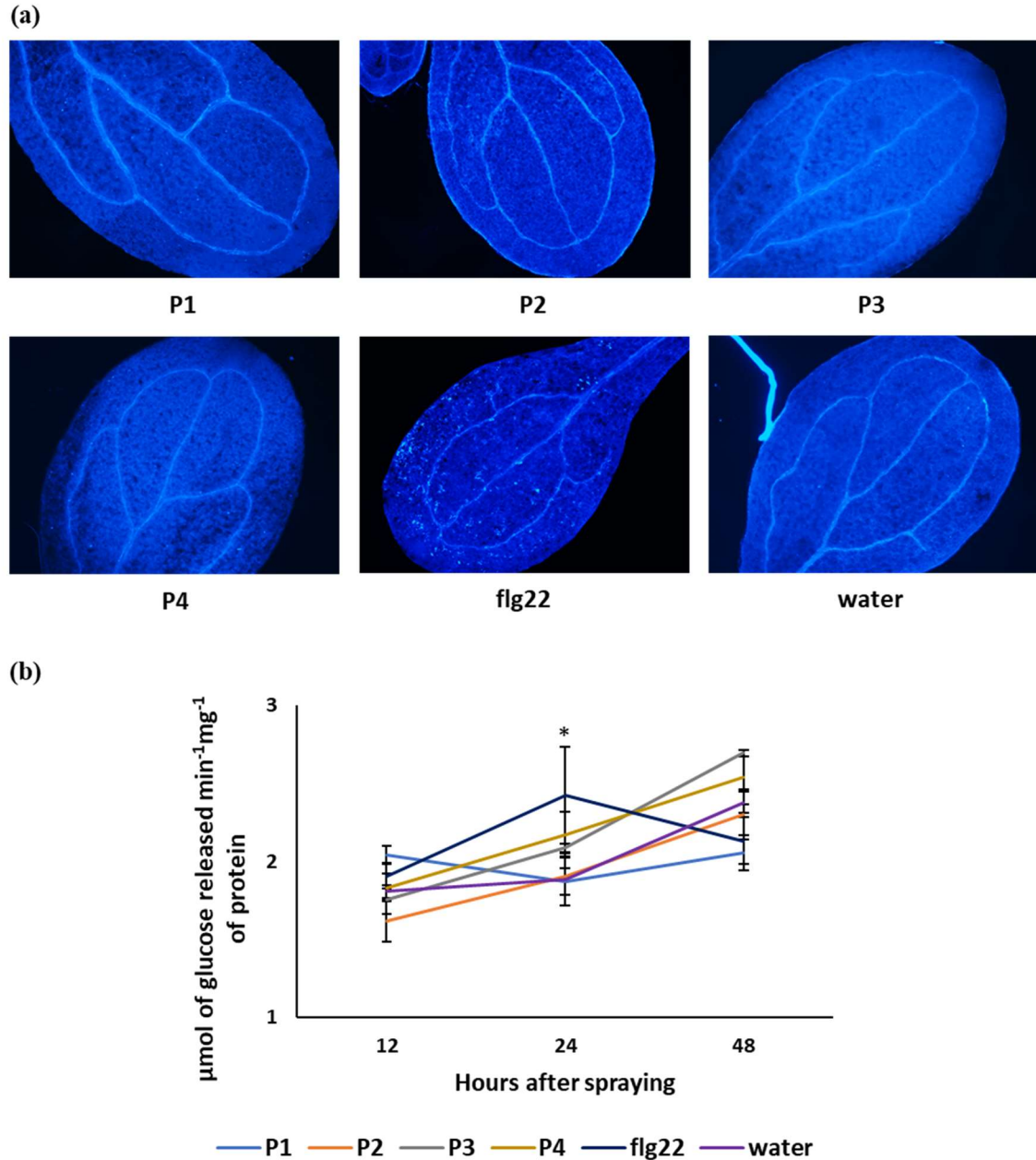


Figure 4.8: Eliciting activities of FgEF1A peptides. (a) Arabidopsis seedlings were treated with 1 μ M each of P1, P2, P3 and P4 for 24 h, stained with 0.01% aniline blue in 150 mM K_2HPO_4 for 2 h and observed for callose under a microscope using DAPI filter. Treatments with 1 μ M flg22 and water served as positive and negative controls, respectively. Images are representative of two independent experiments. (b) β -1,3-

glucanase activity in 10-day-old Roblin seedlings at 12, 24 and 48 h after spraying with 1 μ M each of P1, P2, P3, P4, flg22 or water. Bars represent standard error from two independent experiments, each with three replicates per treatment per time point. Asterisk indicates statistically significant difference compared with the WT ($p < 0.05$).

4.4 Discussion

Bacterial EF-Tu protein is a well-studied elicitor of immunity in plants (Kunze et al., 2004; Furukawa et al., 2014). The abundance of the homologous eukaryotic protein in *F. graminearum*, FgEF1A, was reduced in the secretome of non-pathogenic mutants compared to secretome of the WT (Rampitsch et al., 2013), suggesting that FgEF1A may participate in *F. graminearum* infection. In order to study its role in infection, I attempted to generate both disruption (data not shown) and overexpression transformants of *FgEF1A* gene in *F. graminearum*. Transformation with the cassette for gene disruption did not yield any transformants. This was not surprising since *EF1A* is an important housekeeping gene, and there are no known paralogues in *F. graminearum*. It is likely that disruption of this gene would be lethal to the fungus.

FgEF1A overexpression transformants were developed by replacing *FgEF1A* native promoter with a *GPDA* promoter from *A. nidulans* through homologous recombination. Amplification using primers that bind outside the homologous recombination sites and Southern blotting results showed that a single copy of the overexpression construct was integrated at the desired site in *GPDA:EF1A* transformants. The promoter replacement led to a small but significant increase in *FgEF1A* expression in three out of four *GPDA:EF1A* transformants developed. The expression is not as high as expected from the *GPDA* promoter, which is commonly used for gene overexpression in filamentous fungi (Meyer et al., 2011; Alazi et al., 2018). Substantially higher

expressions of a cerato-platanin gene and two CFEM domain-containing genes in *F. graminearum* were obtained by employing the same *GPDA* promoter (Chapter 2 and 3, respectively).

One possible explanation for the limited increase in *FgEF1A* expression with the *GPDA* promoter is that the strength of *FgEF1A* promoter in *F. graminearum* is comparable to that of *A. nidulans*' *GPDA* promoter. EF1A is one of the most abundant proteins in eukaryotic cells (Merrick, 1992) and is therefore expected to have a strong promoter (Ahn et al., 2007). An experiment in which *Pichia pastoris* translation elongation factor1 (*TEF1*) promoter was compared to its *GPDA* promoter using a bacterial *LIPASE* as a reporter gene showed that expression levels from *TEF1* promoter were comparable to or higher than that from *GPDA* promoter (Ahn et al., 2007). Another study by Nakajima et al. (2014) compared the strength of four *A. nidulans* constitutive promoters in *F. graminearum* using β glucuronidase (*GUS*) as a reporter gene, and found that *TEF1* promoter gave the strongest GUS activity in *F. graminearum* compared to the other promoters, including *GPDA*, used for the comparison (Nakajima et al., 2014). Similarly, strong promoter activities have been shown for *TEF1* promoters from a yeast, *Yarrowia lipolytica* (Muller et al., 1998), and two filamentous fungi, *Ashbya gossypii* (Steiner and Philippsen, 1994) and *Aspergillus oryzae* (Kitamoto et al., 1998). While, promoters for the same gene from different organisms may vary in their strength, it is likely that promoter activities of *FgEF1A* from *F. graminearum* and *GPDA* from *A. nidulans* are comparable and therefore no change in *FgEF1A* expression resulted from replacing the *FgEF1A* promoter with the *GPDA* promoter. Overexpression of *EF1A* in *S. cerevisiae* was achieved by introducing *EF1A* gene on a 2 μ -based plasmid into WT yeast

cells. This resulted in additional copies of *EF1A* which gave higher levels of EF1A protein in the resulting yeast strain (Munshi et al., 2001).

A second possible explanation for the limited increase in *FgEF1A* expression might be that its expression is maintained at or close to basal expression levels by some yet unknown mechanism(s). Eukaryotic EF1A is responsible for carrying out several important cellular functions in addition to its canonical role in protein synthesis, as described in the introduction. Given its role in various important cellular activities, it is possible that *EF1A* expression is tightly regulated by eukaryotic cells. Although *EF1A* overexpression using a 2 μ -plasmid resulted in increased abundance of this protein in yeast, the increase in gene expression as well as protein accumulation was not as high as expected from a 2 μ -plasmid (Tarrant et al., 2016), this was attributed to a low copy number of 2 μ -plasmid with the *EF1A* gene compared with the empty vector control. The authors attributed the low expression to the presence of a regulatory mechanism against overexpression of this gene (Tarrant et al., 2016).

Control of gene expression by small noncoding RNAs is an important mechanism of post-transcriptional regulation of gene expression in eukaryotes (Moazed, 2009; Nicolas et al., 2010). microRNAs (miRNAs) are small noncoding RNAs primarily involved in the post-transcriptional regulation of gene expression in plants and animals (Baulcombe, 2004; Li and Carthew, 2005; Jones-Rhoades et al., 2006). miRNAs regulate gene expression by binding to complementary sequences of their target mRNAs and miRNAs may target mRNAs for degradation or translational repression (reviewed in: Bartel, 2004; Chang et al., 2012). miRNA-like RNAs (milRNAs) have also been reported from different fungal species (Jiang et al., 2012; Zhou et al., 2012a; Zhou et al., 2012b)

including *F. graminearum*, in which 49 miRNA candidates have been identified (Chen et al., 2015). Additionally, the genome of *F. graminearum* contains major RNA silencing components including two dicer proteins, two argonaute proteins and five RNA-dependent RNA polymerases (Chen et al., 2015). Moreover, out of 49 miRNAs, 24 were not detected from a dicer protein deletion mutant, $\Delta FgDICER2$, in *F. graminearum*, indicating that the RNA silencing components are functional in this fungus (Chen et al., 2015). Further experiments are needed to determine whether or not there are small non-coding RNAs that target *FgEF1A* transcripts in *F. graminearum*, and if this explains the limited increase in *FgEF1A* observed.

While the increase in *FgEF1A* expression in *GPDA:EF1A* transformants was small, it was nonetheless statistically significant compared to the WT. It has not been determined whether the small but significant increase in *FgEF1A* expression leads to higher protein abundance. If it does so, and if the increased protein levels have biological significance, the reduced fitness of the *GPDA:EF1A* transformants could be due to the higher *FgEF1A* levels. Increased levels of EF1A has been shown to affect fitness in yeast (Munshi et al., 2001; Tarrant et al., 2016).

FgEF1A overexpression transformants showed lower initial infection and reduced disease spread on wheat spikes compared to WT. This may be a result of delayed macroconidia germination in these transformants, which we know occurs on water agar. Germination of conidia on the inoculated host surface is a pre-requisite for disease establishment. Slower invasion provides enough time for the host plants to mount defense responses which further slow down pathogen growth in the host tissues. The *GPDA:EF1A-CI* transformant was also considerably impaired in its ability to synthesize

DON in axenic culture. However, it has not been determined whether DON accumulation is also decreased during infection and if this explains the lower disease spread observed for *GPDA:EF1A-C1* transformant.

Different regions of bacterial EF-Tu act as PAMPs in different plant species. While N-acetylated first 18 amino acids of EF-Tu (elf18) from *E. coli* triggered immune responses in Brassicaceae (Kunze et al., 2004), 50 amino acids from the middle region of EF-Tu (EFa50) from *Acidovorax avenae* activated immunity in rice (Furukawa et al., 2014). FgEF1A has been detected from the *F. graminearum* secretome; however, there are no studies so far that test whether FgEF1A protein is involved in the interaction of *F. graminearum* with its host plants. Preliminary attempts to purify FgEF1A protein from *E. coli* did not prove successful and hence I was not able to assess whether it activates plant defense responses. However, FgEF1A synthetic peptides with sequence similarity to elf18 or EFa50 epitopes did not induce callose deposition in Arabidopsis or β -1,3-glucanase activity in wheat, suggesting a lack of PAMP-like activity for these peptides.

In summary, a substantial increase in *FgEF1A* expression was not obtained for *GPDA:EF1A* transformants. It may be that the *GPDA* promoter used for overexpression in this work is not much different in strength than the *FgEF1A* native promoter, or that there is a mechanism(s) that regulates *FgEF1A* expression in the cell which has resulted in limited overexpression of this gene. Regardless of the mechanism behind this limited change, a strong growth phenotype was observed, though, as of yet, it is unclear what is responsible for these morphological changes. As a complementary approach to determine the role of FgEF1A in host interactions, I studied the eliciting activities of FgEF1A peptides. Callose deposition in Arabidopsis and β -1,3-glucanase activity in wheat

suggests that the select peptides of FgEF1A do not induce plant immune responses.

However, whether FgEF1A protein itself acts as a PAMP still needs to be determined.

Table 4.1: Primers used for various experiments in this chapter

Primer pair	Primer name	Primer sequence (5'-3') (Tm °C)	Purpose
1	Fg08811-F1 Fg08811-R837	ATGGGTAAGGAGGAGAAGAC (53.2) GCAACAATGAGGTTCTTGAC (51.9)	Amplification of <i>FgEF1A</i> gene
2	Fg08811-f 1698(+) Fg08811-r926(+)	AAAAAGGCCCCAGACAATCT (54.6) CAACTTGGAAGCCCTAACA (55.0)	Amplification of upstream of <i>FgEF1A</i>
3	Fg08811-F1OX Fg08811-R837OX	ggacttaauATGGGTAAGGAGGAGA (55.2) gggtttaauGCAACAATGAGGTTC (54.9)	Amplification of <i>FgEF1A</i> gene with adaptors
4	Fg08811-f1698(+)OX Fg08811-r926(+)OX	ggtcttaauAAAAAGGCCCCAGAC (55.8) ggcattaauCAACTTGGAAGC (54.6)	Amplification of upstream of <i>FgEF1A</i> with adaptors
5	Fg08811-M-2 RF-2	GACGTAGAATGAGGGGCAAGAAAA (57.1) TCTCCTTGCATGCACCATTCCTTG (59.8)	Verification of cross over in <i>GPDA:EF1A</i>
6	RF-3 Fg08811-M-3	TTGCGTCAGTCCAACATTTGTTGCCA (61.7) GGTCTCCTTGATGATCTCCTGGTAA (57.6)	Verification of cross over in <i>GPDA:EF1A</i>
7	Hyg588U Hyg588L	AGCTGCGCCGATGGTTTCTACAA (61.3) GCGCGTCTGCTGCTCCATACAA (62.3)	Amplification of <i>hph</i> gene from <i>GPDA:EF1A</i>
8	EF-SB-F2 EF-SB-R1	CGTGTCCGTCGAGGTCTATT (56.3) AGCTCAACAGAGGGAGGACA (57.9)	Probe synthesis for Southern blotting
9	PgpdA-F3 EF-R3	GCTTTGCCCGGTGTATGAAA (56.1) TCAAGAACCCAGGCGTACTT (56.2)	Amplification and sequencing of <i>FgEF1A</i> gene from <i>GPDA:EF1A</i>
10	EF-F4 EF-R4	CATTCGAATCGCCCTCACAC (56.3) CGGTCGATCTTCTCCTGGAT (56.1)	Amplification and sequencing of <i>FgEF1A</i> gene from <i>GPDA:EF1A</i>
11	EF-F5 EF-R5	ACCACTGAAGTCAAGTCCGT (56.1) AGATGGAGTAGGCTGGAGGA (57.0)	Amplification and sequencing of <i>FgEF1A</i> gene from <i>GPDA:EF1A</i>
12	EF-F6 EF-R6	ACAATGTGCCCTGGTTCATG (55.9) GCACCCACAAAGAGCAAGAA (56.0)	Amplification and sequencing of <i>FgEF1A</i> gene from <i>GPDA:EF1A</i>
13	Fg08811-F1 Fg08811-R1	CTTCAAGTACGCCTGGGTTCT (57.0) GACGGTGACATAGTAGCGAGG (56.9)	Expression analysis of <i>FgEF1A</i> gene in <i>GPDA:EF1A</i> by RT-qPCR
14	B-tub-F B-tub-R	GTTCTGGACGTTGCGCATCTG (59.0) TGATGGCCGCTTCTGACTTCC (59.7)	Normalization of <i>FgEF1A</i> transcript levels

Chapter 5: Summary of findings and future directions

Complete genome sequencing of *Fusarium graminearum* has facilitated research activities in multiple areas including functional genomics to study gene functions in this pathogen. A common approach to study the function of a specific gene is by obtaining knockout mutants for that gene. Over the last two decades, a series of gene knockout mutants have been developed in *F. graminearum* as well as other filamentous fungi with the objective of understanding the function of genes in growth and infection-related processes. Several of them have been discussed in chapter 1.

While knockout mutants are widely used by researchers to understand gene function, they have some limitations. One limitation is that some knockout mutants exhibit little detectable loss-of-function phenotype due to gene redundancies, where one or more than one gene compensates for the absence of the disrupted gene (Giaever et al., 2002). This problem is often resolved by simultaneously knocking out two or three genes with possible functional redundancy in order to obtain a double or triple knockout mutant. This method involves development of more than one deletion construct, each with a unique selection marker to select for integration of each construct into genome. It is difficult to knockout several genes at a time, partly due to the unavailability of multiple selection marker genes suitable for filamentous fungi. Gene editing by Clustered regularly interspaced short palindromic repeats (CRISPR) may provide an alternative strategy since it does not require the use of selection markers and has the potential to simultaneously disrupt several genes by using different guide RNAs along with CRISPR-associated protein 9 (Cas9). This approach has been developed for *F. graminearum* (Gardiner and Kazan, 2018), but is not yet widely used owing to technical challenges.

While knockout mutants are commonly used to study gene function, deletion of certain essential genes can be lethal to the organism and therefore knockout mutants cannot be developed. For instance, I was not able to develop *EF1A* knockout mutant for *F. graminearum*, presumably because this is an essential, non-redundant housekeeping gene. While gene overexpression is not an alternative approach to gene knockout, it can be a complementary approach and provide valuable information regarding gene function.

The *F. graminearum* secretome consists of proteins and secondary metabolites. DON is an example of a secondary metabolite secreted by this pathogen and the role of DON in *F. graminearum* aggressiveness is well-understood. Most of the secreted proteins in *F. graminearum* are uncharacterized and a putative role in infection has been proposed for some of these proteins. I generated gene disruption and overexpression transformants to study a secreted cerato-platanin protein (FgCPP1) and two CFEM-domain containing proteins (FgCFEM1 and FgCFEM2) in *F. graminearum*.

FgCPP1 was detected from the *F. graminearum* secretome and its expression was found to be upregulated during wheat infection, suggesting its involvement in the infection. FgCPP1 and FgCPP2 proteins were reported to exhibit properties similar to expansins, which possess cellulose weakening activity. The recombinant proteins improved the cellulase activity of a fungal β -1,4-glucanase on cellulosic materials including wheat cell wall (Quarantin et al., 2019). However, disruption of *FgCPP1* in *F. graminearum* did not alter its ability to cause disease on wheat (chapter 2), which is similar to findings from a previous study in which aggressiveness of the double knockout mutants for *FgCPP1* and *FgCPP2* were comparable to the WT (Quarantin et al., 2016). The same double knockout mutants also showed increased cellulase activity (Quarantin et

al., 2019). It can, therefore, be assumed that the absence of *FgCPP1* is compensated by the increased cellulase activity in *F. graminearum* and hence no difference was observed in disease. *FgCPP1* overexpression caused a small increase in initial infection of wheat spikes (chapter 2), probably due to its synergistic effect on cellulase activity at wheat cell wall, as recently shown (Quarantin et al., 2019). However, *FgCPP1* disruption or overexpression did not alter the disease spread by the respective mutants (chapter 2), likely because the role of *FgCCP1* in disease spread may be blurred by the effect of DON which is a major determinant of disease spread in wheat.

Additional experiments are needed to elucidate the role of *FgCPP1* in *F. graminearum*-wheat interaction. It has been reported that DON-nonproducing *F. graminearum* is restricted to the inoculated spikelet and cannot spread through the rachis due to cell wall thickening in the rachis node (Proctor et al., 1995; Bai et al., 2002; Jansen et al., 2005). Since recombinant *FgCCP1* was demonstrated to have expansin-like activity on wheat cell wall, one of the future studies I propose is to develop an *FgCPP1* overexpression transformant in a DON-nonproducing background and then study its disease-causing abilities. Additionally, purified *FgCCP1* protein could be co-inoculated with DON-deficient *F. graminearum* to avoid the potential masking effect of DON and to distinguish the effect of *FgCCP1* from that of DON.

FgCFEM1 and *FgCFEM2* disruption mutants were similar to the WT in aggressiveness (chapter 3). However, reduced aggressiveness has been shown for *FgCFEM1* deletion mutants in wheat spikes and coleoptiles (Dufresne et al., 2008; Zhang et al., 2012). I assume that this difference in aggressiveness of *FgCFEM1* deletion mutants is due to different *F. graminearum* strains used, similar to varying infection

phenotypes shown for *CFEM* deletion mutants (*Apth11*) in different *Magnaporthe grisea* strains (DeZwaan et al., 1999). Meanwhile, *FgCFEM1* overexpression transformant exhibited a subtle increase in disease spread in a moderately susceptible wheat cultivar, and not in susceptible or resistant wheat cultivars (chapter 3), suggesting a minor role, if any, for *FgCFEM1* in *F. graminearum* aggressiveness.

Lu and Edwards (2016) reported six putatively secreted *CFEM* proteins from *F. graminearum*. Although only *FgCFEM1* and *FgCFEM2* were detected in the minimum media-based secretome, I believe it is important to study the involvement of the other *CFEM* proteins in host plant infection by *F. graminearum*. I deleted *FgCFEM1* and *FgCFEM2* individually. It seems likely that the *CFEM* encoding genes are functionally redundant in *F. graminearum*, despite the significant sequence diversity present among the *CFEM* proteins. Hydrophobins also exhibit considerable amino acid sequence variability and hydrophobins from different fungal species were partially able to restore the defects of a hydrophobin deletion mutant (*mpg1*) in *M. grisea* (Kershaw et al., 1998), suggesting that functional redundancy is possible even with differences in sequences. I propose as a future direction to perform a time course experiment to study the expression of the remaining four *CFEM* genes in *F. graminearum* during wheat spike infection. The genes which show upregulation during the infection process could be deleted to produce double or triple knockout mutants and characterize them for phenotypes including aggressiveness.

The secretomes of two non-pathogenic *F. graminearum* mutants had reduced abundance of EF1A protein (*FgEF1A*) compared to the WT secretome, suggesting a role of this protein in infection. With the objective of understanding the role of *FgEF1A* in *F.*

graminearum infection, I tried to develop *FgEF1A* disruption and overexpression strains. The disruption strains could not be generated, probably because *FgEF1A* disruption is lethal. A substantially higher expression was not obtained for overexpression strains (chapter 4) either because the *GPDA* promoter used for gene overexpression is not stronger than the *FgEF1A* native promoter or *FgEF1A* expression is probably regulated by the cell.

In order to obtain higher expression for *FgEF1A*, I suggest developing overexpression strains by ectopic integration of an overexpression cassette into the *F. graminearum* genome. The overexpression of the gene can be expected as a result of the *in locus* expression plus the expression from the additional copy of the gene, provided *FgEF1A* expression is not regulated by *F. graminearum*.

The recombinant EF-Tu, the bacterial homologue of FgEF1A, acts as a pathogen-associated molecular pattern (PAMP) and its epitopes, elf18 and EFa50 elicited immunity in Arabidopsis and rice, respectively. My attempts to purify recombinant FgEF1A protein in *E.coli* were not successful and hence I studied the eliciting activities of the FgEF1A peptides with amino acid sequence identity to elf18 or EFa50. The peptides did not induce callose in Arabidopsis or β -1,3-glucanase activity in wheat (chapter 4). It has not yet been determined whether recombinant FgEF1A protein itself can trigger activation of plant immunity.

The recombinant *FgEF1A* could be expressed in a methylotrophic yeast called *Pichia pastoris*. Several fungal recombinant proteins have been successfully purified using this yeast strain. The expression vector pPICZ α A contains a methanol inducible alcohol oxidase 1 (*AOX1*) promoter, an α -factor secretion signal and a C-terminal His tag.

The recombinant protein secreted into the culture medium can be purified with metal affinity chromatography. The purified protein can be tested for its eliciting activities such as extracellular alkalinisation in *Brachypodium distachyon* cell suspension culture, callose deposition in Arabidopsis and β -1,3-glucanase activity in wheat.

Most proteins from the *F. graminearum* secretome are yet to be characterized, and so far, the best characterized protein with a clear role in infection is a secreted lipase (Voigt et al., 2005). While gene silencing by CRISPR-Cas9 has been tested as a proof of concept in some filamentous fungi, gene knockout using homologous recombination is the widely used practice to understanding gene functions. In fact, a combination of approaches could be employed to characterize proteins from the secretome; this may include generation of gene knockout mutants and overexpression strains and the use of purified proteins to study their interaction with host plants.

Bibliography

- Abramson, D., Clear, R.M., and Nowicki, T.W. 1987. *Fusarium species* and trichothecene mycotoxins in suspect samples of 1985 Manitoba wheat. *Can. J. Plant Sci.* 67:611-619.
- Adnan, M., Islam, W., Noman, A., Hussain, A., Anwar, M., Khan, M.U., Akram, W., Ashraf, M.F., and Raza, M.F. 2019a. Q-SNARE protein FgSyn8 plays important role in growth, DON production and pathogenicity of *Fusarium graminearum*. *Microb. Pathog.* 140:103948.
- Adnan, M., Fang, W., Sun, P., Zheng, Y., Abubakar, Y.S., Zhang, J., Lou, Y., Zheng, W., and Lu, G.D. 2019b. R-SNARE FgSec22 is essential for growth, pathogenicity and DON production of *Fusarium graminearum*. *Curr. Genet.*
- Ahn, J., Hong, J., Lee, H., Park, M., Lee, E., Kim, C., Choi, E., Jung, J., and Lee, H. 2007. *Translation elongation factor 1-alpha* gene from *Pichia pastoris*: molecular cloning, sequence, and use of its promoter. *Appl. Microbiol. Biotechnol.* 74:601-608.
- Alazi, E., Knetsch, T., Di Falco, M., Reid, I.D., Arentshorst, M., Visser, J., Tsang, A., and Ram, A.F.J. 2018. Inducer-independent production of pectinases in *Aspergillus niger* by overexpression of the D-galacturonic acid-responsive transcription factor gaaR. *Appl. Microbiol. Biotechnol.* 102:2723-2736.
- Arunachalam, C., and Doohan, F.M. 2013. Trichothecene toxicity in eukaryotes: cellular and molecular mechanisms in plants and animals. *Toxicol. Lett.* 217:149-158.
- Baccelli, I. 2014. Cerato-platanin family proteins: one function for multiple biological roles? *Front. Plant Sci.* 5:769.
- Baccelli, I., Luti, S., Bernardi, R., Scala, A., and Pazzagli, L. 2014. Cerato-platanin shows expansin-like activity on cellulosic materials. *Appl. Microbiol. Biotechnol.* 98:175-184.
- Baccelli, I., Comparini, C., Bettini, P.P., Martellini, F., Ruocco, M., Pazzagli, L., Bernardi, R., and Scala, A. 2012. The expression of the cerato-platanin gene is related to hyphal growth and chlamydospores formation in *Ceratocystis platani*. *FEMS Microbiol. Lett.* 327:155-163.

- Bai, G.H., Desjardins, A.E., and Plattner, R.D. 2002. Deoxynivalenol-nonproducing *Fusarium graminearum* causes initial infection, but does not cause disease spread in wheat spikes. *Mycopathologia* 153:91-98.
- Baillie, G.S., and Douglas, L.J. 1999. Role of dimorphism in the development of *Candida albicans* biofilms. *J. Med. Microbiol.* 48:671-679.
- Baldwin, T.K., Urban, M., Brown, N., and Hammond-Kosack, K.E. 2010. A role for topoisomerase I in *Fusarium graminearum* and *F. culmorum* pathogenesis and sporulation. *Mol. Plant-Microbe Interact.* 23:566-577.
- Barsottini, M.R., de Oliveira, J.F., Adamoski, D., Teixeira, P.J., do Prado, P.F., Tiezzi, H.O., Sforca, M.L., Cassago, A., Portugal, R.V., de Oliveira, P.S., de, M.Z.A.C., Dias, S.M., Pereira, G.A., and Ambrosio, A.L. 2013. Functional diversification of cerato-platanins in *Moniliophthora perniciosa* as seen by differential expression and protein function specialization. *Mol. Plant-Microbe Interact.* 26:1281-1293.
- Bartel, D.P. 2004. MicroRNAs: genomics, biogenesis, mechanism, and function. *Cell* 116:281-297.
- Bata, A., Harrach, B., Ujszaszi, K., Kis-Tamas, A., and Lasztity, R. 1985. Macrocyclic trichothecene toxins produced by *Stachybotrys atra* strains isolated in Middle Europe. *Appl. Environ. Microbiol.* 49:678-681.
- Baulcombe, D. 2004. RNA silencing in plants. *Nature* 431:356-363.
- Bluhm, B.H., Zhao, X., Flaherty, J.E., Xu, J.R., and Dunkle, L.D. 2007. *RAS2* regulates growth and pathogenesis in *Fusarium graminearum*. *Mol. Plant-Microbe Interact.* 20:627-636.
- Blümke, A., Falter, C., Herrfurth, C., Sode, B., Bode, R., Schäfer, W., Feussner, I., and Voigt, C.A. 2014. Secreted fungal effector lipase releases free fatty acids to inhibit innate immunity-related callose formation during wheat head infection. *Plant Physiol.* 165:346-358.
- Boddi, S., Comparini, C., Calamassi, R., Pazzagli, L., Cappugi, G., and Scala, A. 2004. Cerato-platanin protein is located in the cell walls of ascospores, conidia and hyphae of *Ceratocystis fimbriata* f. sp. *platani*. *FEMS Microbiol. Lett.* 233:341-346.

- Boenisch, M.J., and Schäfer, W. 2011. *Fusarium graminearum* forms mycotoxin producing infection structures on wheat. BMC Plant Biol. 11:110.
- Boller, T., and Felix, G. 2009. A renaissance of elicitors: perception of microbe-associated molecular patterns and danger signals by pattern-recognition receptors. Annu. Rev. Plant Biol. 60:379-406.
- Bolton, M.D., van Esse, H.P., Vossen, J.H., de Jonge, R., Stergiopoulos, I., Stulemeijer, I.J., van den Berg, G.C., Borrás-Hidalgo, O., Dekker, H.L., de Koster, C.G., de Wit, P.J., Joosten, M.H., and Thomma, B.P. 2008. The novel *Cladosporium fulvum* lysin motif effector Ecp6 is a virulence factor with orthologues in other fungal species. Mol. Microbiol. 69:119-136.
- Bradford, M.M. 1976. A rapid and sensitive method for the quantitation of microgram quantities of protein utilizing the principle of protein-dye binding. Anal. Biochem. 72:248-254.
- Brotman, Y., Briff, E., Viterbo, A., and Chet, I. 2008. Role of swollenin, an expansin-like protein from *Trichoderma*, in plant root colonization. Plant Physiol. 147:779-789.
- Brown, N.A., Antoniw, J., and Hammond-Kosack, K.E. 2012. The predicted secretome of the plant pathogenic fungus *Fusarium graminearum*: a refined comparative analysis. PLoS One 7:e33731.
- Brown, P.D., Randhawa, H.S., Fetch, J.M., Meiklejohn, M., Fox, S.L., Humphreys, D.G., Green, D., Wise, I., Fetch, T., Gilbert, J., McCallum, B., and Menzies, J. 2015. AAC Tenacious red spring wheat. Can. J. Plant Sci. 95:805-810.
- Bushnell, W.R., Hazen, B.E., and Pritsch, C. 2003. Histology and physiology of *Fusarium* head blight. Pages 44-83 in: *Fusarium head blight of wheat & barley*, K.J. Leonard and W.R. Bushnell, eds. American Phytopathological Society, St. Paul, Minnesota, USA.
- Campbell, A.B., and Czarnecki, E. 1987. Roblin hard red spring wheat. Can. J. Plant Sci. 67:803-804.
- Cao, S., Zhang, S., Hao, C., Liu, H., Xu, J.-R., and Jin, Q. 2016. FgSsn3 kinase, a component of the mediator complex, is important for sexual reproduction and pathogenesis in *Fusarium graminearum*. Sci. Rep. 6:22333.

- Carere, J., Benfield, A.H., Ollivier, M., Liu, C.J., Kazan, K., and Gardiner, D.M. 2017. A tomatinase-like enzyme acts as a virulence factor in the wheat pathogen *Fusarium graminearum*. *Fungal Genet. Biol.* 100:33-41.
- Carvalho, M.D., Carvalho, J.F., and Merrick, W.C. 1984. Biological characterization of various forms of elongation factor 1 from rabbit reticulocytes. *Arch. Biochem. Biophys.* 234:603-611.
- Chang, S.S., Zhang, Z., and Liu, Y. 2012. RNA interference pathways in fungi: mechanisms and functions. *Annu. Rev. Microbiol.* 66:305-323.
- Chen, D., Wang, Y., Zhou, X., Wang, Y., and Xu, J.R. 2014. The Sch9 kinase regulates conidium size, stress responses, and pathogenesis in *Fusarium graminearum*. *PLoS One* 9:e105811.
- Chen, L., Tong, Q., Zhang, C., and Ding, K. 2019a. The transcription factor FgCrz1A is essential for fungal development, virulence, deoxynivalenol biosynthesis and stress responses in *Fusarium graminearum*. *Curr. Genet.* 65:153-166.
- Chen, W., Wei, L., Zhang, Y., Shi, D., Ren, W., Zhang, Z., Wang, J., Shao, W., Liu, X., Chen, C., and Gao, Q. 2019b. Involvement of the two L-lactate dehydrogenase in development and pathogenicity in *Fusarium graminearum*. *Curr. Genet.* 65:591-605.
- Chen, X., Ishida, N., Todaka, N., Nakamura, R., Maruyama, J., Takahashi, H., and Kitamoto, K. 2010. Promotion of efficient saccharification of crystalline cellulose by *Aspergillus fumigatus* Swol. *Appl. Environ. Microbiol.* 76:2556.
- Chen, Y., Gao, Q., Huang, M., Liu, Y., Liu, Z., Liu, X., and Ma, Z. 2015. Characterization of RNA silencing components in the plant pathogenic fungus *Fusarium graminearum*. *Sci. Rep.* 5:12500.
- Chinchilla, D., Bauer, Z., Regenass, M., Boller, T., and Felix, G. 2006. The Arabidopsis receptor kinase FLS2 binds flg22 and determines the specificity of flagellin perception. *Plant Cell* 18:465-476.
- Chuang, S.M., Chen, L., Lambertson, D., Anand, M., Kinzy, T.G., and Madura, K. 2005. Proteasome-mediated degradation of cotranslationally damaged proteins involves translation elongation factor 1A. *Mol. Cell. Biol.* 25:403-413.

- Clear, R.M., and Abramson, D. 1986. Occurrence of *Fusarium* head blight and deoxynivalenol (vomitoxin) in two samples of Manitoba wheat in 1984. *Can. Plant Dis. Surv.* 66:9-11.
- Cuthbert, R.D., DePauw, R.M., Knox, R.E., Singh, A.K., McCaig, T.N., McCallum, B., Fetch, T., and Beres, B.L. 2017. AAC Penhold Canada Prairie Spring Red wheat. *Can. J. Plant Sci.* 98:207-214.
- Cuzick, A., Urban, M., and Hammond-Kosack, K. 2008. *Fusarium graminearum* gene deletion mutants *map1* and *tri5* reveal similarities and differences in the pathogenicity requirements to cause disease on *Arabidopsis* and wheat floral tissue. *New Phytol.* 177:990-1000.
- D'Arcy, C.J., Eastburn, D.M., and Schumann, G.L. 2001. Illustrated glossary of plant pathology. The Plant Health Instructor.
- de Oliveira, A.L., Gallo, M., Pazzagli, L., Benedetti, C.E., Cappugi, G., Scala, A., Pantera, B., Spisni, A., Pertinhez, T.A., and Cicero, D.O. 2011. The structure of the elicitor Cerato-platanin (CP), the first member of the CP fungal protein family, reveals a double psibeta-barrel fold and carbohydrate binding. *J. Biol. Chem.* 286:17560-17568.
- Deng, J., and Dean, R.A. 2008. Characterization of adenylate cyclase interacting protein ACII in the rice blast fungus, *Magnaporthe oryzae*. *Open Mycol. J.* 2:74-81.
- Desjardins, A.E. 2006. *Fusarium* mycotoxins: chemistry, genetics and biology. APS Press, St. Paul, Minn.
- Desjardins, A.E., Hohn, T.M., and McCormick, S.P. 1993. Trichothecene biosynthesis in *Fusarium* species: chemistry, genetics, and significance. *Microbiol. rev.* 57:595-604.
- DeZwaan, T.M., Carroll, A.M., Valent, B., and Sweigard, J.A. 1999. *Magnaporthe grisea* *pth11p* is a novel plasma membrane protein that mediates appressorium differentiation in response to inductive substrate cues. *The Plant Cell* 11:2013-2030.
- Dilks, T., Halsey, K., De Vos, R.P., Hammond-Kosack, K.E., and Brown, N.A. 2019. Non-canonical fungal G-protein-coupled receptors promote *Fusarium* head blight on wheat. *PLoS Pathog.* 15:e1007666.

- Ding, C., Vidanes, G.M., Maguire, S.L., Guida, A., Synnott, J.M., Andes, D.R., and Butler, G. 2011. Conserved and divergent roles of Bcr1 and CFEM proteins in *Candida parapsilosis* and *Candida albicans*. PLoS One 6:e28151.
- Ding, M., Zhu, Q., Liang, Y., Li, J., Fan, X., Yu, X., He, F., Xu, H., Liang, Y., and Yu, J. 2017. Differential roles of three *FgPLD* genes in regulating development and pathogenicity in *Fusarium graminearum*. Fungal Genet. Biol. 109:46-52.
- Ding, S., Mehrabi, R., Koten, C., Kang, Z., Wei, Y., Seong, K., Kistler, H.C., and Xu, J.-R. 2009. Transducin beta-like gene *FTL1* is essential for pathogenesis in *Fusarium graminearum*. Eukaryot. Cell 8:867-876.
- Djonovic, S., Pozo, M.J., Dangott, L.J., Howell, C.R., and Kenerley, C.M. 2006. Sm1, a proteinaceous elicitor secreted by the biocontrol fungus *Trichoderma virens* induces plant defense responses and systemic resistance. Mol. Plant-Microbe Interact. 19:838-853.
- Dufresne, M., van der Lee, T., Ben M'barek, S., Xu, X., Zhang, X., Liu, T., Waalwijk, C., Zhang, W., Kema, G.H., and Daboussi, M.J. 2008. Transposon-tagging identifies novel pathogenicity genes in *Fusarium graminearum*. Fungal Genet. Biol. 45:1552-1561.
- Enz, J. (1995). Climatic summary. In Crop Production Guide No. 6. (North Dakota State University Extension Service. Fargo, ND, USA), pp. 228-232.
- Fan, X., He, F., Ding, M., Geng, C., Chen, L., Zou, S., Liang, Y., Yu, J., and Dong, H. 2019. Thioredoxin reductase is involved in development and pathogenicity in *Fusarium graminearum*. Front. Microbiol. 10:393-393.
- Felix, G., Duran, J.D., Volko, S., and Boller, T. 1999. Plants have a sensitive perception system for the most conserved domain of bacterial flagellin. Plant J. 18:265-276.
- Flor, H.H. 1971. Current status of the gene-for-gene concept. Annu. Rev. Phytopathol. 9:275-296.
- Foroud, A.N., Baines, D., Gagkaeva, Y.T., Thakor, N., Badea, A., Steiner, B., Bürstmayr, M., and Bürstmayr, H. 2019. Trichothecenes in cereal grains - an update. Toxins

- Foroud, N.A., and Eudes, F. 2009. Trichothecenes in cereal grains. *Int. J. Mol. Sci.* 10:147-173.
- Foroud, N.A., McCormick, S.P., MacMillan, T., Badea, A., Kendra, D.F., Ellis, B.E., and Eudes, F. 2012. Greenhouse studies reveal increased aggressiveness of emergent Canadian *Fusarium graminearum* chemotypes in wheat. *Plant Dis.* 96:1271-1279.
- Frandsen, R.J., Frandsen, M., and Giese, H. 2012. Targeted gene replacement in fungal pathogens via *Agrobacterium tumefaciens*- mediated transformation. *Methods Mol Biol.* 835:17-45.
- Frandsen, R.J., Andersson, J.A., Kristensen, M.B., and Giese, H. 2008. Efficient four fragment cloning for the construction of vectors for targeted gene replacement in filamentous fungi. *BMC Mol. Biol.* 9:70.
- Frias, M., Gonzalez, C., and Brito, N. 2011. BcSpl1, a cerato-platanin family protein, contributes to *Botrytis cinerea* virulence and elicits the hypersensitive response in the host. *New Phytol.* 192:483-495.
- Frias, M., Brito, N., Gonzalez, M., and Gonzalez, C. 2014. The phytotoxic activity of the cerato-platanin BcSpl1 resides in a two-peptide motif on the protein surface. *Mol. Plant Pathol.* 15:342-351.
- Frischmann, A., Neudl, S., Gaderer, R., Bonazza, K., Zach, S., Gruber, S., Spadiut, O., Friedbacher, G., Grothe, H., and Seidl-Seiboth, V. 2013. Self-assembly at air/water interfaces and carbohydrate binding properties of the small secreted protein EPL1 from the fungus *Trichoderma atroviride*. *J. Biol. Chem.* 288:4278-4287.
- Fudal, I., Ross, S., Gout, L., Blaise, F., Kuhn, M.L., Eckert, M.R., Cattolico, L., Bernard-Samain, S., Balesdent, M.H., and Rouxel, T. 2007. Heterochromatin-like regions as ecological niches for avirulence genes in the *Leptosphaeria maculans* genome: map-based cloning of *AvrLm6*. *Mol. Plant-Microbe Interact.* 20:459-470.
- Furukawa, T., Inagaki, H., Takai, R., Hirai, H., and Che, F.S. 2014. Two distinct EF-Tu epitopes induce immune responses in rice and Arabidopsis. *Mol. Plant-Microbe Interact.* 27:113-124.

- Gao, F., Zhang, B.-S., Zhao, J.-H., Huang, J.-F., Jia, P.-S., Wang, S., Zhang, J., Zhou, J.-M., and Guo, H.-S. 2019. Deacetylation of chitin oligomers increases virulence in soil-borne fungal pathogens. *Nature Plants* 5:1167-1176.
- Gardiner, D.M., and Kazan, K. 2018. Selection is required for efficient Cas9-mediated genome editing in *Fusarium graminearum*. *Fungal Biol.* 122:131-137.
- Garreau de Loubresse, N., Prokhorova, I., Holtkamp, W., Rodnina, M.V., Yusupova, G., and Yusupov, M. 2014. Structural basis for the inhibition of the eukaryotic ribosome. *Nature* 513:517-522.
- Georgelis, N., Tabuchi, A., Nikolaidis, N., and Cosgrove, D.J. 2011. Structure-function analysis of the bacterial expansin EXLX1. *J. Biol. Chem.* 286:16814-16823.
- Giaever, G., Chu, A.M., Ni, L., Connelly, C., Riles, L., Véronneau, S., Dow, S., Lucau-Danila, A., Anderson, K., André, B., Arkin, A.P., Astromoff, A., El Bakkoury, M., Bangham, R., Benito, R., Brachet, S., Campanaro, S., Curtiss, M., Davis, K., Deutschbauer, A., Entian, K.-D., Flaherty, P., Foury, F., Garfinkel, D.J., Gerstein, M., Gotte, D., Güldener, U., Hegemann, J.H., Hempel, S., Herman, Z., Jaramillo, D.F., Kelly, D.E., Kelly, S.L., Kötter, P., LaBonte, D., Lamb, D.C., Lan, N., Liang, H., Liao, H., Liu, L., Luo, C., Lussier, M., Mao, R., Menard, P., Ooi, S.L., Revuelta, J.L., Roberts, C.J., Rose, M., Ross-Macdonald, P., Scherens, B., Schimmack, G., Shafer, B., Shoemaker, D.D., Sookhai-Mahadeo, S., Storms, R.K., Strathern, J.N., Valle, G., Voet, M., Volckaert, G., Wang, C.-y., Ward, T.R., Wilhelmy, J., Winzeler, E.A., Yang, Y., Yen, G., Youngman, E., Yu, K., Bussey, H., Boeke, J.D., Snyder, M., Philippsen, P., Davis, R.W., and Johnston, M. 2002. Functional profiling of the *Saccharomyces cerevisiae* genome. *Nature* 418:387-391.
- Gilbert, J., Tekauz, A., Mueller, E., and Kromer, U. 1994. Occurrence of *Fusarium* head blight in Manitoba in 1993. *Can. Plant Dis. Surv.*:74-77.
- Gilbert, J., Clear, R.M., Ward, T.J., Gaba, D., Tekauz, A., Turkington, T.K., Woods, S.M., Nowicki, T., and O'Donnell, K. 2010. Relative aggressiveness and production of 3- or 15-acetyl deoxynivalenol and deoxynivalenol by *Fusarium graminearum* in spring wheat. *Can. J. Plant Pathol.* 32:146-152.
- Gomez-Gomez, L., Felix, G., and Boller, T. 1999. A single locus determines sensitivity to bacterial flagellin in *Arabidopsis thaliana*. *Plant J.* 18:277-284.

- Goswami, R.S., and Kistler, H.C. 2004. Heading for disaster: *Fusarium graminearum* on cereal crops. *Mol. Plant Pathol.* 5:515-525.
- Greenshields, D.L., Liu, G., Feng, J., Selvaraj, G., and Wei, Y. 2007. The siderophore biosynthetic gene *SID1*, but not the ferroxidase gene *FET3*, is required for full *Fusarium graminearum* virulence. *Mol. Plant Pathol.* 8:411-421.
- Grosshans, H., Hurt, E., and Simos, G. 2000. An aminoacylation-dependent nuclear tRNA export pathway in yeast. *Genes Dev.* 14:830-840.
- Grove, J.F. 2007. The trichothecenes and their biosynthesis. *Fortschr Chem Org Naturst* 88:63-130.
- Gu, Q., Zhang, C., Liu, X., and Ma, Z. 2015. A transcription factor FgSte12 is required for pathogenicity in *Fusarium graminearum*. *Mol. Plant Pathol.* 16:1-13.
- Gu, S., Li, P., Wu, M., Hao, Z., Gong, X., Zhang, X., Tian, L., Zhang, P., Wang, Y., Cao, Z., Fan, Y., Han, J., and Dong, J. 2014. StSTE12 is required for the pathogenicity of *Setosphaeria turcica* by regulating appressorium development and penetration. *Microbiol. Res.* 169:817-823.
- Guo, Y., Yao, S., Yuan, T., Wang, Y., Zhang, D., and Tang, W. 2019. The spatiotemporal control of KatG2 catalase-peroxidase contributes to the invasiveness of *Fusarium graminearum* in host plants. *Mol. Plant Pathol.* 20:685-700.
- Hohn, T.M., and Beremand, P.D. 1989. Isolation and nucleotide sequence of a sesquiterpene cyclase gene from the trichothecene-producing fungus *Fusarium sporotrichioides*. *Gene* 79:131-138.
- Hong, S.Y., So, J., Lee, J., Min, K., Son, H., Park, C., Yun, S.H., and Lee, Y.W. 2010. Functional analyses of two syntaxin-like *SNARE* genes, *GzSYN1* and *GzSYN2*, in the ascomycete *Gibberella zeae*. *Fungal Genet. Biol.* 47:364-372.
- Hong, Y., Yang, Y., Zhang, H., Huang, L., Li, D., and Song, F. 2017. Overexpression of *MoSM1*, encoding for an immunity-inducing protein from *Magnaporthe oryzae*, in rice confers broad-spectrum resistance against fungal and bacterial diseases. *Sci. Rep.* 7:41037.

- Hou, Z., Xue, C., Peng, Y., Katan, T., Kistler, H.C., and Xu, J.R. 2002. A mitogen-activated protein kinase gene (*MGVI*) in *Fusarium graminearum* is required for female fertility, heterokaryon formation, and plant infection. *Mol. Plant-Microbe Interact.* 15:1119-1127.
- Hu, S., Zhou, X., Gu, X., Cao, S., Wang, C., and Xu, J.R. 2014. The cAMP-PKA pathway regulates growth, sexual and asexual differentiation, and pathogenesis in *Fusarium graminearum*. *Mol. Plant-Microbe Interact.* 27:557-566.
- Ignatius, S.M.J., Chopra, R.K., and Muthukrishnan, S. 1994. Effects of fungal infection and wounding on the expression of chitinases and β -1,3 glucanases in near-isogenic lines of barley. *Physiol. Plant.* 90:584-592.
- Jansen, C., von Wettstein, D., Schäfer, W., Kogel, K.-H., Felk, A., and Maier, F.J. 2005. Infection patterns in barley and wheat spikes inoculated with wild-type and trichodiene synthase gene disrupted *Fusarium graminearum*. *Proc. Natl. Acad. Sci. U. S. A.* 102:16892.
- Janssen, G.M., and Moller, W. 1988. Kinetic studies on the role of elongation factors 1 beta and 1 gamma in protein synthesis. *J. Biol. Chem.* 263:1773-1778.
- Jenczmionka, N.J., Maier, F.J., Losch, A.P., and Schafer, W. 2003. Mating, conidiation and pathogenicity of *Fusarium graminearum*, the main causal agent of the head-blight disease of wheat, are regulated by the MAP kinase *gpmk1*. *Curr. Genet.* 43:87-95.
- Jeong, J.S., Mitchell, T.K., and Dean, R.A. 2007. The *Magnaporthe grisea* *snodprot1* homolog, *MSP1*, is required for virulence. *FEMS Microbiol. Lett.* 273:157-165.
- Jeppesen, M.G., Navratil, T., Spremulli, L.L., and Nyborg, J. 2005. Crystal structure of the bovine mitochondrial elongation factor Tu.Ts complex. *J. Biol. Chem.* 280:5071-5081.
- Jiang, C., Cao, S., Wang, Z., Xu, H., Liang, J., Liu, H., Wang, G., Ding, M., Wang, Q., Gong, C., Feng, C., Hao, C., and Xu, J.-R. 2019. An expanded subfamily of G-protein-coupled receptor genes in *Fusarium graminearum* required for wheat infection. *Nat. Microbiol.* 4:1582-1591.

- Jiang, J., Yun, Y., Yang, Q., Shim, W.B., Wang, Z., and Ma, Z. 2011. A type 2C protein phosphatase FgPtc3 is involved in cell wall integrity, lipid metabolism, and virulence in *Fusarium graminearum*. PLoS One 6:e25311.
- Jiang, L., Yang, J., Fan, F., Zhang, D., and Wang, X. 2010. The type 2C protein phosphatase FgPtc1p of the plant fungal pathogen *Fusarium graminearum* is involved in lithium toxicity and virulence. Mol. Plant Pathol. 11:277-282.
- Jiang, N., Yang, Y., Janbon, G., Pan, J., and Zhu, X. 2012. Identification and functional demonstration of miRNAs in the fungus *Cryptococcus neoformans*. PLoS One 7:e52734.
- Jones-Rhoades, M.W., Bartel, D.P., and Bartel, B. 2006. MicroRNAs and their regulatory roles in plants. Annu. Rev. Plant Biol. 57:19-53.
- Jones, J.D., and Dangl, J.L. 2006. The plant immune system. Nature 444:323-329.
- Jutidamrongphan, W., Andersen, J.B., Mackinnon, G., Manners, J.M., Simpson, R.S., and Scott, K.J. 1991. Induction of beta-1,3-glucanase in barley in response to infection by fungal pathogens. Mol. Plant-Microbe Interact. 4:234-238.
- Kaku, H., Nishizawa, Y., Ishii-Minami, N., Akimoto-Tomiyama, C., Dohmae, N., Takio, K., Minami, E., and Shibuya, N. 2006. Plant cells recognize chitin fragments for defense signaling through a plasma membrane receptor. Proc. Natl. Acad. Sci. U. S. A. 103:11086-11091.
- Kazemi-Pour, N., Condemine, G., and Hugouvieux-Cotte-Pattat, N. 2004. The secretome of the plant pathogenic bacterium *Erwinia chrysanthemi*. Proteomics 4:3177-3186.
- Kerff, F., Amoroso, A., Herman, R., Sauvage, E., Petrella, S., Filee, P., Charlier, P., Joris, B., Tabuchi, A., Nikolaidis, N., and Cosgrove, D.J. 2008. Crystal structure and activity of *Bacillus subtilis* YoaJ (EXLX1), a bacterial expansin that promotes root colonization. Proc. Natl. Acad. Sci. U. S. A. 105:16876-16881.
- Kershaw, M.J., Wakley, G., and Talbot, N.J. 1998. Complementation of the mpg1 mutant phenotype in *Magnaporthe grisea* reveals functional relationships between fungal hydrophobins. EMBO J. 17:3838-3849.

- Kim, J.E., Myong, K., Shim, W.B., Yun, S.H., and Lee, Y.W. 2007. Functional characterization of acetylglutamate synthase and phosphoribosylamine-glycine ligase genes in *Gibberella zeae*. *Curr. Genet.* 51:99-108.
- Kim, J.E., Lee, H.J., Lee, J., Kim, K.W., Yun, S.H., Shim, W.B., and Lee, Y.W. 2009. *Gibberella zeae* chitin synthase genes, *GzCHS5* and *GzCHS7*, are required for hyphal growth, perithecia formation, and pathogenicity. *Curr. Genet.* 55:449-459.
- Kim, Y., Kim, H., Son, H., Choi, G.J., Kim, J.-C., and Lee, Y.-W. 2014. MYT3, a Myb-like transcription factor, affects fungal development and pathogenicity of *Fusarium graminearum*. *PloS one* 9:e94359-e94359.
- King, R., Urban, M., Hammond-Kosack, M.C.U., Hassani-Pak, K., and Hammond-Kosack, K.E. 2015. The completed genome sequence of the pathogenic ascomycete fungus *Fusarium graminearum*. *BMC Genomics* 16:544.
- Kitamoto, N., Matsui, J., Kawai, Y., Kato, A., Yoshino, S., Ohmiya, K., and Tsukagoshi, N. 1998. Utilization of the *TEF1-a* gene (*TEF1*) promoter for expression of polygalacturonase genes, *pgaA* and *pgaB*, in *Aspergillus oryzae*. *Appl. Microbiol. Biotechnol.* 50:85-92.
- Kong, X., van Diepeningen, A.D., van der Lee, T.A.J., Waalwijk, C., Xu, J., Xu, J., Zhang, H., Chen, W., and Feng, J. 2018. The *Fusarium graminearum* histone acetyltransferases are important for morphogenesis, DON biosynthesis, and pathogenicity. *Front. Microbiol.* 9:654.
- Kou, Y., Tan, Y.H., Ramanujam, R., and Naqvi, N.I. 2017. Structure-function analyses of the Pth11 receptor reveal an important role for CFEM motif and redox regulation in rice blast. *New Phytol.* 214:330-342.
- Kulkarni, R.D., and Dean, R.A. 2004. Identification of proteins that interact with two regulators of appressorium development, adenylate cyclase and cAMP-dependent protein kinase A, in the rice blast fungus *Magnaporthe grisea*. *Mol. Genet. Genomics* 270:497-508.
- Kulkarni, R.D., Kelkar, H.S., and Dean, R.A. 2003. An eight-cysteine-containing CFEM domain unique to a group of fungal membrane proteins. *Trends Biochem. Sci.* 28:118-121.

- Kulkarni, R.D., Thon, M.R., Pan, H., and Dean, R.A. 2005. Novel G-protein-coupled receptor-like proteins in the plant pathogenic fungus *Magnaporthe grisea*. *Genome Biol.* 6:R24.
- Kunze, G., Zipfel, C., Robatzek, S., Niehaus, K., Boller, T., and Felix, G. 2004. The N terminus of bacterial elongation factor Tu elicits innate immunity in Arabidopsis plants. *Plant Cell* 16:3496-3507.
- Kurasawa, Y., Numata, O., Katoh, M., Hirano, H., Chiba, J., and Watanabe, Y. 1992. Identification of *Tetrahymena* 14-nm filament-associated protein as elongation factor 1 alpha. *Exp. Cell Res.* 203:251-258.
- Langevin, F., Eudes, F., and Comeau, A. 2004. Effect of trichothecenes produced by *Fusarium graminearum* during Fusarium head blight development in six cereal species. *Eur. J. Plant Pathol.* 110:735-746.
- Letunic, I., Doerks, T., and Bork, P. 2015. SMART: recent updates, new developments and status in 2015. *Nucleic Acids Res.* 43:257-260.
- Li, B., Dong, X., Zhao, R., Kou, R., Zheng, X., and Zhang, H. 2019a. The t-SNARE protein FgPep12, associated with FgVam7, is essential for ascospore discharge and plant infection by trafficking Ca²⁺ ATPase FgNeo1 between Golgi and endosome/vacuole in *Fusarium graminearum*. *PLoS Pathog.* 15:e1007754.
- Li, D., Wei, T., Abott, C.M., and Harrich, D. 2013. The unexpected roles of eukaryotic translation elongation factors in RNA virus replication and pathogenesis. *Microbiol. Mol. Biol. Rev.* 77:253-266.
- Li, L., Zhu, T., Song, Y., Luo, X., Feng, L., Zhuo, F., Li, F., and Ren, M. 2019b. Functional characterization of target of rapamycin signaling in *Verticillium dahliae*. *Front. Microbiol.* 10:501.
- Li, X., and Carthew, R.W. 2005. A microRNA mediates EGF receptor signaling and promotes photoreceptor differentiation in the Drosophila eye. *Cell* 123:1267-1277.
- Li, Y., Wang, C., Liu, W., Wang, G., Kang, Z., Kistler, H.C., and Xu, J.R. 2011. The *HDF1* histone deacetylase gene is important for conidiation, sexual reproduction, and pathogenesis in *Fusarium graminearum*. *Mol. Plant-Microbe Interact.* 24:487-496.

- Li, Y., Li, B., Liu, L., Chen, H., Zhang, H., Zheng, X., and Zhang, Z. 2015. FgMon1, a guanine nucleotide exchange factor of FgRab7, is important for vacuole fusion, autophagy and plant infection in *Fusarium graminearum*. *Sci. Rep.* 5:18101.
- Liu, G., Tang, J., Edmonds, B.T., Murray, J., Levin, S., and Condeelis, J. 1996. F-actin sequesters elongation factor 1alpha from interaction with aminoacyl-tRNA in a pH-dependent reaction. *J. Cell Biol.* 135:953-963.
- Liu, N., Wu, S., Dawood, D.H., Tang, G., Zhang, C., Liang, J., Chen, Y., and Ma, Z. 2019a. The b-ZIP transcription factor FgTfmI is required for the fungicide phenamacril tolerance and pathogenecity in *Fusarium graminearum*. *Pest Manag. Sci.* 75:3312-3322.
- Liu, S., Wu, B., Yang, J., Bi, F., Dong, T., Yang, Q., Hu, C., Xiang, D., Chen, H., Huang, H., Shao, C., Chen, Y., Yi, G., Li, C., and Guo, X. 2019b. A cerato-platanin family protein FocCP1 is essential for the penetration and virulence of *Fusarium oxysporum* f. sp. *cubense* tropical race 4. *Int. J. Mol. Sci.* 20:3785.
- Liu, X., Xu, J., Wang, J., Ji, F., Yin, X., and Shi, J. 2015. Involvement of threonine deaminase FgIlv1 in isoleucine biosynthesis and full virulence in *Fusarium graminearum*. *Curr. Genet.* 61:55-65.
- Liu, X., Jiang, Y., Zhang, Y., Yu, M., Jiang, H., Xu, J., and Shi, J. 2019c. FgIlv3a is crucial in branched-chain amino acid biosynthesis, vegetative differentiation, and virulence in *Fusarium graminearum*. *J. Microbiol.* 57:694-703.
- Lopez-Berges, M.S., Rispail, N., Prados-Rosales, R.C., and Di Pietro, A. 2010. A nitrogen response pathway regulates virulence functions in *Fusarium oxysporum* via the protein kinase TOR and the bZIP protein MeaB. *Plant Cell* 22:2459-2475.
- Lu, S., and Edwards, M.C. 2016. Genome-wide analysis of small secreted cysteine-rich proteins identifies candidate effector proteins potentially involved in *Fusarium graminearum*-wheat interactions. *Phytopathology* 106:166-176.
- Luderer, R., Takken, F.L., de Wit, P.J., and Joosten, M.H. 2002. *Cladosporium fulvum* overcomes Cf-2-mediated resistance by producing truncated AVR2 elicitor proteins. *Mol. Microbiol.* 45:875-884.

- Luna, E., Pastor, V., Robert, J., Flors, V., Mauch-Mani, B., and Ton, J. 2011. Callose deposition: a multifaceted plant defense response. *Mol. Plant-Microbe Interact.* 24:183-193.
- Luti, S., Martellini, F., Bemporad, F., Mazzoli, L., Paoli, P., and Pazzagli, L. 2017. A single amino acid mutation affects elicitor and expansins-like activities of ceratoplatanin, a non-catalytic fungal protein. *PLoS One* 12:e0178337.
- Maier, F.J., Miedaner, T., Hadel, B., Felk, A., Salomon, S., Lemmens, M., Kassner, H., and Schafer, W. 2006. Involvement of trichothecenes in fusarioses of wheat, barley and maize evaluated by gene disruption of the trichodiene synthase (Tri5) gene in three field isolates of different chemotype and virulence. *Mol. Plant Pathol.* 7:449-461.
- Mary Wanjiru, W., Zhensheng, K., and Buchenauer, H. 2002. Importance of cell wall degrading enzymes produced by *Fusarium graminearum* during infection of wheat heads. *Eur. J. Plant Pathol.* 108:803-810.
- Mayer, C.F. 1953. Endemic panmyelotoxicosis in the Russian grain belt. I. The clinical aspects of alimentary toxic aleukia (ATA); a comprehensive review. *Mil. Surg.* 113:173-189.
- McMullen, M., Jones, R., and Gallenberg, D. 1997. Scab of wheat and barley: a re-emerging disease of devastating impact. *Plant Dis.* 81:1340-1348.
- Merrick, W.C. 1992. Mechanism and regulation of eukaryotic protein synthesis. *Microbiol. rev.* 56:291-315.
- Mesterházy, Á. 2003. Breeding wheat for *Fusarium* head blight resistance in Europe. Pages 211-240 in: *Fusarium Head Blight of Wheat and Barley*, K.J. Leonard and W.R. Bushnell, eds. American Phytopathological Society, St. Paul, MN, USA.
- Meyer, V., Wanka, F., van Gent, J., Arentshorst, M., van den Hondel, C.A.M.J.J., and Ram, A.F.J. 2011. Fungal gene expression on demand: an inducible, tunable, and metabolism-independent expression system for *Aspergillus niger*. *Appl. Environ. Microbiol.* 77:2975-2983.
- Miller, J.D., and Blackwell, B.A. 1986. Biosynthesis of 3-acetyldeoxynivalenol and other metabolites by *Fusarium culmorum* HLX 1503 in a stirred jar fermentor. *Can. J. Bot.* 64:1-5.

- Miller, J.D., Young, J.C., and Sampson, D.R. 1985. Deoxynivalenol and *Fusarium* head blight resistance in spring cereals. *J. Phytopathol.* 113:359-367.
- Miller, J.D., Greenhalgh, R., Wang, Y., and Lu, M. 1991. Trichothecene chemotypes of three *Fusarium* species. *Mycologia* 83:121-130.
- Mirocha, C.J., Abbas, H.K., Windels, C.E., and Xie, W. 1989. Variation in deoxynivalenol, 15-acetyldeoxynivalenol, 3-acetyldeoxynivalenol, and zearalenone production by *Fusarium graminearum* isolates. *Appl. Environ. Microbiol.* 55:1315-1316.
- Miya, A., Albert, P., Shinya, T., Desaki, Y., Ichimura, K., Shirasu, K., Narusaka, Y., Kawakami, N., Kaku, H., and Shibuya, N. 2007. CERK1, a LysM receptor kinase, is essential for chitin elicitor signaling in *Arabidopsis*. *Proc. Natl. Acad. Sci. U. S. A.* 104:19613-19618.
- Moazed, D. 2009. Small RNAs in transcriptional gene silencing and genome defence. *Nature* 457:413-420.
- Muller, S., Sandal, T., Kamp-Hansen, P., and Dalboge, H. 1998. Comparison of expression systems in the yeasts *Saccharomyces cerevisiae*, *Hansenula polymorpha*, *Kluyveromyces lactis*, *Schizosaccharomyces pombe* and *Yarrowia lipolytica*. Cloning of two novel promoters from *Yarrowia lipolytica*. *Yeast* 14:1267-1283.
- Munshi, R., Kandl, K.A., Carr-Schmid, A., Whitacre, J.L., Adams, A.E., and Kinzy, T.G. 2001. Overexpression of translation elongation factor 1A affects the organization and function of the actin cytoskeleton in yeast. *Genetics* 157:1425-1436.
- Murashige, T., and Skoog, F. 1962. A revised medium for rapid growth and bioassays with tobacco tissue cultures. *Physiol. Plant.* 15:473-497.
- Nakajima, Y., Tokai, T., Maeda, K., Tanaka, A., Takahashi-Ando, N., Kanamaru, K., Kobayashi, T., and Kimura, M. 2014. A set of heterologous promoters useful for investigating gene functions in *Fusarium graminearum*. *JSM Mycotoxins* 64:147-152.
- Nicolas, F.E., Moxon, S., de Haro, J.P., Calo, S., Grigoriev, I.V., Torres-Martinez, S., Moulton, V., Ruiz-Vazquez, R.M., and Dalmay, T. 2010. Endogenous short RNAs

generated by Dicer 2 and RNA-dependent RNA polymerase 1 regulate mRNAs in the basal fungus *Mucor circinelloides*. Nucleic Acids Res. 38:5535-5541.

Oide, S., Berthiller, F., Wiesenberger, G., Adam, G., and Turgeon, B.G. 2014. Individual and combined roles of malonichrome, ferricrocin, and TAFC siderophores in *Fusarium graminearum* pathogenic and sexual development. Front. Microbiol. 5:759.

Pan, Y., Wei, J., Yao, C., Reng, H., and Gao, Z. 2018. SsSm1, a Cerato-platanin family protein, is involved in the hyphal development and pathogenic process of *Sclerotinia sclerotiorum*. Plant Sci. 270:37-46.

Paper, J.M., Scott-Craig, J.S., Adhikari, N.D., Cuomo, C.A., and Walton, J.D. 2007. Comparative proteomics of extracellular proteins *in vitro* and *in planta* from the pathogenic fungus *Fusarium graminearum*. Proteomics 7:3171-3183.

Pazzagli, L., Cappugi, G., Manao, G., Camici, G., Santini, A., and Scala, A. 1999. Purification, characterization, and amino acid sequence of cerato-platanin, a new phytotoxic protein from *Ceratocystis fimbriata* f. sp. *platani*. J. Biol. Chem. 274:24959-24964.

Perez, A., Pedros, B., Murgui, A., Casanova, M., Lopez-Ribot, J.L., and Martinez, J.P. 2006. Biofilm formation by *Candida albicans* mutants for genes coding fungal proteins exhibiting the eight-cysteine-containing CFEM domain. FEMS Yeast Res. 6:1074-1084.

Perez, A., Ramage, G., Blanes, R., Murgui, A., Casanova, M., and Martinez, J.P. 2011. Some biological features of *Candida albicans* mutants for genes coding fungal proteins containing the CFEM domain. FEMS Yeast Res. 11:273-284.

Pestka, J.J. 2010. Deoxynivalenol: mechanisms of action, human exposure, and toxicological relevance. Arch. Toxicol. 84:663-679.

Petersen, T.N., Brunak, S., von Heijne, G., and Nielsen, H. 2011. SignalP 4.0: discriminating signal peptides from transmembrane regions. Nat. Methods 8:785-786.

Pfaffl, M.W., Horgan, G.W., and Dempfle, L. 2002. Relative expression software tool (REST) for group-wise comparison and statistical analysis of relative expression results in real-time PCR. Nucleic Acids Res. 30:e36-e36.

- Pinton, P., Braicu, C., Nougayrede, J.P., Laffitte, J., Taranu, I., and Oswald, I.P. 2010. Deoxynivalenol impairs porcine intestinal barrier function and decreases the protein expression of claudin-4 through a mitogen-activated protein kinase-dependent mechanism. *J. Nutr.* 140:1956-1962.
- Pinton, P., Accensi, F., Beauchamp, E., Cossalter, A.M., Callu, P., Grosjean, F., and Oswald, I.P. 2008. Ingestion of deoxynivalenol (DON) contaminated feed alters the pig vaccinal immune responses. *Toxicol. Lett.* 177:215-222.
- Poland, J.A., Balint-Kurti, P.J., Wisser, R.J., Pratt, R.C., and Nelson, R.J. 2009. Shades of gray: the world of quantitative disease resistance. *Trends Plant Sci.* 14:21-29.
- Proctor, R.H., Hohn, T.M., and McCormick, S.P. 1995. Reduced virulence of *Gibberella zeae* caused by disruption of a trichothecene toxin biosynthetic gene. *Mol. Plant-Microbe Interact.* 8:593-601.
- Puhalla, J.E., and Spieth, P.T. 1983. Heterokaryosis in *Fusarium moniliforme*. *Exp. Mycol.* 7:328-335.
- Puri, K.D., and Zhong, S. 2010. The 3-ADON population of *Fusarium graminearum* found in North Dakota is more aggressive and produces a higher level of DON than the prevalent 15-ADON population in spring wheat. *Phytopathology* 100:1007-1014.
- Qi, P.-F., Zhang, Y.-Z., Liu, C.-H., Zhu, J., Chen, Q., Guo, Z.-R., Wang, Y., Xu, B.-J., Zheng, T., Jiang, Y.-F., Wang, J.-P., Zhou, C.-Y., Feng, X., Kong, L., Lan, X.-J., Jiang, Q.-T., Wei, Y.-M., and Zheng, Y.-L. 2018. *Fusarium graminearum* ATP-binding cassette transporter gene *FgABCC9* is required for its transportation of salicylic acid, fungicide resistance, mycelial growth and pathogenicity towards wheat. *Int. J. Mol. Sci.* 19:2351.
- Qin, J., Wu, M., and Zhou, S. 2019. FgEaf6 regulates virulence, asexual/sexual development and conidial septation in *Fusarium graminearum*. *Curr. Genet.*
- Quarantin, A., Glasenapp, A., Schafer, W., Favaron, F., and Sella, L. 2016. Involvement of the *Fusarium graminearum* cerato-platanin proteins in fungal growth and plant infection. *Plant Physiol. Biochem.* 109:220-229.

- Quarantin, A., Castiglioni, C., Schäfer, W., Favaron, F., and Sella, L. 2019. The *Fusarium graminearum* cerato-platanins loosen cellulose substrates enhancing fungal cellulase activity as expansin-like proteins. *Plant Physiol. Biochem.* 139:229-238.
- Ramamoorthy, V., Cahoon, E.B., Thokala, M., Kaur, J., Li, J., and Shah, D.M. 2009. Sphingolipid C-9 methyltransferases are important for growth and virulence but not for sensitivity to antifungal plant defensins in *Fusarium graminearum*. *Eukaryot. Cell* 8:217-229.
- Rampitsch, C., Day, J., Subramaniam, R., and Walkowiak, S. 2013. Comparative secretome analysis of *Fusarium graminearum* and two of its non-pathogenic mutants upon deoxynivalenol induction *in vitro*. *Proteomics* 13:1913-1921.
- Rittenour, W.R., and Harris, S.D. 2008. Characterization of *Fusarium graminearum* Mes1 reveals roles in cell-surface organization and virulence. *Fungal Genet. Biol.* 45:933-946.
- Rittenour, W.R., and Harris, S.D. 2013. Glycosylphosphatidylinositol-anchored proteins in *Fusarium graminearum*: inventory, variability, and virulence. *PLoS One* 8:e81603.
- Rossi, V., Terzi, V., Moggi, F., Morcia, C., Faccioli, P., Haidukowski, M., and Pascale, M. 2007. Assessment of *Fusarium* infection in wheat heads using a quantitative polymerase chain reaction (qPCR) assay. *Food Addit. Contam.* 24:1121-1130.
- Rotter, B.A., Prelusky, D.B., and Pestka, J.J. 1996. Toxicology of deoxynivalenol (vomitoxin). *J. Toxicol. Environ. Health* 48:1-34.
- Ruest, L.B., Marcotte, R., and Wang, E. 2002. Peptide elongation factor eEF1A-2/S1 expression in cultured differentiated myotubes and its protective effect against caspase-3-mediated apoptosis. *J. Biol. Chem.* 277:5418-5425.
- Sabnam, N., and Barman, S.R. 2017. WISH, a novel CFEM GPCR is indispensable for surface sensing, asexual and pathogenic differentiation in rice blast fungus. *Fungal Genet. Biol.* 105:37-51.
- Sampedro, J., and Cosgrove, D.J. 2005. The expansin superfamily. *Genome Biol.* 6:242.

- Sasikumar, A.N., Perez, W.B., and Kinzy, T.G. 2012. The many roles of the eukaryotic elongation factor 1 complex. Wiley interdisciplinary reviews. RNA 3:543-555.
- Saville, S.P., Lazzell, A.L., Monteagudo, C., and Lopez-Ribot, J.L. 2003. Engineered control of cell morphology in vivo reveals distinct roles for yeast and filamentous forms of *Candida albicans* during infection. Eukaryot. Cell 2:1053-1060.
- Scala, A., Pazzagli, L., Comparini, C., Santini, A., Tegli, S., and Cappugi, G. 2004. Cerato-platanin, an early induced protein by *Ceratocystis fimbriata* f.sp. *platani*, elicits phytoalexin synthesis in host and non-host plants. J. Plant Pathol. 86:27-33.
- Schaafsma, A.W., Ilinic, L.T., Miller, J.D., and Hooker, D.C. 2001. Agronomic considerations for reducing deoxynivalenol in wheat grain. Can. J. Plant Pathol. 23:279-285.
- Schenk, S.T., and Schikora, A. 2015. Staining of Callose Depositions in Root and Leaf Tissues. Bio-protocol 5:e1429.
- Schmale III, D.G., and Bergstrom, G.C. 2003. Fusarium head blight in wheat. The Plant Health Instructor. DOI:10.1094/PHI-I-2003-0612-01.
- Schroeder, H.W., and Christensen, J.J. 1963. Factors affecting resistance of wheat to scab caused by *Gibberella zeae* Phytopathology 42:720-727.
- Scott, P.M. 1984. Effects of food processing on mycotoxins. J. Food Prot. 47:489-499.
- Seidl, V., Marchetti, M., Schandl, R., Allmaier, G., and Kubicek, C.P. 2006. Epl1, the major secreted protein of *Hypocrea atroviridis* on glucose, is a member of a strongly conserved protein family comprising plant defense response elicitors. FEBS J. 273:4346-4359.
- Seo, B.W., Kim, H.K., Lee, Y.W., and Yun, S.H. 2007. Functional analysis of a histidine auxotrophic mutation in *Gibberella zeae*. Plant Pathol. J. 23:51-56.
- Seong, K., Hou, Z., Tracy, M., Kistler, H.C., and Xu, J.R. 2005. Random insertional mutagenesis identifies genes associated with virulence in the wheat scab fungus *Fusarium graminearum*. Phytopathology 95:744-750.

- Seong, K.Y., Pasquali, M., Zhou, X., Song, J., Hilburn, K., McCormick, S., Dong, Y., Xu, J.R., and Kistler, H.C. 2009. Global gene regulation by *Fusarium* transcription factors Tri6 and Tri10 reveals adaptations for toxin biosynthesis. *Mol. Microbiol.* 72:354-367.
- Shimizu, T., Nakano, T., Takamizawa, D., Desaki, Y., Ishii-Minami, N., Nishizawa, Y., Minami, E., Okada, K., Yamane, H., Kaku, H., and Shibuya, N. 2010. Two LysM receptor molecules, CEBiP and OsCERK1, cooperatively regulate chitin elicitor signaling in rice. *Plant J.* 64:204-214.
- Singh, P., Piotrowski, M., Klopstech, K., and Gau, A.E. 2004. Investigations on epiphytic living *Pseudomonas* species from *Malus domestica* with an antagonistic effect to *Venturia inaequalis* on isolated plant cuticle membranes. *Environ. Microbiol.* 6:1149-1158.
- Sinha, R.C., Savard, M.E., and Lau, R. 1995. Production of monoclonal antibodies for the specific detection of deoxynivalenol and 15-acetyldeoxynivalenol by ELISA. *J. Agric. Food Chem.* 43:1740-1744.
- Sobrova, P., Adam, V., Vasatkova, A., Beklova, M., Zeman, L., and Kizek, R. 2010. Deoxynivalenol and its toxicity. *Interdiscip. Toxicol.* 3:94-99.
- Sock, J., Rohringer, R., and Kang, Z. 1990. Extracellular beta-1,3-glucanases in stem rust-affected and abiotically stressed wheat leaves : Immunocytochemical localization of the enzyme and detection of multiple forms in gels by activity staining with dye-labeled laminarin. *Plant Physiol.* 94:1376-1389.
- Sperschneider, J., Gardiner, D.M., Thatcher, L.F., Lyons, R., Singh, K.B., Manners, J.M., and Taylor, J.M. 2015. Genome-wide analysis in three *Fusarium* pathogens identifies rapidly evolving chromosomes and genes associated with pathogenicity. *Genome Biol. Evol.* 7:1613-1627.
- Spolti, P., Barros, N.C., Gomes, L.B., dos Santos, J., and Del Ponte, E.M. 2012. Phenotypic and pathogenic traits of two species of the *Fusarium graminearum* complex possessing either 15-ADON or NIV genotype. *Eur. J. Plant Pathol.* 133:621-629.
- Sprinzel, M. 1994. Elongation factor Tu: a regulatory GTPase with an integrated effector. *Trends Biochem. Sci.* 19:245-250.

- Sridhar, P.S., Trofimova, D., Subramaniam, R., González-Peña Fundora, D., Foroud, N.A., Allingham, J.S., and Loewen, M.C. 2020. Ste2 receptor-mediated chemotropism of *Fusarium graminearum* contributes to its pathogenicity against wheat. *Sci. Rep.* 10:10770.
- St.Clair, D.A. 2010. Quantitative disease resistance and quantitative resistance loci in breeding. *Annu. Rev. Phytopathol.* 48:247-268.
- Stack, R.W. 2003. History of *Fusarium* head blight with emphasis on North America. Pages 1-34 in: *Fusarium Head Blight of Wheat and Barley*, K.J. Leonard and W.R. Bushnell, eds. APS Press, St. Paul, MN.
- Stapulionis, R., Kolli, S., and Deutscher, M.P. 1997. Efficient mammalian protein synthesis requires an intact F-actin system. *J. Biol. Chem.* 272:24980-24986.
- Steiner, S., and Philippsen, P. 1994. Sequence and promoter analysis of the highly expressed *TEF* gene of the filamentous fungus *Ashbya gossypii*. *Mol. Gen. Genet.* 242:263-271.
- Stergiopoulos, I., and de Wit, P.J.G.M. 2009. Fungal Effector Proteins. *Annu. Rev. Phytopathol.* 47:233-263.
- Tarrant, D.J., Stirpe, M., Rowe, M., Howard, M.J., von der Haar, T., and Gourlay, C.W. 2016. Inappropriate expression of the translation elongation factor 1A disrupts genome stability and metabolism. *J. Cell Sci.* 129:4455-4465.
- Taylor, D.R., Frank, J., and Kinzy, T.G. 2007. Structure and function of the eukaryotic ribosome and elongation factors. Pages 59-85 in: *Translational Control in Biology and Medicine*, N. Sonenberg, J.W.B. Hershey, and M.B. Mathews, eds. Cold Spring Harbor Laboratory Press, Cold Spring Harbor.
- Tekauz, A., McCallum, B., and Gilbert, J. 2000. Review: *Fusarium* head blight of barley in western Canada. *Can. J. Plant Pathol.* 22:9-16.
- Tendulkar, S.R., Gupta, A., and Chattoo, B.B. 2003. A simple protocol for isolation of fungal DNA. *Biotechnol. Lett.* 25:1941-1944.

- Thornton, S., Anand, N., Purcell, D., and Lee, J. 2003. Not just for housekeeping: protein initiation and elongation factors in cell growth and tumorigenesis. *J Mol Med (Berl)* 81:536-548.
- Tini, F., Beccari, G., Benfield, A.H., Gardiner, D.M., and Covarelli, L. 2019. Role of the *XylA* gene, encoding a cell wall degrading enzyme, during common wheat, durum wheat and barley colonization by *Fusarium graminearum*. *Fungal Genet. Biol.* 136:103318.
- Trail, F. 2009. For blighted waves of grain: *Fusarium graminearum* in the postgenomics era. *Plant Physiol.* 149:103-110.
- Trail, F., and Common, R. 2000. Perithecial development by *Gibberella zeae*: a light microscopy study. *Mycologia* 92:130-138.
- Trail, F., Xu, H., Loranger, R., and Gadoury, D. 2002. Physiological and environmental aspects of ascospore discharge in *Gibberella zeae* (anamorph *Fusarium graminearum*). *Mycologia* 94:181-189.
- Ueno, Y. 1977. Mode of action of trichothecenes. *Pure Appl. Chem.* 49:1737–1745.
- Ueno, Y. 1985. The toxicology of mycotoxins. *Crit. Rev. Toxicol.* 14:99-132.
- Vaknin, Y., Shadkchan, Y., Leviansky, E., Morozov, M., Romano, J., and Osherov, N. 2014. The three *Aspergillus fumigatus* CFEM-domain GPI-anchored proteins (CfmA-C) affect cell-wall stability but do not play a role in fungal virulence. *Fungal Genet. Biol.* 63:55-64.
- Van den Ackerveken, G.F., Van Kan, J.A., Joosten, M.H., Muisers, J.M., Verbakel, H.M., and De Wit, P.J. 1993. Characterization of two putative pathogenicity genes of the fungal tomato pathogen *Cladosporium fulvum*. *Mol. Plant-Microbe Interact.* 6:210-215.
- Vanderplank, J.E. 1968. Disease resistance in plants, Academic Press; New York, USA.
- Voigt, C.A., and Somerville, S.C. 2009. Callose in biotic stress (pathogenesis): biology, biochemistry and molecular biology of callose in plant defence: callose deposition and turnover in plant–pathogen interactions. Pages 525-562 in: Chemistry,

Biochemistry, and Biology of 1-3 Beta Glucans and Related Polysaccharides, A. Bacic, G.B. Fincher, and B.A. Stone, eds. Academic Press, San Diego.

- Voigt, C.A., Schafer, W., and Salomon, S. 2005. A secreted lipase of *Fusarium graminearum* is a virulence factor required for infection of cereals. *Plant J.* 42:364-375.
- Walkowiak, S., Rowland, O., Rodrigue, N., and Subramaniam, R. 2016. Whole genome sequencing and comparative genomics of closely related Fusarium Head Blight fungi: *Fusarium graminearum*, *F. meridionale* and *F. asiaticum*. *BMC Genomics* 17:1014.
- Walkowiak, S., Bonner, C.T., Wang, L., Blackwell, B., Rowland, O., and Subramaniam, R. 2015. Intraspecies interaction of *Fusarium graminearum* contributes to reduced toxin production and virulence. *Mol. Plant-Microbe Interact.* 28:1256-1267.
- Wan, J., Zhang, X.C., Neece, D., Ramonell, K.M., Clough, S., Kim, S.Y., Stacey, M.G., and Stacey, G. 2008. A LysM receptor-like kinase plays a critical role in chitin signaling and fungal resistance in Arabidopsis. *Plant Cell* 20:471-481.
- Wang, L., Mogg, C., Walkowiak, S., Joshi, M., and Subramaniam, R. 2014. Characterization of NADPH oxidase genes *NoxA* and *NoxB* in *Fusarium graminearum*. *Can. J. Plant Pathol.* 36:12-21.
- Wang, Y., Wu, J., Kim, S.G., Tsuda, K., Gupta, R., Park, S.Y., Kim, S.T., and Kang, K.Y. 2016. *Magnaporthe oryzae*-secreted protein MSP1 induces cell death and elicits defense responses in rice. *Mol. Plant-Microbe Interact.* 29:299-312.
- Wang, Y., Liu, W., Hou, Z., Wang, C., Zhou, X., Jonkers, W., Ding, S., Kistler, H.C., and Xu, J.R. 2011. A novel transcriptional factor important for pathogenesis and ascosporeogenesis in *Fusarium graminearum*. *Mol. Plant-Microbe Interact.* 24:118-128.
- Wang, Y.Z., and Miller, J.D. 1988. Effects of *Fusarium graminearum* metabolites on wheat tissue in relation to Fusarium head blight resistance. *J. Phytopathol.* 122:118-125.
- Ward, T.J., Clear, R.M., Rooney, A.P., O'Donnell, K., Gaba, D., Patrick, S., Starkey, D.E., Gilbert, J., Geiser, D.M., and Nowicki, T.W. 2008. An adaptive evolutionary shift in Fusarium head blight pathogen populations is driving the

- rapid spread of more toxigenic *Fusarium graminearum* in North America. Fungal Genet. Biol. 45:473-484.
- Watt, S.A., Wilke, A., Patschkowski, T., and Niehaus, K. 2005. Comprehensive analysis of the extracellular proteins from *Xanthomonas campestris* pv. *campestris* B100. Proteomics 5:153-167.
- Weissman, Z., and Kornitzer, D. 2004. A family of *Candida* cell surface haem-binding proteins involved in haemin and haemoglobin-iron utilization. Mol. Microbiol. 53:1209-1220.
- Wilson, L.M., Idnurm, A., and Howlett, B.J. 2002. Characterization of a gene (*sp1*) encoding a secreted protein from *Leptosphaeria maculans*, the blackleg pathogen of *Brassica napus*. Mol. Plant Pathol. 3:487-493.
- Windels, C.E. 2000. Economic and social impacts of Fusarium head blight: changing farms and rural communities in the northern great plains. Phytopathology 90:17-21.
- Yagen, B., and Joffe, A.Z. 1976. Screening of toxic isolates of *Fusarium poae* and *Fusarium sporotrichioides* involved in causing alimentary toxic aleukia. Appl. Environ. Microbiol. 32:423-427.
- Yamaji, Y., Kobayashi, T., Hamada, K., Sakurai, K., Yoshii, A., Suzuki, M., Namba, S., and Hibi, T. 2006. *In vivo* interaction between Tobacco mosaic virus RNA-dependent RNA polymerase and host translation elongation factor 1A. Virology 347:100-108.
- Yan, Z. 2012. Recombinant EXLX1 from *Bacillus subtilis* for enhancing enzymatic hydrolysis of corn stover with low cellulase loadings. Afr. J. Biotechnol. 11.
- Yang, Tang, L., Gong, Y., Xie, J., Fu, Y., Jiang, D., Li, G., Collinge, D.B., Chen, W., and Cheng, J. 2018. A cerato-platanin protein SsCP1 targets plant PR1 and contributes to virulence of *Sclerotinia sclerotiorum*. New Phytol. 217:739-755.
- Yang, C., Liu, H., Li, G., Liu, M., Yun, Y., Wang, C., Ma, Z., and Xu, J.R. 2015. The MADS-box transcription factor FgMcm1 regulates cell identity and fungal development in *Fusarium graminearum*. Environ. Microbiol. 17:2762-2776.

- Yang, Y., Zhang, H., Li, G., Li, W., Wang, X., and Song, F. 2009. Ectopic expression of MgSM1, a cerato-platanin family protein from *Magnaporthe grisea*, confers broad-spectrum disease resistance in Arabidopsis. *Plant Biotechnol. J.* 7:763-777.
- Yennawar, N.H., Li, L.C., Dudzinski, D.M., Tabuchi, A., and Cosgrove, D.J. 2006. Crystal structure and activities of EXPB1 (*Zea m 1*), a beta-expansin and group-1 pollen allergen from maize. *Proc. Natl. Acad. Sci. U. S. A.* 103:14664-14671.
- Yu, D., Zhang, S., Li, X., Xu, J.-R., Schultzhaus, Z., and Jin, Q. 2017. A Gin4-like protein kinase GIL1 involvement in hyphal growth, asexual development, and pathogenesis in *Fusarium graminearum*. *Int. J. Mol. Sci.* 18:424.
- Yu, H.Y., Seo, J.A., Kim, J.E., Han, K.H., Shim, W.B., Yun, S.H., and Lee, Y.W. 2008. Functional analyses of heterotrimeric G protein G alpha and G beta subunits in *Gibberella zeae*. *Microbiology* 154:392-401.
- Yun, S.-H., Arie, T., Kaneko, I., Yoder, O.C., and Turgeon, B.G. 2000. Molecular organization of mating type loci in heterothallic, homothallic, and asexual *Gibberella/Fusarium species*. *Fungal Genet. Biol.* 31:7-20.
- Zhang, C., Lin, Y., Wang, J., Wang, Y., Chen, M., Norvinyeku, J., Li, G., Yu, W., and Wang, Z. 2016a. FgNoxR, a regulatory subunit of NADPH oxidases, is required for female fertility and pathogenicity in *Fusarium graminearum*. *FEMS Microbiol. Lett.* 363:fnv223.
- Zhang, D., Fan, F., Yang, J., Wang, X., Qiu, D., and Jiang, L. 2010. FgTep1p is linked to the phosphatidylinositol-3 kinase signalling pathway and plays a role in the virulence of *Fusarium graminearum* on wheat. *Mol. Plant Pathol.* 11:495-502.
- Zhang, H., Li, B., Fang, Q., Li, Y., Zheng, X., and Zhang, Z. 2016b. SNARE protein FgVam7 controls growth, asexual and sexual development, and plant infection in *Fusarium graminearum*. *Mol. Plant Pathol.* 17:108-119.
- Zhang, L., Li, B., Zhang, Y., Jia, X., and Zhou, M. 2016c. Hexokinase plays a critical role in deoxynivalenol (DON) production and fungal development in *Fusarium graminearum*. *Mol. Plant Pathol.* 17:16-28.
- Zhang, X.-W., Jia, L.-J., Zhang, Y., Jiang, G., Li, X., Zhang, D., and Tang, W.-H. 2012. In planta stage-specific fungal gene profiling elucidates the molecular strategies of *Fusarium graminearum* growing inside wheat coleoptiles. *The Plant Cell* 24:5159.

- Zhang, Y.-Z., Wei, Z.-Z., Liu, C.-H., Chen, Q., Xu, B.-J., Guo, Z.-R., Cao, Y.-L., Wang, Y., Han, Y.-N., Chen, C., Feng, X., Qiao, Y.-Y., Zong, L.-J., Zheng, T., Deng, M., Jiang, Q.-T., Li, W., Zheng, Y.-L., Wei, Y.-M., and Qi, P.-F. 2017a. Linoleic acid isomerase gene *FgLAI12* affects sensitivity to salicylic acid, mycelial growth and virulence of *Fusarium graminearum*. *Sci. Rep.* 7:46129-46129.
- Zhang, Y.-Z., Chen, Q., Liu, C.-H., Lei, L., Li, Y., Zhao, K., Wei, M.-Q., Guo, Z.-R., Wang, Y., Xu, B.-J., Jiang, Y.-F., Kong, L., Liu, Y.-L., Lan, X.-J., Jiang, Q.-T., Ma, J., Wang, J.-R., Chen, G.-Y., Wei, Y.-M., Zheng, Y.-L., and Qi, P.-F. 2019. *Fusarium graminearum* *FgCWM1* encodes a cell wall mannoprotein conferring sensitivity to salicylic acid and virulence to wheat. *Toxins* 11:628.
- Zhang, Y., Liang, Y., Qiu, D., Yuan, J., and Yang, X. 2017b. Comparison of ceratoplatanin family protein BcSpl1 produced in *Pichia pastoris* and *Escherichia coli*. *Protein Expr. Purif.* 136:20-26.
- Zhang, Y., Gao, Y., Liang, Y., Dong, Y., Yang, X., Yuan, J., and Qiu, D. 2017c. The *Verticillium dahliae* SnodProt1-like protein VdCP1 contributes to virulence and triggers the plant immune system. *Front. Plant Sci.* 8:1880.
- Zhang, Y.Z., Chen, Q., Liu, C.H., Liu, Y.B., Yi, P., Niu, K.X., Wang, Y.Q., Wang, A.Q., Yu, H.Y., Pu, Z.E., Jiang, Q.T., Wei, Y.M., Qi, P.F., and Zheng, Y.L. 2016d. Chitin synthase gene *FgCHS8* affects virulence and fungal cell wall sensitivity to environmental stress in *Fusarium graminearum*. *Fungal Biol.* 120:764-774.
- Zhang, Z.N., Wu, Q.Y., Zhang, G.Z., Zhu, Y.Y., Murphy, R.W., Liu, Z., and Zou, C.G. 2015. Systematic analyses reveal uniqueness and origin of the CFEM domain in fungi. *Sci. Rep.* 5:13032.
- Zheng, D., Zhang, S., Zhou, X., Wang, C., Xiang, P., Zheng, Q., and Xu, J.-R. 2012. The *FgHOG1* pathway regulates hyphal growth, stress responses, and plant infection in *Fusarium graminearum*. *PloS one* 7:e49495-e49495.
- Zheng, H., Zheng, W., Wu, C., Yang, J., Xi, Y., Xie, Q., Zhao, X., Deng, X., Lu, G., Li, G., Ebbole, D., Zhou, J., and Wang, Z. 2015. Rab GTPases are essential for membrane trafficking-dependent growth and pathogenicity in *Fusarium graminearum*. *Environ. Microbiol.* 17:4580-4599.
- Zhou, J., Fu, Y., Xie, J., Li, B., Jiang, D., Li, G., and Cheng, J. 2012a. Identification of microRNA-like RNAs in a plant pathogenic fungus *Sclerotinia sclerotiorum* by high-throughput sequencing. *Mol. Genet. Genomics* 287:275-282.

- Zhou, Q., Wang, Z., Zhang, J., Meng, H., and Huang, B. 2012b. Genome-wide identification and profiling of microRNA-like RNAs from *Metarhizium anisopliae* during development. *Fungal Biol.* 116:1156-1162.
- Zhu, Q., Sun, L., Lian, J., Gao, X., Zhao, L., Ding, M., Li, J., and Liang, Y. 2016. The phospholipase C (*FgPLC1*) is involved in regulation of development, pathogenicity, and stress responses in *Fusarium graminearum*. *Fungal Genet. Biol.* 97:1-9.
- Zhu, W., Wei, W., Wu, Y., Zhou, Y., Peng, F., Zhang, S., Chen, P., and Xu, X. 2017. BcCFEM1, a CFEM domain-containing protein with putative GPI-anchored site, is involved in pathogenicity, conidial production, and stress tolerance in *Botrytis cinerea*. *Front. Microbiol.* 8:1807.
- Zipfel, C., Kunze, G., Chinchilla, D., Caniard, A., Jones, J.D., Boller, T., and Felix, G. 2006. Perception of the bacterial PAMP EF-Tu by the receptor EFR restricts *Agrobacterium*-mediated transformation. *Cell* 125:749-760.